

**Best
Available
Copy**

AD-755 814

SELECTED MATERIAL FROM SOVIET TECHNICAL
LITERATURE, DECEMBER 1972

Stuart G. Hibben

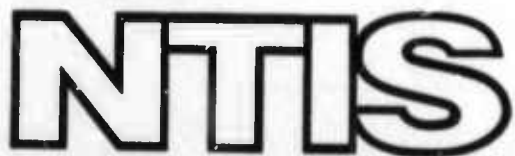
Informatics, Incorporated

Prepared for:

Air Force Office of Scientific Research

26 January 1973

DISTRIBUTED BY:



National Technical Information Service
U. S. DEPARTMENT OF COMMERCE
5285 Port Royal Road, Springfield Va. 22151

informatics inc

SELECTED MATERIAL
FROM
SOVIET TECHNICAL LITERATURE

December 1972

Sponsored by
Advanced Research Projects Agency

Reproduced by
**NATIONAL TECHNICAL
INFORMATION SERVICE**
U S Department of Commerce
Springfield VA 22151

SELECTED MATERIAL
FROM
SOVIET TECHNICAL LITERATURE

December 1972

Sponsored by
Advanced Research Projects Agency

ARPA Order No. 1622-3

January 26, 1973

ARPA Order No. 1622-3
Program Code No: 62701D2F10
Name of Contractor:
Informatics Inc.
Effective Date of Contract:
January 3, 1972
Contract Expiration Date:
December 31, 1972
Amount of Contract: \$250,000

Contract No. F44620-72-C-0053
Principal Investigator:
Stuart C. Hibben
Tel: (301) 779-2850 or
(301) 770-3000
Short Title of Work:
"Soviet Technical Selections"

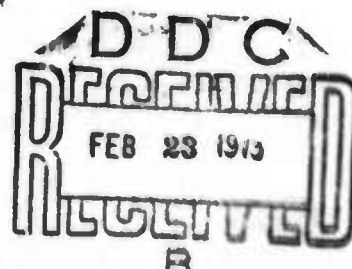
This research was supported by the Advanced Research Projects Agency of the Department of Defense and was monitored by the Air Force Office of Scientific Research under Contract No. F44620-72-C-0053. The publication of this report does not constitute approval by any government organization or Informatics Inc. of the inferences, findings, and conclusions contained herein. It is published solely for the exchange and stimulation of ideas.

Approved for public release; distribution unlimited

informatics inc

Systems and Services Company
6000 Executive Boulevard
Rockville, Maryland 20852
(301) 770-3000 Telex 89-521

II



UNCLASSIFIED

Security Classification

DOCUMENT CONTROL DATA - R & D

(Security classification of title, body of abstract and indexing annotation must be entered when the overall report is classified)

1. ORIGINATING ACTIVITY (Corporate author)

Informatics Inc.
6000 Executive Boulevard
Rockville, Maryland 20852

2a. REPORT SECURITY CLASSIFICATION

UNCLASSIFIED

2b. GROUP

3. REPORT TITLE

Selected Material from Soviet Technical Literature, December, 1972

4. DESCRIPTIVE NOTES (Type of report and inclusive dates)

Scientific . . . Interim

5. AUTHOR(S) (First name, middle initial, last name)

Stuart G. Hibben

6. REPORT DATE

January 26, 1973

7a. TOTAL NO. OF PAGES

165

7b. NO. OF REFS

8a. CONTRACT OR GRANT NO

F44620-72-C-0053

9a. ORIGINATOR'S REPORT NUMBER(S)

8b. PROJECT NO

1622-3

9b. OTHER REPORT NO(S) (Any other numbers that may be assigned this report)

c.

62701D

d.

AFOSR - TR - 73 - 0264

10. DISTRIBUTION STATEMENT

Approved for public release; distribution unlimited.

11. SUPPLEMENTARY NOTES

Tech. Other

12. SPONSORING MILITARY ACTIVITY

Air Force Office of Scientific Research
1400 Wilson Boulevard *11 PG*
Arlington, Virginia 22209

13. ABSTRACT

This report includes abstracts and bibliographic lists on major contractual subjects that were completed in December, 1972. The major topics are: laser technology, effects of strong explosions, geosciences, and particle beams. Sections on material science and on items of miscellaneous interest are included as optional topics. A preliminary draft report on Soviet Developments in Climatology has been published under separate cover as an additional optional topic.

To avoid duplication in reporting, only laser entries concerning high-power effects are routinely included, since all current laser material appears regularly in the quarterly bibliographies.

An index identifying source abbreviations and a first-author index to the abstracts are appended. Since this is the final report for 1972, a cumulative author index for all 1972 abstracts has also been included.

I

DD FORM 1 NOV 68 1473

UNCLASSIFIED

INTRODUCTION

This report includes abstracts and bibliographic lists on major contractual subjects that were completed in December, 1972. The major topics are: laser technology, effects of strong explosions, geosciences, and particle beams. Sections on material science and on items of miscellaneous interest are included as optional topics. A preliminary draft report on Soviet Developments in Climatology has been published under separate cover as an additional optional topic.

To avoid duplication in reporting, only laser entries concerning high-power effects are routinely included, since all current laser material appears regularly in the quarterly bibliographies.

An index identifying source abbreviations and a first-author index to the abstracts are appended. Since this is the final report for 1972, a cumulative author index for all 1972 abstracts has also been included.

TABLE OF CONTENTS

1. Laser Technology	
A. Abstracts	1
B. Recent Selections	18
2. Effects of Strong Explosions	
A. Abstracts	20
B. Recent Selections	54
3. Geosciences	
A. Abstracts	68
B. Recent Selections	95
4. Particle Beams	
A. Abstracts	101
B. Recent Selections	109
5. Material Science	
A. Abstracts	115
B. Recent Selections	121
6. Miscellaneous Interest	
A. Abstracts	135
B. Recent Selections	147
7. List of Source Abbreviations 150
8. Author Index to Abstracts 156
9. Cumulative Author Index, January - December 1972 158

IV

1. Laser Technology

A. Abstracts

Danileyko, Yu. K., A. A. Manenkov, V. S.
Nechitaylo, A. M. Prokhorov, and V. Ya.
Khaimov-Mal'kov. Role of absorbing
inclusions in the destruction of transparent
dielectrics by laser radiation. ZhETF, v. 63,
no. 3, 1972, 1031-1035.

A theory is presented on the process of thermal destruction of transparent dielectrics, accounting for nonlinearities of the absorbing inclusions as well as the surrounding matrix. The theory attempts to prove that the destruction is clearly of a threshold nature and is always accompanied by high-temperature radiation spark similar to laser breakdown in gases.

An equation of thermal conductivity is used to describe the laser heating of an absorbing spherical particle of radius a and its surrounding medium. For temperature nonlinearities of the value $Q(I, T)$, representing the thermal source power, various laws and approximations may be used based on the radiation absorption mechanism or the temperature interval. The authors selected an experimental temperature dependence for the $Q(I, T)$ value, and an inversely proportional dependence for the thermal conductivity $K(T)$ value. Two solutions for the thermal conductivity equation were analyzed as a function of the laser pulse duration. For long pulses when $t \gtrsim r_x = T_0 C_1 \rho_1 a^2 / \alpha_1$, (where T_0 is the initial specimen temperature; and C_1 , ρ_1 , α_1 are the specific heat, density and the constant of the particle matter, respectively), the solution of the thermal conductivity equation is given in the form of an implicit integral relationship between t_{thresh} and Q_{thresh} . The t threshold value denotes the time preceding the moment when the temperature in the center of an inclusion begins to rise rapidly, similar to an avalanching and equivalent to the onset of destruction. The other threshold value, Q , is the threshold capacity of destruction. The analysis indicates that the destruction process is of a thermal explosion nature. The maximum

attainable temperature in the absorbing inclusion is not pertinent in determinations of destruction thresholds. The latter temperature value governs the magnitude of maximum stresses in the surrounding matrix; and consequently, also the nature, scope and the dynamics of destructions in the matrix. For short laser pulses when $\tau \ll \tau_x$, it is concluded that it is not necessary to determine the critical temperature in order to estimate the Q_{thresh} for medium-size nonlinearity parameters.

The theory developed in the article proves that the threshold of destruction strongly depends on the size of inclusions, the thermal and optical constants, and the temperature nonlinearity. Numerical estimates are given for the threshold destruction of glass with $2a = 10^{-5}$ cm platinum inclusions from a laser pulse of $\tau = 3 \times 10^{-8}$ sec, yielding an I_{thresh} of $\approx 8 \times 10^7$ watt/cm². For ruby crystals with $2a = 3 \times 10^{-6}$ cm nickel particle inclusions and pulse duration $\tau = 3 \times 10^{-8}$ sec, with $\tau \gg \tau_x$, $Q_{\text{thresh}} \approx 2 \times 10^{14}$ watt/cm² and $I_{\text{thresh}} \approx 7 \times 10^9$ watt/cm² values are obtained.

Lokhov, Yu. N., G. V. Rozhnov, and I. I. Shvyrkova. Kinetics of forming a liquid phase from the action of a point heat source, taking heat of phase transition into account.
FiKhOM, no. 3, 1972, 9-17.

The article presents a quantitative description of the melting process of semiinfinite heat-conducting solids under the impact of a surface point heat source of constant intensity with allowance for the phase transition temperature. Analytical assumptions are: 1) the source surface power density does not exceed 10^6 w/cm², thus avoiding the problem of material vaporization and the related gas-dynamic effects; 2) the material is an ideal black body; 3) the liquid and solid phase thermophysical parameters are not a function of temperature; 4) the material density remains constant during the melting process and 5) the stabilization time of the maximum melting radius for most metals does not exceed hundredths of a millisecond allowing the heat exchange between the liquid and solid phases and the environment to be

ignored and reducing the problem to a spherically-symmetrical one.

The spherically-symmetrical problem is given as a set of heat conductivity equations for liquid and solid phase temperature distributions with corresponding initial and boundary conditions. For the solution, the velocity of phase transition boundary motion is determined from the energy balance. For small time intervals the velocity is much higher than that of diffusion in a liquid medium. Experimental data have shown that turbulence in this medium controls the hydrodynamic nature of heat transfer in a melted material. The turbulent temperature conductivity is of the order of $0.1 \text{ cm}^2/\text{sec}$, which results in a rapid mixing and levelling of temperature up to the melting temperature T_m .

At specific material heat source parameters and thermo-physical properties, the solution obtained enables the size of the melted zone to be determined as well as the r_m value, for the time of heat source exposure needed to form the melted zone. Both the zone size and the r_m are dependent on the melting temperature. The solutions obtained confirm the assumption that for most metals the liquid phase temperature is constant over the total time interval (steel is the only exception due to its low heat conductivity).

The authors demonstrate the qualitative agreement of estimates derived from the formulas with experimental data obtained using a focused laser pulse as a point heat source (energy - 0.1 joule, duration - $\tau = 1 \text{ ms}$, under the conditions $\tau \geq r_m$). Temperature distribution data along the solid phase are also presented in computer-aided numerical solution form. It is shown that the stationary state stabilization and the heating depth of the solid phase are largely a function of the phase transition temperature.

Batanov, V. A., F. V. Bunkin, A. M.
Prokhorov, and V. B. Fedorov.
Vaporization of metal targets from high-intensity optical radiation. ZhETF, v. 63,
no. 2, 1972, 586-608.

In an extensive study of laser interaction with metals, theoretical and experimental data are given on metal liquid-vapor phase transition, the increased transparency wave in metals, ejection of matter and recoil impulses at the target, and laser irradiation of Bi and Pb targets. Calculations indicate that when the intensity of incident radiation exceeds some threshold value I_{thresh} the target surface temperature of a $\sim 10^{-3}$ cm thick layer will be higher than either the normal boiling temperature or melting temperature; the vaporization consequently proceeds from the liquid metal.

Evidence is shown that at a critical intensity I_{md} a "transparency wave" appears in the vapor products, at the front of which the metal vapor takes on dielectric properties. The authors then trace the behaviour of the complex dielectric permittivity of target matter when radiation intensity passes through the point I_{md} . At this moment, the coefficient of reflection R from the target drops to one fifth of its initial value, but with further increases $I > I_{\text{md}}$ the coefficient decreases more slowly (see Fig. 1).

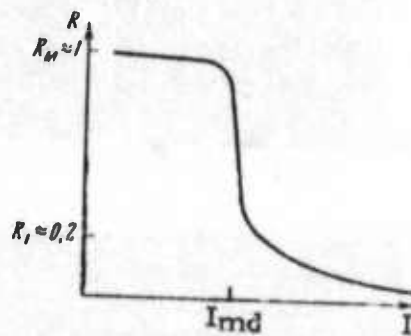


Fig. 1. Dependence of reflection coefficient R on intensity I of incident light. Decrease of R in the region $I > I_{\text{md}}$ follows the law $R \sim 1/I^2$.

An increase of radiation intensity above I_{md} does not increase the target surface temperature; rather the resulting energy is used in moving the front of the increased-transparency wave deeper into the target. The velocity of the increased-transparency wave D in relation to "cold" metals is computed from the laws of conservation of matter, pulse and energy. It is shown that at the initial stage of increased transparency, when the excess intensity I over the transparency threshold $I_{\mu d}$ (μ is the absorption coefficient) is low, D is linearly dependent on I.

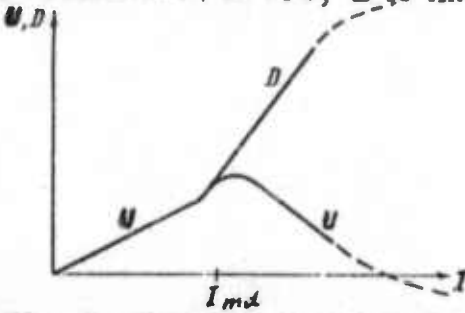


Fig. 2. Dependence of the rate of front vaporization U and the velocity of the increased-transparency wave D on incident light intensity.

Dependence of the rate of vaporization of the front wave U on intensity I of incident radiation is also examined. A sharp deviation of linear dependence $U(I)$ at the threshold point I_{md} is caused by an increase in absorptive capacity $(1 - R)$ of the target surface. At $I = I_{md}$ the velocity of U reaches a maximum, but a further increase of I stops the vaporization front($U = 0$), and immediately removes it from the "cold" metal ($U < 0$), as seen in Fig. 2.

Ejection of matter and recoil impulses provide additional experimental data on processes at the target, as predetermined by conditions at the phase boundary. Formulas are given for specific values of the recoil pulse J and ejected mass Δm with respect to their relations to total energy E_0 in the radiation pulse. Experiments were conducted with

lasers of up to 10 J at a pulse duration of $\tau = 0.8$ millisecond, permitting operation on large radiation-exposed spots to achieve uniform vaporization. Tests were carried out at atmospheric pressure using Bi and Pb targets. Experimental data were obtained that verified the suggested mechanism of metal vaporization under the impact of a high-intensity laser beam. From experimental relations D/E_0 , maxima were traced at the I_{md} values $\approx 3 \times 10^6$ w/cm² for bismuth, and $\approx 2.5 \times 10^7$ w/cm² for lead. The corresponding values for T_{md} were $\approx 2500^\circ$ K for Bi and $\approx 3350^\circ$ K for Pb.

Aluminum targets were also tested and it was determined that the crater shape had a strong effect on the recoil impulse. The authors present additional data on the vaporization of metal targets by high-intensity laser beams and conclude that the gas-dynamic structure of a plasma flare is time-independent; its shock wave is fixed with respect to the target, and the ambient pressure is < 1 atm. This is of particular importance for the evaluation of ejecta, since it bypasses the role of the liquid phase, in contrast to the usual method of weighing the target before and after the test.

Batanov, B. A., F. V. Bunkin, A. M. Prokhorov, and V. B. Fedorov. Self-focusing of light in plasma and a supersonic ionization wave in the laser beam.
ZhETF P, v. 16, no. 7, 1972, 378-382.

A plasma flare was generated, characterized by almost total absorption of internal laser radiation. The process occurred during progressive vaporization of a bismuth target in a helium atmosphere (pressure $P_0 = 2.5-5$ atm) by a laser beam ($\lambda = 1.06\mu$ at an intensity of

$I_0 \approx 10^7$ w/cm² and 1 ms pulse width). A time scan of the bismuth plasma flare is presented containing a time stabilized flare cross-section which shows that as a result of flare expansion the internal pressure P becomes equal to the external pressure P_0 . The plasma is sustained by the beam in a slow burning mode. The condition for maintaining the plasma in the beam is expressed by $aI = Q$, where Q is the radiation recombination loss. The plasma temperature T and electron density n_e are calculated from the condition $P = P_0$ by the time and length averaged coefficient of inhibition $a \approx 0.4$ cm⁻¹. Self-focusing instability also develops in a plasma cloud at $P = P_0$. The laser beam, at a level $n_e \sim P_0/T \sim P_0/I$, generates a plasma cross-section profile $\epsilon = 1 - \text{const} \times n_e$, similar to the profile I , with a maximum on the beam axis. The plasma beam itself focuses on the profile ϵ , which is made possible by the plasma low thermal conductivity. As a result of self-focusing and an absorption burst, a plasma bunch is formed in cold vapor. The characteristics of this process are: 1) taking beam attenuation into account, plasma lens focus intensity $I_{sf} \gtrsim 1.5 \times 10^7$ w/cm² is lower than the optical breakdown threshold; 2) the bunch is formed at the target and not in the plasma lens focus; and 3) the burst takes much longer to develop ($\sim 10^{-4}$ - 10^{-5} sec) than breakdown into avalanche ionization. The bunch movement toward the beam is in the form of a supersonic ionization wave along the cold vapor between the target and the drifting plasma; one-dimensional propagation of the wave proceeds through laser beam energy absorption in the wave. The velocity of the burst luminescence region exceeds that of the plasma cloud drifting away from the target. The bunch then overtakes the drifting plasma and the process repeats itself. Six cycles of instability self-focusing with increased periodicity were established.

geometry are far more effective in capturing and retaining bunches of dense laser-produced plasma than the plug-type traps (probkotrons). A ruby laser, 150 x 12 mm at an energy of 0.15 joule and 50 nsec pulse duration was focused on a flat titanium target surface in a vacuum chamber at 3×10^{-6} torr. A plasma bunch front of $n > 10^{13} \text{ cm}^{-3}$ density moved along the trap axis at a velocity $v = (4-5) \cdot 10^6 \text{ cm/sec}$. The total number of particles in the plasma bunch was determined from the mean energy of the bunch, target mass measurements, and chamber pulse pressure variations. In all three cases the total was determined to be $N = 3 \times 10^{16}$ particles. An SHF generator ($\lambda = 0.8 \text{ cm}$) was used to measure laser plasma physical characteristics. The SHF cutoff of the freely expanding plasma bunch 5 cm from the target was $\tau = 1.2-1.4 \mu\text{sec}$. This value increased sharply with an increase in magnetic field intensity in the trap. Results are: in antiplug traps $\tau = 160 \mu\text{sec}$ at an intensity of $H = 6 \text{ koe}$; in plug-type traps τ was 25 μsec at 7-8 koe. The injected plasma in the trap was photographed during the trapping process and two different patterns were again observed as a function of trap geometry. In the antiplug traps, the plasma bunch moving along the magnetic field filled the trap; as revealed by the photographs, part of the bunch was disk-shaped and remained stable longer. Increases of τ were accompanied by increased flow energy q moving through the trap equatorial slot. It was observed that for the plug-type traps, although an increase of field resulted in a specific increase in time during which the plasma remained in the trap, this dependence is rather weak; with increased intensity, the plasma was also compressed into a narrow filament. The authors suggest that the brevity of plasma entrapment may be due to the nonuniformity of trap filling.

Alkhimov, A. P., V. F. Klimkin, A. I.
Ponomarenko, and R. I. Soloukhin. On
the development of a discharge initiated
by a laser spark. 10th Int. Conf. Phenomena
Ioniz. Gases, Oxford, 1971. Oxford,
1971, 227 (RZh Mekh, 8/72, no. 8 B196)
(Translation)

A study is made of the initial stages of the formation of a laser-initiated discharge in air at atmospheric pressures (Al electrodes 10 cm in diameter, gap 15 mm, voltage - about 35 kv). The time relationships of the radiation intensity of a Nd laser (pulse~30 nanosec, power ~ 20 Mw) and the discharge current are registered; in addition a study is made, by means of an electronicoptical converter under conditions of scanning and frame photography, of the pattern of discharge development over nanosecond intervals. The discharge commences with the formation of a plasmoid in the cathode region independently of the point of laser-beam focusing with progressive development of a streamer moving toward the anode (rate of motion $\sim 10^9$ cm/sec) and closure of the gap. An examination is made of the qualitative pattern of the physical processes taking place during this time.

Arifov, T. U., and I. M. Rayevskiy.
Laser plasma charging of magnetic
traps. ZhTF, no. 8, 1972, 1764-1766.

Data are presented on plasma behaviour in magnetic traps of two different configurations, referred to as "plug-type" and "antiplug-type". Experiments have shown that magnetic traps with "anti-plug"

Knyazev, I. N., and V. S. Letokhov.

Stimulated radiation in the far vacuum u-v
from fast heating of an electron plasma
by ultrashort optical pulses. OiS, v. 33,
no. 1, 1972, 110-115.

Laser excitation in a rising electron avalanche is not advantageous in the short-wave range because: 1) as long as the neutral gas predominates in the plasma, the electron avalanche proceeds at a high speed but owing to photoabsorption there is no emission at short-wave transitions; and 2) when neutral gas burns out and the plasma becomes transparent for transitions in the far vacuum ultraviolet, ionization velocity drops drastically, hindering inversion. The authors propose using ultrashort pulses of an electric or optical field with $\omega > \omega_p$ for electron heating in a dense plasma where $n \approx 10^{18} - 10^{20} \text{ cm}^{-3}$ and $z \approx 5$. The heating should proceed until a temperature is reached sufficient to excite the upper operating level without substantially increasing the electron density. The use of short-wave electric pulses does not require the same high degree of initial plasma density typical of light pulses. The above method yields the maximum critical excitation velocity on the order of the collision frequency ν_{eff} between ions and electrons; energy absorbed by the plasma is used for electron heating. Optimal excitation of operating levels of the above type of short-wave laser occurs when electrons are heated to an energy that corresponds to the maximal cross-section, at a time $\Delta t \ll A_{12}^{-1}$, which is smaller than the reciprocal value of the operating transition probability; it is thus feasible to obtain amplification factors $\approx 10-10^3 \text{ cm}^{-1}$ in the vicinity of $\lambda \approx 500\text{\AA}$. The authors calculate inversion excitation during propagation of ultrashort light pulses in plasma. Results suggest that by using a neodymium laser pulse of $\Delta t = 10^{-11} \text{ sec}$ duration and 1 joule energy it is possible to heat plasma of $n_e \approx 2 \times 10^{19} \text{ cm}^{-3}$ and $z=5$ to an energy of $\sim 160 \text{ ev}$. This energy may be optimally used at an $\sim 1.5 \text{ cm}$ length and $\approx 10^{-3} \text{ cm}^2$ cross-section area.

Rezvov, A. V. Effective boundary conditions in the theory of e-m wave penetration into plasma. ZhTF, no. 6, 1972, 1120-1129.

The spatial structure of an e-m field in a semi-bounded plasma is calculated for incidence of a p-polarized plane wave at an angle θ (vector E lies in the plane of incidence), or surface wave propagation along the boundary. The specific case is analyzed of a frequency range satisfying the inequalities $\omega^2 > v^2$; $\omega^2 > v_T^2/c^2 \cdot \omega_p^2$; $\omega - \omega_p > \omega_p v_T^2/c^2 \sin \theta$, which permits omission of the effects of particle collisions. A Maxwellian distribution of particle velocities is assumed. The author proceeds from expressions for Fourier components of the e-m field which were obtained from a simultaneous solution of the Maxwell equation and the Boltzmann kinetic equation.

The spatial distribution of a plasma e-m field includes both plane waves and a spatially anharmonic component, and comprises a superposition of free oscillations. The latter are determined from the analytical properties of permittivity dispersion functions and particle interactions with the plasma surface. Solutions are given for the mirror reflection model and for the conditions of particle diffuse scattering on the plasma boundary. Based on the values obtained for longitudinal and transverse wave amplitudes induced in plasma, the author concludes that the same results may also be obtained by the standard phenomenological method if the boundary conditions of the e-m field components are supplemented or slightly modified. Such effective boundary conditions are outlined by the authors in solving the problem of plane e-m wave incidence on a plasma boundary at the angle θ .

Tyurin, Ye. L., and V. A. Shcheglov.
Radiant heat wave in a moving plasma.
ZhTF, no. 8, 1972, 1586-1590.

The article presents an analytical solution to a problem of heated plasma flow with a preset density and random time dependence of flow velocity $v(t)$. At the boundary $x = 0$, a laser energy flow occurs with a random time form $I_o(t)$. This corresponds to the physical condition when plasma is heated by powerful laser radiation in the energy range of 10--100 joules per pulse, and pulse duration τ which agrees with the gas-dynamical plasma dispersion τ_{gd} , and equals 10^{-9} sec. Plasma heating by two or more pulses is examined which improves the heating quality when the process is essentially unstable and absorption is determined by the number of discharge particles.

Radiation transfer and energy conservation equations are solved for a medium where $n = \text{const}$ and $v \ll c$ at the preset boundary conditions. The solutions describe the process of heat wave propagation in a moving radiation absorbing medium. The solutions are applicable to any form of absorption coefficient K temperature dependence and cover a broad range of initial conditions. Heating of sufficient intensity generates a sharp front wave $x = x_o$, where $\partial t / \partial x$ is maximal and the temperature $T_{fr} = \text{const}$. As a function of current time t and setting time t_s when $dx_{fr} / dt = 0$, two heat wave propagation modes were noted: at $t < t_s$ the heat wave motion is unstable and it propagates into the plasma; at $t = t_s$ the front comes to a stop, and its motion and other wave parameter variations are subsequently dependent on changes in the plasma flow velocity $v(t)$ and radiation energy velocity $I_o(t)$. In other words, when $t \geq t_s$ the heating process becomes stabilized and at the boundary $x = 0$ this leads to equality between plasma radiation energy flow $I_o(t)$ and heat energy flow. Heat wave parameters were computed under two conditions: 1) $v = \text{const}$ is the plasma

flow average velocity under the pulse effect; and 2) $v \sim \sqrt{T_0}$ accounts for an increase in plasma velocity during the heating process. It was proven that variations in velocity in relation to heating had only a slight effect on the time t_s but doubled the heating time. Numerical estimates are given for t_s and the maximum depth of heat wave penetration into plasma x_{\max} , under typical laser heating conditions. At $I_0 = 10^{13} \text{ w/cm}^2$, $n = 10^{21} \text{ cm}^{-3}$, and $v = 2 \times 10^7 \text{ cm/sec}$, the values $t_s = 5 \times 10^{-9} \text{ sec}$ and $x_{\max} = 5 \times 10^{-2} \text{ cm}$ were obtained. At a relatively high pulse energy ϵ expressed in joules per square centimeter, the heat wave possibly approaches the non-transparent plasma layer where $n \geq n_{\text{crit}}$, which leads to the reflection of laser energy from the target.

The solutions obtained by the authors permit estimates of the optimal duration τ_{opt} of single or pulse packets from specific ϵ , n , v and plasma absorption layer thickness values with non-reflecting characteristics and under maximum temperature conditions. It was also demonstrated that only about one half of radiation energy was used for plasma heating, the remainder being dissipated in the plasma.

Zayko, Yu. N., L. I. Kats, N. N.

Kireyev, and S. A. Smolyanskiy.

Electromagnetic wave propagation
in a rarefied plasma in a variable
magnetic field. TVT, no. 2, 1972,
232-242.

The complex index of refraction is calculated for a single-component, spatially homogeneous infinite Lorentz plasma in a spatially uniform alternating magnetic field $\vec{H}(t) = \vec{h}_0 H_0 \cos \Omega t$. Stress vector orientations of stationary and alternating external fields, the magnetic fields and the electromagnetic wave are arbitrary. The alternating magnetic field $\vec{H}_1(t)$ and the induced electric field $\vec{E}_1(t)$ are regarded as strong, and $\vec{E}_2(t) \ll \vec{E}_1(t)$ is the weak electric field of the wave. The response of the system to the plasma electric field is analyzed for $E = \vec{E}_1(t) + \vec{E}_2(x, t)$.

Chastov, A. A. Transmission of a powerful beam in semicolloidal dye solutions. ZhPS, v. 16, no. 4, 1972, 649-653.

Ruby laser beams in semicolloidal dye solutions were investigated under the condition that the size of micelles and the inhomogeneities formed around them was smaller than the beam wavelength. Aluminum chlorophthalocyanine in o-dichlorbenzene, vanadyl phthalocyanine in chloroform, and 1,2-aluminum phthalocyanine in o-dichlorbenzene and quinoline solutions were used. Experiments have shown that with increased radiation intensity the transmissibility of colloidal solutions first rises and then drops; intensities of the order of several Mw/cm^2 produce nonlinear scattering.

The author computed the attenuation of a parallel light beam in a semicolloidal dye solution and concluded that the scattering coefficient has a square-law dependence on radiation intensity. An initial stage of increased transmissibility was traced to the brightening of dye monomers. The dye linear absorption decreased under weak and moderate fluxes and the number of aggregated molecules increased. At strong fluxes the transmission characteristic of the solution dropped and the number of bonded molecules rose from the increased nonlinear scattering. The difference in the transmissibility of semicolloidal solution layers of various thickness is reduced with an increase of radiation intensity. The phenomena discussed are cited as having application in the study of interactions of powerful radiation with absorbing solutions. The author suggests using the factor of a decrease of transmission in semicolloidal solutions exposed to high radiation intensities for detecting tiny concentrations of aggregates, when spectral methods are insensitive.

The average oscillation value for the alternating magnetic field is not derived. When computing the tensor of plasma electric conductivity, the authors based their calculations on the equation of electron motion in a nonrelativistic approximation.

A perturbation theory approximation method is used to solve the specific problem $\lambda = \frac{H_1}{H} \ll 1$. Results yielded: 1) a relationship that determines the plasma conductivity matrix by a value order (the matrix may also be determined by approximations, disregarding perturbation theory); and 2) an explicit expression for the complex plasma refraction index; $n_m(\omega) = n'_m(\omega) + i n''_m(\omega)$. The complex formulas are analyzed for five physically different cases when the vectors k , h_o and h_i are paired perpendicularly or are parallel. Since the final formulas for the complex refraction index are too cumbersome, only those results are given that agree with $|n'_n(\omega) \gg n''_n(\omega)|$.

The left-hand and right-hand wave polarizations are examined. Conditions are established under which resonances occur. The resonances are evidently a function of the alternating magnetic field amplitude, which results in additional resonance points. The signal cutoff pattern is recorded for the five cited physical cases and the two wave polarizations. Conditions are given for the occurrence of windows in some of the cases, i.e. when $n'_n(\omega) = 1$, $n''_n(\omega) = 0$. Exact formulas must be used to determine the complex refraction index. In all cases, plasma brightening becomes feasible due to the position of the magnetic field variable component.

Petukhova, T. M., V. V. Bukhalenkov,
and V. I. Grokhovskiy. Metal surface
condition after laser irradiation. EOM,
no. 4, 1972, 28-31.

An analysis is given of physical and chemical changes in the surface of several iron and steel targets following laser irradiation. The laser used was a type K-3M free-running ruby with 3 millisec., 1.5 j pulses, and focused on the target surface at $f = 10$ mm. A wide range of crater geometries was obtained by profilometer, as listed in Table I.

Table I. Crater Characteristics

Structure type	Material and heat treatment	Crater dia., mm	Crater depth, mm	Max. ejecta ridge hgt., mm	Ejecta range, mm
Perlite	U 12 steel, heated to 850°C , oven-cooled	0.40	0.030	0.060	0.65
	Iron with globular graphite, heated to 890°C , air-cooled	0.30	0.030	0.035	0.75
	Ductile iron, heated to 870°C , air cooled	0.30	0.035	0.040	0.75
Austenite	1X18N8 steel, heated to 1100°C , water quenched	0.30	0.010	0.010	0.40
Martensite	U 12 steel, heated to 850°C , water quenched	0.40	0.030	0.080	0.70
	Iron with globular graphite, heated to 890°C , oil quenched	0.45	0.030	0.040	0.80

Similarities and differences in the crater profiles are discussed; Fig. 1 compares ejecta profiles for austenite and martensite types. Laser hardening effects were also recorded; it was noted that ejecta peaks give anomalously high hardness readings, whereas the base material in some cases suffers a loss in hardness after irradiation. Strain hardening patterns are illustrated, together with data on exoelectron emission variations which can be used to detect phase change in the target material.

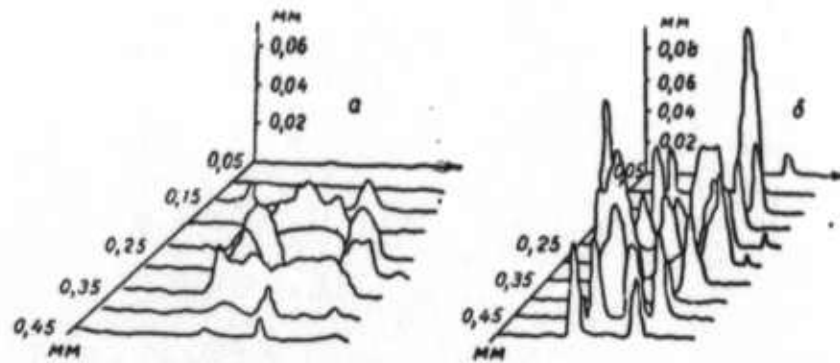


Fig. 1. Relief profiles in the crater region for austenite (a) and martensite (b) targets. Vertical - x 1000, horizontal - x 200.

B. Recent Selections

i. Beam Target Effects

Aksel'rod, I. L., and A. Z. Volynets. Development of a sublimation process in a monochromatic electromagnetic radiation field. EOM, no. 5, 1972, 52-55.

Apanasevich, P. A., and V. G. Dubovets. Theoretical analysis of interaction of high-power polarized radiation with an isotropic resonant medium. ZhPS, v. 17, no. 5, 1972, 796-803.

Batanov, V. A., F. V. Bunkin, A. M. Prokhorov, and V. B. Fedorov. Gasodinamicheskaya struktura plazmennogo fakela, voznikayushchego pri isparenii metallov moshchnym opticheskim izlucheniym (Gas dynamic structure of a plasma flare generated from vaporization of metals by high power optical radiation). AN SSSR, Fizicheskiy institut, Preprint no. 50, Moskva, 1972, 23 p. (KL Dop vyp, 10/72, no. 21613)

Kolomiyets, B. T., E. A. Lebedev, and E. A. Smorgonskaya. Problem of the breakdown mechanism in chalcogenide glass. FTP, no. 10, 1972, 2073-2075.

Rarov, N. N., A. A. Uglov, and I. V. Zuyev. Effect of heat source parameters on the depth and size of surface deformation in the liquid phase. DAN SSSR, v. 207, no. 1, 1972, 83-85.

Rubanov, A. S., Ye. V. Ivakin, and I. P. Petrovich. Relaxation of thermal phase in a lattice. IAN B, Seriya fiz.-mat. nauk, no. 6, 1972, 123-126.

Sklizkov, G. V., S. I. Fedotov, and A. S. Shikanov. Issledovaniye pogloshcheniya izlucheniya Nd-lazera pri nagreve tonkoy misheni (Investigating Nd-laser radiation absorption from heating of thin targets). AN SSSR, Fizicheskiy institut, Preprint no. 45, Moskva, 1972, 20 p. (KL Dop vyp, 10/72, no. 22189)

Vsesoyuznoyeo veshchaniye po fizike vozdeystviya opticheskogo izlucheniya na kondensirovannyye sredy, 2-e. Leningrad, 24-27 April 1972. (Second All-Union Conference on physics of effects of optical radiation on condensed media, Leningrad, 24-27 April 1972). AN SSSR, Fizicheskiy institut, Preprint no. 41, Moskva, 1972, 45p. (KL Dop vyp, 10/72, no. 21609)

ii. Beam-Plasma Interaction

Anan'in, O. B., Yu. A. Bykovskiy, N. N. Degtyarenko, Yu. P. Kozyrev, S. M. Sil'nov, and B. Yu. Sharkov. Obtaining C and Al nuclei in a laser source of multicharged ions. ZhETF P, v. 61, no. 10, 1972, 543-548.

Bass, F. G. Properties of electron plasma in a powerful electromagnetic field. ZhETF, v. 63, no. 5, 1972, 1664-1671.

Norinskiy, L. V., V. A. Pryadein, and L. A. Rivlin. Investigation of optically-initiated directional electrical breakdowns in a gas. ZhETF, v. 63, no. 5, 1972, 1649-1652.

Silin, V. P. Relaxation processes in a parametrically unstable plasma. ZhETF, v. 63, no. 5, 1972, 1686-1697.

2. Effects of Strong Explosions

A. Abstracts

Polyakov, Yu. A., and G. N. Nikolayev.
Radiative heat transfer behind a reflected shock wave in a two-phase flow. IN:
Teplo-i massoperenos, v. 1, part 3.
Minsk, 1972, 265-269 (RZhMekh, 9/72,
9B296)

High-temperature gas-dust mixtures participate in plasmochemical processes, are present in the boundary layer of supersonic-vehicle ablation materials, and form during the propagation of strong shock waves along the ground surface. It is important here to evaluate the influence of the finely dispersed solid phase upon the intensity of gas radiation. Investigation of heat exchange behind a reflected wave was conducted in a shock tube which permitted supersonic shockwaves from 3 to 6 km/sec to be generated in a gas-dust mixture. Dimensions of the low-pressure chamber were: length 4 m, diameter 30 mm. An oxygen-hydrogen-helium mixture was introduced as driver gas into the high-pressure chamber; this mixture was ignited at $P_1 = 20 - 50$ atm. The wave velocity was measured by ionization sensing elements; the state of the gas behind the reflected wave was determined on the basis of the velocity and initial state of the gas by means of the laws of conservation, with account taken of dissociation and ionization. In order to create a two-phase medium, a weighed sample of Al_2O_3 powder was introduced into the shock tube from a dosing cylinder.

Golovachev, Yu. P., and F. D. Popov.
Calculation of supersonic viscous gas flow
around blunt bodies at high Reynolds
numbers. ZhVMMF, v. 12, no. 5, 1972,
1292-1303.

A solution to a supersonic viscous gas flow problem is obtained on the basis of simplified equations of mass, momentum, and energy continuity. The equations describe the total flow in front of a blunt body, since separate treatment of the inviscid flow and the boundary layer is inadmissible in some practically important cases of supersonic flow. The gas flow calculated therefore encompasses the total shock layer from the shock wave, which is assumed to be a discontinuity surface, up to the body surface. The initial set of equations expressed in spherical coordinates r and θ is simplified by transforming the shock layer into a rectangular region expressed in spatial variables

$$\begin{aligned}x &= \frac{\ln(1+H\xi)}{\ln(1+H)}, & y = \theta, \\ \xi &= \frac{r - G(\theta)}{F(0,t) - G(0)}, & H > 0.\end{aligned}\tag{1}$$

A rectangular grid is introduced, and the simplified set of equations is represented by difference equations with second-order approximation and the weight α . The nonlinear set of equations obtained can be used to calculate flow at a considerable distance from the symmetry axis, since the density ratio across the shock wave can be arbitrary. The set of equations is solved by iteration. Each successive iteration deals with a set of linear equations, and in the iteration process the set of difference equations is broken down into independent subsets along individual radial lines. Each subset is solved by successive elimination of matrix vectors. The gas dynamic parameters and the new shock wave position are determined along all

radial lines. Iteration is normally repeated 2-3 times, until the relative variations of all functions in any grid node start to decrease for two time layers and the maximum variation is $<\Delta t \times 10^{-3}$. The method is illustrated by calculation of perfect gas flow around a thermally-insulated sphere at $M_\infty = 2$ and $Re = 5 \times 10^2 - 10^5$.

Shvets, A. I. Flow around a body with base injection. IN: Sbornik Nauchnaya konferentsiya. Institut mekhaniki Moskovskogo universiteta, 22-24 May 1972. Moskva, 1972, 25-26 (RZhMekh, 9/72, no. 9B477). (Translation)

It was established that a weak injection into the stagnation region in a subsonic flow does not increase base pressure. The base pressure in supersonic flow peaks at a relative air blowing rate of about 1%.

Blagosklonov, V. I., and A. N. Minaylos. Supersonic ideal gas flow around a circular cylinder. IN: Uchenyye zapiski TsAGI, v. 3, no. 2, 1972, 130-134. (RZhMekh, 9/72, no. 9B460) (Translation)

Theoretical numerical data are presented on flow around a cylinder at Mach numbers in the 1.5-1,000 range and 1.05 to 1.66 gas specific heat ratios. Empirical similarity criteria for flow characteristics are given, permitting the data to be presented in analytical form.

Gilinskiy, S. M., T. S. Novikova,
and V. B. Taranchuk. Two-dimensional
nonstationary supersonic flow around a
body by hot gas mixtures. IN: Sbornik.
Nauchnaya konferentsiya. Institut mekha-
niki Moskovskogo universiteta, 22-24 May,
1972. Tezisy dokladov, Moskva, 1972, 13 -
14 (RZhMekh, 9/72, no. 9B458)(Translation)

Nonstationary spiking conditions during high-velocity motion
of a body in a combustible gas mixture are analyzed. An approximate solution
is obtained to the problem of hypersonic flow around a blunt body. Kinetic
models are applied in the vicinity of the stagnation boundary with distributed
heat transfer and heat release at the flame front. An analytical and
numerical investigation is conducted by the method of "truncated distributions".

Afonina, N. Ye., and V. G. Gromov.
Investigation of supersonic viscous flow
of a CO₂ gas mixture around a body. IN:
Sbornik. Nauchnaya konferentsiya. Institut
mekhaniki Moskovskogo universiteta, 22-24
May, 1972. Tezisy dokladov. Moskva, 1972,
6. (RZhMekh, 9/72, no. 9B461)(Translation).

Theoretical data are given on the viscous flow of a CO₂-N₂
gas mixture at R numbers in the 10^{2.5} to 10^{5.5} range in the vicinity of a
stagnation streamline. Calculations are performed based on a set of
equations which were derived by the method of "truncated distributions" as
a single-term approximation of a complete set of Navier-Stokes equations.

Bogolyubskiy, I. L. Hypersonic radiant gas flow around a pointed cone. IN: Trudy XV i XVI nauchnykh konferentsiy Moskovskogo fiziko-tehnicheskogo instituta, 1969-1970. Seriya Aerofizika i prikladnaya matematika. Part 1. Dolgoprudnyy, 1971, 9-23 (RZhMekh, 9/72, no. 9B464)(Translation)

A solution to the problem of flow around a pointed cone is obtained in a first approximation using the k- parametric expansion of the equations for an inviscid, radiating and absorbing gas. The parameter is $k = \rho_\infty / \rho_s$, where ρ_∞ and ρ_s are the densities of the oncoming gas and the gas behind a shock, respectively. Calculation is performed for a multistep model of radiating gas flow around a cone with a vertex half-angle of 30 to 60 degrees. Temperature and enthalpy fields are determined, a shock wave profile is plotted, and radiant flux distributions along the cone generatrix are obtained.

Zak, L. I., and V. A. Levin. Problem of strong surface injection in supersonic flow around a body. IN: Sbornik. Nauchnaya konferentsiya. Institut mekhaniki Moskovskogo universiteta, 22-24 May, 1972. Tezisy dokladov. Moskva, 1972, 17. (RZhMekh, 9/72, no. 9B466) (Translation)

The problem is analyzed of supersonic flow around a plate, a wedge, and a cone of finite dimensions in the presence of a strong injection of a compressible or noncompressible fluid. Allowance is made for conditions at the trailing edge.

Gershbeyn, E. A. Hypersonic flow around a blunt body under strong injection. IN: Sbornik Nauchnaya konferentsiya. Institut mekhaniki Moskovskogo universiteta, Moskva, 22-24 May, 1972. Tezisy dokladov. Moskva, 1972, 12. (RZhMekh, 9/72, no. 9B467)
(Translation)

A solution based on a hypersonic approximation is obtained to the problem of multicomponent gas flow in a shock layer around flat or axisymmetric bodies, with intensive injection of extraneous gases.

Gorinov, A. S., and K. M. Magomedov.
Application of a boundary layer decomposition method to calculation of chemically-non-equilibrium, viscous gas flow. IN: Trudy Konferentsii Moskovskogo fiziko-tehnicheskogo instituta, 1970. Seriya Aerofizika. Prikladnaya matematika. Moskva, 1971, 3-13. (RZhMekh, 9/72, no. 9B468)(Translation).

The steady supersonic flow is analyzed of a chemically-nonequilibrium viscous gas around the front surface of a blunt body near the stagnation streamline. The initial set of equations is simplified by the assumption of a thin compressed shock layer. The boundary conditions are formulated by a unified Rankine-Hugoniot relation at the shock wave and a condition of nonpenetration through a nondisintegrating surface. In view of the difficulties in solving the derived system by successive approximations of the matrix, or by the method of adjustments, the authors propose to split

the system, at the expense of deriving a more complicated algorithm, into weakly-correlated pairs of equations which can be solved by the usual successive scalar approximations. The method is closely related to the method of boundary layer corrections of Vishik and Lyusternik, but with no expansions. As a rule, the presence of a small parameter is not required. As an illustration of the method the nonequilibrium air flow around a spherical blunt body is calculated over a wide range of Reynolds numbers and with allowance for six reactions. It is noted that the boundary layer and relaxation region of electrons are significantly thicker than those of neutral particles.

Savinov, K. G. Investigation of three-dimensional supersonic flow around triaxial ellipsoids. IN: Sbornik Nauchnaya konferentsiya. Institut mekhaniki Moskovskogo universiteta, 22-24 May 1972. Moskva, 1972, 33 (RZhMekh, 9/72, no. 9B471). (Translation).

Numerical data are presented on three-dimensional, supersonic, perfect gas flow around the nose of a triaxial ellipsoid. Particular attention is devoted to flow without a symmetry plane. The gas dynamic parameters distribution over the body and across the shock layer is shown. Positions of the shock and acoustic surfaces are indicated.

Pilyugin, N. N. Radiant heat flux distribution on a spherical surface in hypersonic inviscid radiant gas flow. IN: Sbornik Nauchnaya konferentsiya. Institut mehaniki Moskovskogo universiteta, 22-24 May, 1972. Tezisy dokladov. Moskva, 1972, 30. (RZhMekh, 9/72, no. 9B919).
(Translation)

A theoretical study is presented of the stabilized, uniform hypersonic flow of an inviscid, radiant perfect gas around a sphere. An approximation of volume deexcitation is applied. Analytical expressions in a first approximation are derived for all gas dynamic parameters.

Moshnenko, Yu. I., and V. A. Velichkin.
Aerodynamic heating dispersion from a lifting shell in supersonic flow. IN:
Teplo-i massoperenos. v. 1, part 3. Minsk,
1972, 233-238 (RZhMekh, 9/72, no. 9B910)
(Translation)

In order to determine the scattering characteristics of the temperature conditions of lifting shells, the Monte Carlo method of statistical tests is used; this method is based on the multiple realization of a theoretically calculated model for the thermal load of a structure with random sampling of the initial data. An investigation was conducted of the aerodynamic heating of a weakly conical shell, reinforced by a set of force stringers, under conditions of supersonic streamline flow within the range of the parameters $2 \times 10^6 < R < 3.4 \times 10^8$, $0.17 < T_w/T_e < 0.9$, and $M > 1.3$.

Nikolayev, F. A., Yu. V. Novitskiy, V. B.
Rozanov, and Yu. P. Sviridenko. Fluctuation characteristics in dense plasma of high current discharges generated by electric explosion of metal wire in a vacuum. ZhETF, v. 63, no. 3, 1972, 844-853.

Fluctuation characteristics were studied in a plasma generated by vacuum discharge of capacitors (discharge geometry was straight Z-pinch, $W_{\text{stored}} = 22.5 \text{ kJ}$, $\tau_{\text{disch}} = 120 \mu\text{sec}$, and $I_{\text{max}} = 220 \text{ kA}$) across lithium wires with initial diameters $d_0 = 0.17, 0.34$, and 1.0 mm . The random fluctuations of plasma parameters which occur during the initial $35-40 \mu\text{sec}$ were determined by correlation processing of signals recorded by magnetic sensing elements, and by dimensional analysis of magnetohydrodynamic equations. In addition to their independent value, such data make it possible to accurately analyze integral discharge characteristics. Both the correlation of oscilloscope traces of local magnetic fields and the theoretical analysis revealed a discharge turbulence during the first quarter period. Plasma structural and luminescence inhomogeneities during this period attain a mean linear dimension of $\sim 1 \text{ cm}$ and propagate through the plasma at sonic velocity. The plasma mean density ρ and temperature T fluctuations may be of the order of $1.7 \times 10^{-5} \text{ g/cm}^3$ and 3 eV for a 0.17 mm wire. Plasma turbulence decreases, bunch dimension increases, and their velocity decreases when the wire diameter is increased. Instabilities generated in a dense ($n = 10^{17}-10^{18} \text{ cm}^{-3}$), optically transparent plasma generate and sustain turbulent discharges. Turbulence dissipates after $\sim 40 \mu\text{sec}$ owing to instability decay. It is suggested that plasma line spectra are directly correlated with decay of superheated instabilities. Comparison of the theoretical T , ρ and p fluctuations data with previously determined mean values of these parameters led to the conclusion that plasma turbulence does not qualitatively affect the discharge characteristics.

Lebedev, S. V., A. I. Savvatimskiy, and
 Yu. B. Smirnov. Electrical explosion method
and measurement of heat of fusion and electrical
conductivity of refractory metals. ZhTF, no. 8,
 1972, 1752-1760.

Earlier measurements by the authors (TVT, no. 3, 1971, 635) of the heat of fusion E_f and electrical resistivities ρ_s and ρ_ℓ of refractory metals are here extended to Ir and Au. The method of exploding wires was again used. The wire resistance $R(t)$ and energy $E(t)$ absorbed by the wire during melting were evaluated from oscilloscope measurements of the voltage variations across the wire ($V_R(t)$ and a calibrated resistance $V_r(t)$). Iridium wire specimens, 1-2 cm long and ~ 0.1 mm in diam, and gold wires 1-6 cm long and 0.1 mm in diam were exploded in air at atmospheric pressure using $(2.5-5.6)\times 10^{10}$ a/m² rectangular current pulses, and in air or water using 4.25×10^{10} and 1.3×10^{10} a/m² pulses, respectively. The experimental E_f data for Au (Table 1) agree, within experimental error, with known experimental values from the literature. The Au experimental ρ_s and ρ_ℓ data differ from

Table 1. Ir and Au heats of fusion $E_{1, 2}$ measured by the electrical explosion method.

Metal	Number of samples	$E_{1, 2}$ mean value, j/g	% Deviation from the mean		Probable systematic error, %
			Arithmetical mean	Maximum	
Ir	19	200	2	5	3
Au	17	70	1.5	3.5	3

the most reliable literature data obtained in a slow process (Table 2).

Table 2. Resistivity of solid (ρ_s) and liquid (ρ_l) Ir and Au at mp

Metal Source	Metal characteristics		Number of samples tested	ρ_s , μohm cm	$\delta^1)$ %	ρ_l , μohm cm	$\delta^1)$ %	$\frac{\rho_s}{\rho_l}$
	purity, %	ρ at room temperature μohm . cm.						
Ir Authors	99.9	6.79	19	70.3	1.3	92.0	2	1.31
Au data	99.99	2.235	17	13.1	1.2	29.1	1.2	2.22
Au Literature	-	2.316	3	13.50	-	30.82	-	2.28
Au data	99.95	-	-	(13.68) ²	-	31.2	-	(1.28) ²

1) Arithmetic mean error. Possible systematic error in authors' data - 1.5%.

Corresponding data for other metals obtained by the same method are close to the ρ_s and ρ_l data in the tables. E_f , ρ_s and ρ_l data for Ir were not found in the literature. The second break on the $I_{ph}(t)$ oscilloscope trace of Au did not coincide with the second break on the $V_R(t)$ trace. This was attributed to wire nonhomogeneity and did not justify a correction of the E_f data obtained from V_R oscilloscope traces. It is concluded that the E_f data obtained by the method of exploding wires coincide with the equilibrium values, confirming the applicability of the method to measurements of E_f and high-temperature ρ of refractory metals. The accuracy of the measurement is estimated to be 2-3% for ρ and ~5% for E_f .

Sychev, V. V., A. D. Kozlov, and G.

A. Spiridonov. Thermodynamic properties

of air in the 150-1000° K temperature

interval at pressures to 1000 bar. IN:

Sbornik.Teplofizicheskiye svoystva veshchestv

i materialov. Moskva, Izd-vo standartov,

no. 5, 1972, 4-20. (RZhF, 8/72, no. 8 Yel5)

(Translation)

A new equation of state for air describes all reliable experimental thermal data with an error $\leq 0.1\%$ of the compressibility factor $z = pv/RT$. The following thermodynamic properties of air are calculated within the given temperature range: specific volume, enthalpy, specific heats C_p and C_v , entropy, sound velocity, the adiabatic Joule-Thomson effect, volatility, coefficients of volume expansion and isothermal compression, the thermal pressure coefficient, and the adiabatic exponent.

Lomakin, B. N., and V. Ye. Fortov.

Dynamic method for investigation of

the equation of state of a nonideal cesium

plasma. DAN SSSR, v. 206, no. 3, 1972,

576-579.

A comparative analysis is made of P-V isentropes, isotherms, and constant enthalpy curves calculated for a highly imperfect cesium plasma, using an experimental equation of state in caloric form (cf. Feb. 1972 Report p. 67). The dynamic method for measuring the shock wavefront velocity $D = 1.4-2.1 \text{ km/sec}$ and plasma density $\rho = V^{-1}$ at initial $P_0 = 0.15-$

0.5 bar is described briefly.* In principle, the method is based on the compression and irreversible heating of the substance in the shock wave-front. In view of the limitations to imperfect plasma diagnostics, the method takes advantage of the correlation between kinematic parameters of the shock wave propagation and the thermodynamic characteristics of the shock-compressed medium. The experimental range of parameters was extended by recording the state behind the front of a reflected shock wave. The measured parameters were used to calculate the equation of state and temperature T behind the shock wavefront. The experimental P-V isotherms plotted against the isotherms, calculated in a perfect gas approximation, indicate that experimental P exceeds calculated P. Analysis of the isotherms and the constant enthalpy curves led to the conclusion that the contribution of the discrete spectrum of the partially-ionized plasma to the equation of state is greatly diminished as the effect of the free charges interaction on thermodynamic functions and the ionic equilibrium is lessened. The absence of kinks on the experimental P-V isentropes points to the absence of phase transitions in an imperfect cesium plasma over the range of parameters studied. It is highly improbable that there is a two-phase region in the reflected shock wave, because the slope of isentropes is nearly identical to that in the approximation of a perfect gas.

* A more extensive description and essentially the same analysis of the experimental data were given in a longer paper previously published in ZhETF, v. 63, no. 1, 1972, 92-103.

Klyatskin, V. I., and V. I. Tatarskiy.
Statistical theory of light propagation in
a turbulent medium (Review). IVUZ
Radiofiz, no. 10, 1972, 1433-1455.

Theoretical research data (1958-1972) on electromagnetic wave propagation in a medium with large scale random inhomogeneities are comprehensively reviewed. Some 90% of the source materials are of Soviet origin and include numerous publications of the present authors. The inadequacy of the smooth perturbations method (SPM) for describing the strong fluctuations effect was initially established experimentally by Gracheva and Gurvich, and later confirmed by these and other Soviet authors. Theoretical research was subsequently oriented towards the development of a diffusion approximation method to describe wave propagation in an inhomogeneous medium. This research trend is discussed and basic stochastic wave equations, such as scalar wave and parabolic equations, are presented. The derivation of these equations is outlined on the basis of a random diffusion approximation of wave propagation in a medium with large scale inhomogeneities.

The solution of the parabolic wave equation is shown to obey certain exact conditions, e.g., a causality condition. In the first or random diffusion approximation, closed integral equations for the wave field statistical moments $M_{n, m}$ can be obtained, assuming the longitudinal correlation radius $\ell_{||}$ of the fluctuating permittivity component $\tilde{\epsilon}$ is negligible ($\ell_{||} = 0$). This assumption is equivalent to substituting the delta-correlation B_{ϵ}^{eff} for the true correlation function B_{ϵ} of the refractive index, which describes the statistical characteristics of $\tilde{\epsilon}$ in a Gaussian distribution of the refractive index fluctuations. Using a Gaussian distribution and delta-correlation, the authors reduced the closed integral equations to a differential equation.

Tatarskiy has derived an equivalent equation of the Einstein-Fokker type for the characteristic functional of the field function $u(x, \rho)$, which describes the field statistically. It follows that the wave propagation approximation in a medium with Gaussian, delta-correlated fluctuations of $\tilde{\epsilon}$ can be assimilated to a diffusion approximation. The authors applied successive approximation to find a more exact solution of the parabolic wave equation. Using the Furutsu-Novikov formula, a closed equation was obtained in a second approximation of the field $\langle u \rangle$. The solution U_2 of the second approximation differed no more than 2.5% from the exact solution

$$\bar{u}(x) = u_0 \exp[-\mu(\tau - 1 + e^{-\nu})], \quad (1)$$

for $\mu = k^2 l^2 \sigma_{\epsilon}^2 / 4 = 0.2$, where l is the correlation radius of $\tilde{\epsilon}$, $k^2 = \omega^2 / C^2 \langle \epsilon \rangle$.

The boundary conditions of the first approximation are deduced from analysis of the second approximation. The conditions show that the first or diffusion approximation is applicable to strong field fluctuations. Using the radiation transfer equation for a small angle approximation, Dolin has developed a linear differential equation of the mutual coherence function Γ_2 , which is analogous to the differential equation obtained by the authors from the cited equation of $M_{n, m}$ in a diffusion approximation. Dolin solved the equation for Γ_2 by the method of characteristics. Kon and Tatarskiy extend this solution to partially coherent sources and arrive at a simple formula for Γ_2 in the case of a plane incident wave. Dolin's solutions for Γ_2 and the averaged wave intensity are compared with the experimental 1971 data of other Soviet authors. A statistical description of light beam amplitude and phase fluctuations was attempted by the SPM and diffusion approximation methods. Using the latter method, Klyatskin derived an expression for amplitude level fluctuations σ_x^2 which disagrees with the experiment. This discrepancy is explained in terms of a geometrical

optics approximation. Zavorotnyy and Klyatskin have recently shown that amplitude and phase statistical characteristics are determined by those of rays. The amplitude level X and phase gradient S are described by a single dynamic ray trajectory equation with boundary conditions. This equation shows that ray propagation is not a random diffusion process. Calculation of X and S in diffusion and geometrical-optics approximations is correct only if certain boundary conditions for a turbulent medium are satisfied.

Berlyand, O. S., V. N. Petrov, and D. A. Severov. Long range propagation of [radioactive] impurities for a vertical diffusion coefficient varying in time and altitude. FAiO, no. 9, 1972, 994-997.

Near-surface concentration q_0 of radioactive impurities was evaluated as a function of vertical diffusion coefficient K_z variation in time and altitude. Such an evaluation is related to the solution of problems of long range propagation of radioactive impurities. Diurnal variations of K_z are described by the function

$$K_z = K_{z_0} (1 - \epsilon \cos \omega t). \quad (1)$$

where K_{z_0} is the nocturnal diffusion coefficient, $\omega = 2.62 \times 10^{-1}$ /hr is the earth angular rotation velocity, and ϵ is the amplitude of K_z variation. Calculation of K_z in the near-surface atmospheric layer was based on selective vertical concentration profile $q(z)$ data, measured by Soviet authors in a radioactive inert gas stream from underground nuclear explosions. The average K_z values calculated from the tabulated data are 10, 12, 16, and $40 \text{ m}^2/\text{sec}$ during spring, summer, summer under convection conditions,

and winter, respectively. The ϵ value was accordingly assigned 0, 1, 2, and 3 values. Using the K_z and ϵ values thus obtained, $q(0, h, t)$ profiles were calculated by solving the diffusion equation. The $q(0, h, t)$ plots (Fig. 1) show that q_0 may decrease by a factor of 2 to 3 when ϵ varies.

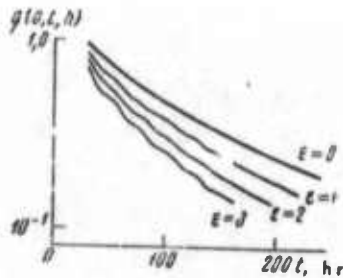


Fig. 1. Near-ground volume concentration versus time at different ϵ values.

The effect of K_z variations on $q(x, y, z, t, h)$ at the ground below the impurities source at an altitude h was evaluated by solving a set of diffusion equations for q_2 at $z = 0$ and taking horizontal diffusion and wind direction into account. The plotted $q(t)$ data show that during the first 2-3 days the near-ground impurities concentration and consequently the fallout density vary significantly, when K_z above $z^* = 0-0.5$ increases by an order of magnitude and $h = 2-4$ km.

Alimov, V. A., and G. P. Komrakov.

Fading of scattered signals during an ionospheric F_{sp} event. IVUZ Radiofiz., no. 10, 1972, 1581-1583.

Results are reported of F-spread observations carried out in March 1971 by r-f pulse probing of the ionosphere. Other researchers have concluded that pure ionospheric scattering of radiowaves during F-spreading is insignificant. The experimental procedure used by these researchers included selection of a receiver bandwidth equal to the spectral width of the probe pulse and nonpolarized reflected signal reception, which apparently had a significant error effect on the data obtained. The present authors therefore used revised experimental procedures to test for F_{sp} effects. The probe pulse had a 50 Hz repetition rate and 100 μ sec. duration, the receiver bandwidth was 30 kHz, and the 2.4 MHz reflected signal was polarized at the receiving end. The time-sweep of the scattered signal was displayed on an oscilloscope and recorded by camera. The distribution function W(R) of the scattered signal fluctuations was plotted (Fig. 1) for a fixed ionospheric height and 1 min observation period. Fig. 1 shows that experimental

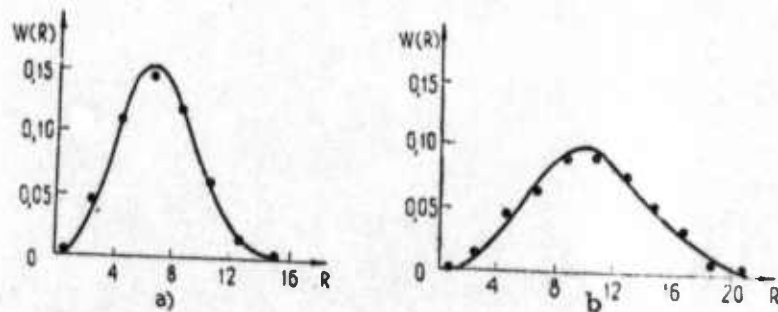


Fig. 1. Amplitude distribution of a scattered signal extended over ~ 300 km: a) leading edge, b) mid-signal. Solid lines - Nakagami's m-distribution for $m = 2$ and $R^2 = 54.86$ (a) or 144.4 (b). Points are experimental values.

$W(R)$ values are well approximated by Nakagami's m-distribution for $m \approx 1.1-2.5$ ($m = R^2 \sqrt{R^2 - R'^2}$, where R' is the mean square fluctuation of signal amplitude). The m-distribution is for a signal composed of m statistically-independent rays with random phases, i.e., m separate, completely diffuse beams. Previous experimental $W(R)$ data obtained under conditions of F-spread may also be considered as amplitude fluctuation m-distributions of a composite multiple-beam signal with $m \approx 1-5$. The presence of a "mirror" component in the reflected signal may be interpreted as the result of averaging of strong amplitude fluctuations of the completely diffuse beams. This interpretation also adequately explains other research data on the inhomogeneous ionosphere structure, such as the correlation between F-spread and fading of radio signals from discrete sources, and the experimental angular spread of the reflected signal spectrum.

Kapitanov, V. A., Yu. V. Mel'nichuk,
and A. A. Chernikov. Spectral configuration
of radar signals from precipitation. FAiO,
no. 9, 1972, 963-972.

A theoretical and experimental study is presented of radar echo spectra from precipitation. The frequency range studied corresponds to a spectral density $S_E(f)$ below the -15 to -20 db level in reference to the spectral maximum, at the spectral edge. The study was prompted by advances in radar technology and the increased stability of powerful SHF generators. Analysis of spectral edge formation indicated that collisions in the HF range (above 150-200 Hz), between scattering particles, e.g., rain drops or snow flakes, may have a significant effect on the spectral configuration. Collisions may be caused either by a spread of the particle fallin rate I or air turbulence. For an intermediate $I = 3 \text{ mm/h}$, it was estimated that $S_E(f)$ begins to decrease at $f^* \sim 15 \text{ Hz}$ in accordance with the f^{-4} law,

owing to the effect of turbulent fluctuations of particle velocity. At a small elevation angle the effect of particle vibrations may be significant in the range from 30-50 and 100-200 Hz. Two other factors (coalescence of raindrops and wind-caused changes in the number of scatterers in a given volume) are suggested as affecting the spectrum configuration to a lesser extent. The experimental 3.2 cm radar echo spectra obtained from rain and snowfall of intermediate I (1-4 mm/h) and at small elevation angles up to 6° , closely fit a Gaussian curve $S(f) \sim f^{-6}$ within the range of $S_E(f)$ from the maximum to about the -30 db level, corresponding to $f \sim 100$ Hz. It is assumed that the Gaussian approximation adequately describes the radar echo spectra down to the -40 db level. At lower levels, a noticeable deviation of the spectra from a Gaussian curve is expected with spectral edge formation. The data obtained have application in Doppler radar measurements of particle size distribution in clouds and precipitation.

Arsen'yan, T. I., F. F. Pashkov, A. A. Semenov,
A. A. Tishchenko, and N. N. Rimskiy. Inter-
ferometric investigation of phase fluctuation of
coherent optical radiation in the atmosphere.

IVUZ Radiofiz., no. 8, 1972, 1228-1232.

Atmospheric phase fluctuations of laser radiation were investigated at $\lambda = 0.63 \mu$ and beam radius = 1.2 cm. The beams were generated using a Zhamen-type interferometer. A microphotometer measured a visible interference image recorded on film, which was directly related to the structural function of phase fluctuations under normal distribution conditions. Signal characteristics were statistically analyzed in relation to the beam separation base ρ of the interferometer. Statistical

parameters of a real atmosphere were simultaneously determined by an apparatus for quick-response measurements of temperature pulsations. The structural constant of temperature fluctuations C_t^2 can be used to accurately determine the structural constant of the air reflection factor C_n^2 , which is related by formulas to the structural function of phase fluctuation $D\varphi(\rho)$:

$$C_n^2 = \frac{80 \cdot 10^{-6} \rho}{T^2} C_t^2 \quad \text{and} \quad D\varphi(\rho) = 0,73 C_t^2 k^2 L \rho^{5/3} \left(1 - \frac{5}{6} \frac{L^2}{k^2 a^4} \right),$$

where k is the wave number, L - path length, a - beam radius, and $C_{2\epsilon}^2 = 4C_n^2$. Measurement data on a 120-meter path, under conditions in the formulas, are compared with theoretical data computed for $D\varphi$ in Table 1.

$C_t^2 (cm^{-2/3})$	$\rho (cm)$	0,6	1,0	1,5	2,0	2,5	3,0
$8,8 \cdot 10^{-16}$	$D\varphi$ theor.	0,03	0,07	0,16	0,25	0,38	0,54
	$D\varphi$ exper.	0,03	0,07	0,16	0,25	0,31	0,4
$4,4 \cdot 10^{-15}$	$D\varphi$ theor.	0,16	0,38	0,74	1,21	1,75	2,34
	$D\varphi$ exper.	0,16	0,38	0,74	1,16	1,68	2,2
$6,3 \cdot 10^{-15}$	$D\varphi$ theor.	0,24	0,55	1,08	1,77	2,55	3,39
	$D\varphi$ exper.	0,24	0,51	1,06	1,51	2,28	3,0

Table 1. Experimental and theoretical data for the $D\varphi$ structural function on a 120-meter path.

Data analysis shows that at $\rho \leq 2$ cm the relationship $D \sim \rho^{5/3}$ is obtained. Interferometric methods were also used to analyze the correlation coefficients and radii and their dependence on path length and lateral velocities. Measurements were taken on 7.5 to 20 meter paths and 1.5 meters above the base. Experimental data obtained by the authors show a strong dependence of phase variations on lateral velocities: the experimental range of variations in time correlation radii of phase fluctuations was 0.05 to 0.6 sec, decreasing with an increase in transfer velocities. With decreased path length, the time correlation radii increased.

The main advantage of the cited method is the high accuracy of statistical signal characteristic determinations. The structural function of phase fluctuation in the first series of experiments was determined with an error not exceeding 4%. In the second series of experiments, the error in recording the positional variations of the interference band on a continuous film (speed from 2 to 4 cm/sec) was 5 to 7%. A drawback of the method is the inapplicability to measuring phase fluctuations in excess of the π value; the method is hence applicable to small fluctuations only.

Magnitskiy, B. V., and B. A. Tverskoy.

Vertical currents in conjugate points.

Geomagnetizm i aeronomiya, no. 4, 1972,
708-711.

The effect on an asymmetric current loop of various conductivities in the ionospheric E-layer and the northern and southern polar caps is analyzed. The work continues that of the co-author Tverskoy (DAN SSSR, 188, 1969, 575, and NIIYaF MGU Preprint 70-337-100) on sub-storm processes and current generation in the magnetosphere in a region of trapped radiation, and the relationship of these currents to polar cap ionospheric currents. Calculation assumptions include a loop current characterized by drift polarization, charges compensated by currents along

magnetic field lines of force, and current contact through the E-layer. The magnetic field was considered to be near-dipole, and a plasma cloud was assumed to be generated by hot protons and cold electrons in an equatorial plane intersecting lines of force to the ionosphere at high latitudes. Proton and electron characteristics are described by continuity equations for distribution functions. The proton continuity equation allows for magnetic and electrical drift; the electron continuity equation allows for the electrical drift and the electron current density. Solutions to the equations yield zero harmonics for the longitudinally-asymmetric current density propagating from one hemisphere to the other and a related DP2 system. The first harmonics in a given expression define the current density propagating along magnetic lines of force and limited from the north and south by Hall electric currents which develop in the ionosphere during a DP1 system with an accompanying bay. For numerical analysis of the bay first harmonic of electron current density $j_{\parallel}^{(1)} - j_{\perp}^{(1)}$, an arbitrary potential difference amplitude of 15 kv is used. Assuming that the peak coordinate of the longitudinally-symmetric portion of the proton pressure is 5, the E-layer thickness is $3 \cdot 10^6$ cm, and the Peterson conductivity is $10 \cdot 10^5$ esu for the Northern and $2 \cdot 10^5$ esu for the Southern hemispheres, it is determined that the current density propagating from one hemisphere to the other during a bay is ~ 1 esu, which agrees with the current density value associated with an ionospheric plasma reported by the co-author Tverskoy (NIIYaF MGU Preprint 70-337-100).

Kopytenko, Yu. A., O. M. Raspopov, V. A.
Troitskaya, and R. Shlish. Analysis of
stable geomagnetic pulsations of Pc4 type
using network observations. Geomagnetizm
i aeronomiya, no. 4, 1972, 720-726.

Spectrum analysis data are given for Pc4 pulsations within the magnetic conjugate points of Sogra ($\Phi = 57.5N$, $\Lambda = 122$ deg) and Kergelen ($\Phi = 58S$, $\Lambda = 123.7$ deg) and from three Northern Hemisphere network stations located approximately in the same meridian:

Lovozero ($\Phi = 63N$, $\Lambda = 116.4$ deg),
Suysar' ($\Phi = 57N$, $\Lambda = 113$ deg), and
Borok ($\Phi = 53N$, $\Lambda = 114$ deg).

Pulses were recorded at all stations using identical equipment (scan: 6 mm/min, sensitivity: $0.14 \gamma/mm$ along H and D horizontal components). Magnetogram data were processed on 16 Pc4 pulsation events in 1966, periods II, III, and IV, and 1964, period IX. Six of the clearest of these were selected for spectrum analysis. Pulsation event transcriptions for 1966, periods II-IV and VII-XII, and for 1968 from Sogra and Kergelen were also analyzed, for a total of 50 pulsation events. A general conclusion from the analysis is that the Pc4 pulsations are a local phenomenon on the earth surface as well as in the magnetosphere, since pulsation amplitude and polarization vary substantially over distance of ~ 500 km. The pulsation total horizontal vector value varies concurrently within a network of remote stations during a Pc4 event, and normally increases at high latitudes. Maximum amplitude pulsation events were occasionally observed at medium latitudes. Most of the spectral density maxima were observed during like periods at all stations; but the H and D components relationship of these maxima is a function of the pulsation polarization characteristics at the individual stations. The spectral density maxima position may vary during a given Pc4 event. The pulsation amplitude, periodicity, direction of horizontal vector rotation, and spectral maxima position varied synchronously within

the conjugate points; also the q-factor increased during high amplitude pulsations.

Vinogradov, A. I., A. L. Devirts, E. I.
Dobkina, B. I. Ogorodinkov, and I. V.
Petryanov. Stratospheric concentrations
of C¹⁴ in 1967-1969. DAN SSSR, v. 205,
no. 4, 1972, 824-826.

Radioactive carbon levels over the Central European sector of the USSR between 1967 and 1969 were measured in-flight by aerostats at altitudes from 12.5 to 31 km. During the flights CO₂ was frozen for one hour in a heat exchanger-collector cooled by liquid nitrogen. The CO₂ was defrosted postflight and placed in bubblers containing a 20% solution of KOH. The CO₂ gas absorption was almost total in the first bubbler, since CO₂ was only rarely observed in a second series-installed bubbler. BaCO₃ was precipitated, screened, scrubbed, and after drying, suspended to determine the amount of CO₂ recorded during the flight. Specimens were maintained in hermetic polyethylene containers prior to radiometric analysis. The C¹⁴ levels were determined by gas or scintillation analyses as a function of the precipitated BaCO₃. The resulting C¹⁴ beta-particle measurement error rate was within 1 to $\pm 2\%$. Radioactive CO₂ data at various altitudes are presented in Table 1 and Figure 1. The experimental C¹⁴ concentration data for the upper and lower stratosphere reflect a systematic reduction of atmospheric CO₂ radioactivity since the 1961-62 nuclear test explosions despite the continuing inflow of C¹⁴ into the upper layers. The radioactive carbon concentration level at an altitude of 25 km has decreased by a factor 4.8 in 1968 and 5.7 in 1969 from the C¹⁴ levels in 1 g of air reported for the stratosphere in the Northern Hemisphere in 1963 by Feeley et al (Tellus, 18, no. 2, 1966, 316). Results also yield a CO₂ half-life in the upper stratosphere of about five years.

(1)	(2)	(3)	(4)	(5)	(1)	(2)	(3)	(4)	(5)
Лабора- торный номер пробы	Дата отбора	Сред- няя высота полета, км	Избыток количества атомов C^{14} в 1 г воздуха, 10^{-5}	Счет- ное вещес- тво	Лабора- торный номер пробы	Дата отбора	Сред- няя высота полета, км	Избыток количества атомов C^{14} в 1 г воздуха, 10^{-5}	Счет- ное вещес- тво
Mo-742	07.10.67	30,7	235	CO ₂	Mo-736	30.07.68	31,2	183	CO ₂
Mo-512	25.10.67	23,3	371	C ₂ H ₆	No-547	27.03.69	12,5	119	C ₂ H ₆
Mo-514	06.03.68	25,4	197	C ₂ H ₆	No-549	29.05.69	30,7	166	C ₂ H ₆
Mo-738	06.03.68	25,4	195	CO ₂	Mo-531	01.07.69	24,8	165	C ₂ H ₆
Mo-517	23.03.68	19,5	150	C ₂ H ₆	Mo-740	04.07.69	20,9	155	CO ₂
Mo-515	12.04.68	19,8	187	C ₂ H ₆	Mo-532	23.08.69	31,9	157	C ₂ H ₆
Mo-739	23.05.68	13,0	93	CO ₂	Mo-526	05.09.69	13,0	38	C ₂ H ₆
Mo-516	11.06.68	12,9	108	C ₂ H ₆	Mo-530	21.10.69	22,4	156	C ₂ H ₆
Mo-518	22.06.68	13,0	78	C ₂ H ₆	Mo-741	21.10.69	22,4	159	CO ₂

Table 1. C^{14} concentration in stratosphere over Northern Hemisphere. (1) laboratory probe no., (2) sampling date, (3) average flight altitude, km, (4) excess atmospheric C^{14} in 1 g of air, 10^{-5} , and (5) counter material.

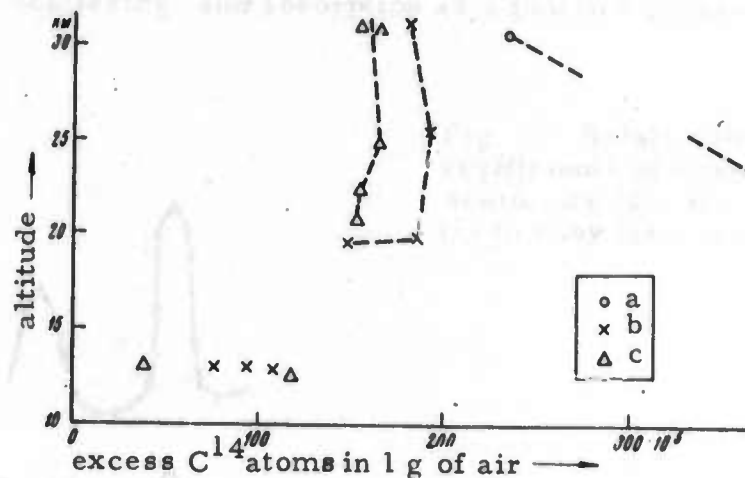


Figure 1. Stratospheric C^{14} distribution at various altitudes.
a - 1967, b - 1968, c - 1969.

Zuyev, V. Ye., A. V. Sosnin, and S. S. Khmelevtsov. Attenuation of ruby laser radiation in the surface boundary layer from temperature retuning of its wavelength. ZhPS, v. 17, no. 2, 1972, 361-363.

Surface boundary layer absorption spectra were investigated in the 6942 to 6945 Å range using medium resolution laser spectrometry. A ruby laser in the free running mode was used. The emission line half-width varied only slightly during spectrum retuning and was equivalent to 0.2 Å while crystal temperature was varied from 4 to 60° C. The experimental setup, similar to one used earlier by the authors (FAiO, 5, 859, 1963) included a 1:20 mirror collimator aperture ratio and an output pupil of 100 mm. Single pulses up to 1 msec were recorded; measured pulses were converted into a short duration sequential series with a total pulse output proportional to the energy or the average current of the measured pulse. The experimental results plotted in Fig. 1 are based on coefficients of attenuation, scattering, and absorption as a function of laser wavelength.

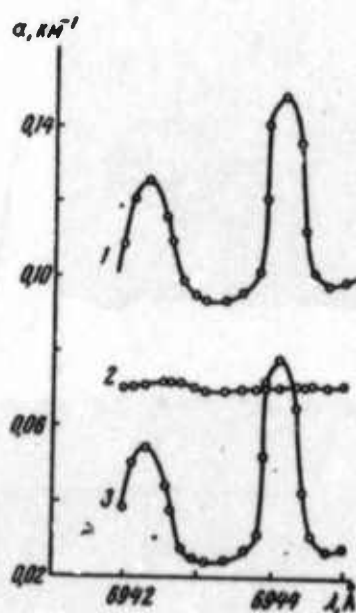


Fig. 1. Relationship of coefficients of attenuation (1), scattering (2), and absorption (3) to ruby laser wavelength.

Two absorption lines with centers at 6942.4 and 6943.9 Å were identified and satisfactorily compared with spectral line data reported by Long (Proc. IEEE, 51, 5, 859, 1963). Absorption coefficient calculations using data from Fig. 1 varied between 0.022 and 0.078 km⁻¹. The absorption coefficient data are not generally recommended for calculations of ruby laser or precipitated water layer absorption since the measurements were made using a generator with the same emission line width as the investigated absorption line width. A line width substantially narrower than that of the atmospheric absorption spectra is recommended.

Boronin, A. P., Yu. A. Medvedev, and
B. M. Stepanov. Electric pulses from volume
pulsation of explosion charge products. DAN
SSSR, v. 206, no. 3, 1972, 580-583.

Oscilloscope traces of low-frequency electrical pulses were recorded for 2-3 msec several meters from an explosion of 54-660 g charges of TNT-RDX 50/50 ignited by a fuse. The recordings were used to quantitatively describe the pulse field at a greater distance and over a longer time period, and to correlate pulse parameters with the self-similar gasdynamic parameters of an explosion. The authors earlier studied only the initial explosion period for shock waves of $\sim 20 r_0$, (explosive charge radius) and typically over a $\sim 150 \mu\text{sec}$ period for a 50 g charge. Oscilloscope traces exhibit fairly pronounced peaks of the primary negative signal at $t_2 \approx 600$, $t_4 \approx 1600$, and $t_6 \approx 2500 \mu\text{sec}$. The pulse amplitude and characteristic width increases with an increase of the charge mass m , without affecting the pulse shape.

On the basis of a statistical analysis of several hundred oscilloscope traces obtained from about 100 tests at different distances R from the explosion site, the electrical pulse can be described by

$$\frac{E(t^0)}{E^*(t_2^0)} = \Psi(t^0) \left[\frac{2.5}{R} \right]^\beta \left[\frac{m}{54} \right]^\alpha. \quad [m] = r, \quad [R] = m, \quad (1)$$

where $t^0 = tm^{-1/3}$ is dimensionless time, $\Psi(t^0)$ is a universal function of t^0 , $E^*(t_2^0)$ is the pulse field potential at a time t_2 and 2.5 m from the explosion of a 54 g. charge, $\alpha = 0.99 \pm 0.2$, and $\beta = 2.6 \mp 0.7$. Eq. (1) shows that for a ten to hundreds gram charge the pulse amplitude is proportional to m and $\sim R^{-3}$, and the pulse shape is described by $\Psi(t^0)$. The self-similarity of the $\Psi(t^0)$ function (Fig. 1a) indicates that the physical mechanism of electrical field excitation is correlated with gas dynamic processes.

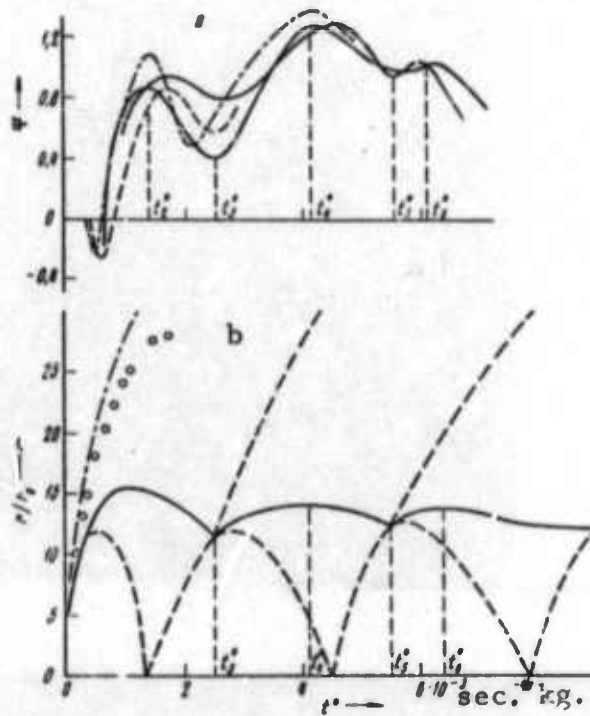


Fig. 1. a- Experimental pulse shape versus self-similar time t^0 curves: solid - $m = 54$ g., dotted - $m = 660$ g., and dot-dash - $m = 225$ g. b- dimensionless radius versus t^0 curves: solid - theoretical at the detonation products front, dot-dash - at the main shock wave front in air, dotted - at the reflected and refracted shock wave fronts; small circles - experimental data on the propagation boundary detonation products.

Fig. 1b shows that the extreme positions of the experimental $r(t^0)r_0$ curves, at t_3^0 , t_4^0 , t_5^0 , and t_6^0 times, coincide (within the experimental error) with the corresponding positions on the theoretical curve. It is concluded that the oscillatory structure of a pulse field can be satisfactorily correlated with the volume pulsations of detonation products. This conclusion confirms that low-frequency electrical pulse generation relates directly to a nonstationary expansion of detonation products. The electrical field source is assumed to be an effective electric dipole with a nonuniform charge distribution in its volume. Two hypotheses are proposed to explain the source structure. The first hypothesis that the electric charges are concentrated near the detonation products front agrees with the experimental signal amplitude dependence on charge mass. In this case, the particle total electric charge is proportional to the surface layer mass of the explosive charge. The second hypothesis that the charges are distributed uniformly in the detonation products volume contradicts the experiment, since the hypothetical pulse amplitude would be proportional to $m^{4/3}$.

Markov, A. A. Investigation of reliability of self-similar solutions to theory of explosions in the atmosphere. DAN SSSR, v. 206, no. 1, 1972, 47-50.

A theoretical analysis is made of the adiabatic propagation of an inviscid perfect gas, generated by a point explosion in an exponential atmosphere. In contrast to the earlier studies of Rayzer, the equations of gas motion and the relations for the upward and downward shock waves contain two dimensionless parameters which represent the effects of Earth

gravity (Ag) and counterpressure (Ap). It is shown that when $Ap = Ag = 0$, the mixed boundary-value problem has a single solution for perturbation, and the boundary values of gasdynamic parameters depend on a self-similar solution. The exact solution nonuniformly approaches the self-similar model as the Lagrangian self-similar variable $\eta \rightarrow \infty$. The difference between the exact and self-similar solutions can be evaluated. Analogous solutions were obtained for $Ap^2 + Ag^2 > 0$.

Mel'nikova, N. S. Explosion in a medium with variable density, taking alternating counterpressure into account. PMiM, v. 36, no. 4, 1972, 26-635.

The initial and subsequent stages of an explosion in a medium with variable initial density ρ_1 and initial pressure p_1 are analyzed. The medium is defined by

$$\rho_1 = Ar^{-\alpha}, \quad p_1 = Cr^{-\gamma} \quad (1),$$

where r is a Eulerian coordinate. The explosion-generated adiabatic turbulent motion of the medium is described by three differential equations which satisfy the boundary conditions

$$v(r_2, t) = v_2, \quad \rho(r_2, t) = \rho_2, \quad p(r, t) = p_2 \quad (2)$$

at a shock wave front with a radius $r_2(t)$. Solution of the explosion equations is sought in the form of the dimensionless quantities

$$f = \frac{v}{c}, \quad g = \frac{\rho}{\rho_2}, \quad h = \frac{p}{p_2} \quad (3),$$

as the functions of two variables

$$\lambda = \frac{r}{r_1}, \quad q = \frac{a_1^2}{c^2}, \quad a_1 = a(r_1) \quad (4)$$

and the symmetry constant $\nu = 1, 2, 3$; adiabatic exponent γ ; ω ; and x . An exact solution for the initial explosion stage was obtained only when

$$\omega = \omega_1 = \frac{3\nu - 2 + \gamma(2 - \nu)}{\gamma + 1} \quad (5)$$

In this case, the self-similar solution, omitting the effect of counterpressure, was made possible by linearization of the initial set of equations. The problem becomes non-self-similar when counterpressure is considered. The characteristic functions of turbulent gas motion are described by the equations

$$\begin{aligned} \frac{p}{p_1} &= 1 + \frac{H_1 p_1 r_1}{(\gamma + 2) p_1} (1 - \lambda^{\alpha+2}) - \frac{p_1 r_1}{p_1} \lambda^{\alpha+2} (H_2 + H_3 \ln \lambda) \ln \lambda \\ \frac{v}{v_1} &= (1 - H_4 \ln \lambda) \lambda, \quad \frac{p}{p_1} = \lambda^\alpha, \quad \alpha = \nu \left(\frac{p_1}{p_1} - 1 \right) - \omega \frac{p_1}{p_1}, \quad \lambda = \frac{r}{r_1} \end{aligned} \quad (6)$$

and the H_1 - H_4 functions of these equations are defined. Equations (6) were derived by integration of the initial set of equations using the formula

$$r = c(t) \xi^{\alpha_1(t)} + b \quad (7),$$

where ξ is the Lagrangian coordinate. Eqs. (2) and (6) show that all characteristics of turbulent gas motion can be expressed through the $r_2(t)$ function, which is determined from the integral equation of the energy continuity. The equation of shock wave motion is derived from the integral equation and solution of Eq. 6. The linearized and nonlinearized solutions are used to calculate the $h_1(\lambda)$, $g_1(\lambda)$, $f_1(\lambda)$, $p/p_2(\lambda)$, $\rho/\rho_2(\lambda)$, and $v/v_2(\lambda)$ functions for $\nu = 2$ and 3 and various x , γ , ω , and q values.

Zvolinskiy, N. V. Hydrodynamic theory
of explosion effects and an incompressibility
diagram. PMiM, v. 36, no. 4, 1972, 726-731.

The continuum motion from an explosion is analyzed using an incompressibility diagram. The diagram is a set of hypotheses on the incompressibility and ideal state of the medium, assuming small-magnitude deformations and displacements. These conditions may be close to reality in the first stage of the explosion-generated motion of a continuum. Motion of an ideal compressible medium under small scale deformations is described in a linear approximation by the scalar wave equation

$$\Delta p - \frac{1}{a^2} \frac{\partial^2 p}{\partial t^2} = 0, \quad a^2 = \frac{k^2}{\rho_0} \quad (1)$$

where ρ_0 is the constant density. Equation (1) is used to determine the pressure field $p(M, t)$ in a random space B with a piecewise continuous boundary surface S. The solution to the motion problem of a compressible medium subjected to a given limit load is thereby reduced to a mixed boundary value solution of the wave equation. Based on (1), the velocity field is determined from

$$v(M, t) = - \frac{1}{\rho_0} \int_0^t \text{grad } p(M, \tau) d\tau \quad (2)$$

The solution is simplified by introducing the incompressibility diagram, i.e., assuming the medium is incompressible and the process is stabilized after a characteristic time τ . The boundary values of dynamic $p(M, t)$ and $v(M, t)$ can then be respectively calculated from

$$\Pi(Q) = \int_0^\tau f(Q, t) dt \quad (3)$$

and

$$v = -\rho_0^{-1} \text{grad} \Pi \quad (4)$$

$\Pi(Q)$ is the pressure pulse in a point of S . The p and v functions thus calculated are independent of t , in agreement with the concept of an extremely short duration asymptotic process. Mathematical proof is obtained that the mean pressure pulse $P_o(M)$ is a harmonic function of the set B and its boundary value on S is

$$P_o(Q) = F_o(Q), \quad Q \in S, \quad F_o(Q) = \lim_{t \rightarrow \infty} \left(\frac{1}{t} \int_0^t f(Q, \tau)(t - \tau) d\tau \right) \quad (5)$$

The boundary value of the mean velocity is

$$V_o(M) = -\rho_o^{-1} \operatorname{grad} P_o(M) \quad (6)$$

The $V_o(M)$ is correlated with $P_o(M)$ by the formula

$$v(M, t) = -\frac{1}{\rho_o} \operatorname{grad} \int_0^t p(M, \tau) d\tau \quad (7)$$

The incompressibility diagram describes the compressible medium problem in an integral asymptotic form at $t \rightarrow \infty$. Application of the diagram is limited to problems in which the solution depends on the integral explosion effect, and to the case of high-velocity waves.

B. Recent Selections

i. Shock Wave Effects

Anafriyev, B. F., V. M. Baranov, and Yu. V. Miloserdin. Application of shock-excited ultrasonic oscillations to measurements of material physical and mechanical properties. IN: Nauchnyye trudy vuzov LatSSR. Ul'trazvukh, v. 3, 1971, 31-36. (LZhS, 46/72, no. 153860)

Bagdoyev, A. G., and Z. N. Danoyan. Study of motion of a medium near a shock wave contact point using linear and nonlinear formulation. ZhVMMF, no. 6, 1972, 1512-1529.

Borovoy, V. Ya., and Ye. V. Sevast'yanova. Techeniye gaza i teploobmen v zone vzaimodeystviya laminarnogo pogranichnogo sloya s udarnoy volnoy vblizi polukryla, ustanovленного на пластине (Gas flow and heat transfer in a laminar boundary layer interaction zone with a shock wave near a half wing mounted on a plate). IN: Trudy TsAGI, Moskva, no. 410, 1972, 19p. (KL, 48/72, no. 38607)

Gvozdeva, L. G., and A. K. Stanyukovich. Reflection from a terrestrial surface of shock waves generated from meteorite impact. Astronomicheskiy vestnik, v. 6, no. 4, 1972, 228-236.

Kolodyazhnnyy, A. V. Buckling dynamics of finite length cylindrical shells under non-axisymmetric shock wave loading. IN: Sbornik. 4-ya Vsesoyuznaya konferentsiya po problemam ustoychivosti v stroitel'noy mehanike, Moskva, 1972, 169-170. (RZhMekh, 11/72, no. 11V413)

Korobeynikov, V. P., and Yu. M. Nikolayev. Shock waves and magnetic field configuration in interplanetary space. Cosmic Electrodynamics, v. 3, no. 1, 1972, 25-44. (RZhF, 10/72, no. 10G84)

Kuskov, A. M. Calculating diffraction from weak shock wave interactions on a plate. VLU, no. 19, 1972, 9E-102.

Kutateladze, S. S., A. P. Burdukov, V. V. Kuznetsov, V. Ye. Nakoryakov, B. G. Pokusayev, and I. R. Shreyber. Structure of a weak shock wave in a gas-liquid medium. DAN SSSR, v. 207, no. 2, 1972, 313-315.

Losev, S. A. Training seminar on shock wave studies, 6-16 April 1972, Moskva. FGIV, no. 3, 1972, 448-450.

Naugol'nykh, K. A. Conversion of shock waves into acoustic waves, Akusticheskiy zhurnal, no. 4, 1972, 579-583.

Pelinovskiy, Ye. N., and V. Ye. Fridman. Statistical phenomena of shock wave generation. Akusticheskiy zhurnal, no. 4, 1972, 590-594.

Pelinovskiy, Ye. N., A. I. Saichev, and V. Ye. Fridman. Shock wave generation in a statistically-nonuniform gas. Akusticheskiy zhurnal, no. 4, 1972, 627-629.

Shremenko, L. S. Shock tube generation of shock waves. VMU, Seriya fizika, astronomiya, no. 5, 1972, 607-611.

Vilyunov, V. N. Gas-phase model of solid fuel ignition in a shock tube. FGIV, no. 3, 1972, 355-361.

Zaslonko, I. S., S. M. Kogarko, Ye. V. Mozhukhin, and Yu. P. Petrov. Thermal decomposition of nitromethane in shock waves. KiK, v. 13, no. 5, 1972, 1113-1118.

ii. Hypersonic Flow

Alekseyev, B. V. Pogranichnyy sloy s khimicheskimi reaktsiyami (Boundary layers with chemical reactions). AN SSSR, Vychislitel'nyy tsentr, Moskva, 1967, 128p. (RZhMekh, 11/72, no. 11B680 K)

Burago, S. G. Three-dimensional supersonic flow around a smooth generatrix body. IVUZ Avia, no. 2, 1972, 5-13.

Buyanov, Ye. Ye. Issledovaniye obtekaniya tel vrashcheniya segmental'no-konicheskoy formy pri dozvukovykh i sverkhzvukovykh skorostyakh potoka. (Studies of subsonic and supersonic flow around segmented-conic bodies of revolution). IN: Trudy TsAGI, no. 1406, 1972, 23p. (KL, 46/72, no. 37309)

Chushkin, P. I. Metod kharakteristik dlya prostranstvennykh sverkhzvukovykh techeniy (Method of characteristics for three-dimensional supersonic flow). AN SSSR, Vychislitel'nyy tsentr, Moskva, 1968, 122p. (RZhMekh, 11/72, no. 11B340 K)

Galkin, M. S. Dynamic strength of membranes in supersonic gas flow. IN: Sbornik. 4-ya Vsesoyuznaya konferentsiya po problemam ustoychivosti v stroitel'noy mehanike, Moskva, 1972, 151. (RZhMekh, 11/72, no. 11B407)

Gorskiy, V. B. Eddy-free relativistic gas flow. DAN SSSR, v. 207, no. 2, 1972, 309-312.

Kozlov, N. P., L. V. Leskov, Yu. S. Procasov, and V. I. Khvesyuk. Probe method for Mach number measurements in hypersonic plasma flow. IN: Sbornik. Tezisy dokladov V Vsesoyuzno konferentsii po generatoram nizkotemperaturnoy plazmy, Novosibirsk, v. 2, 1972, 130-132. (RZhMekh, 11/72, no. 11B1000)

Kutukhin, V. P., L. D. Fedorova, and B. A. El'gudina. Study of optimum lifting body configuration in hypersonic flow. IN: Uchenyye zapiski TsAGI, v. 3, no. 3, 1972, 100-106. (RZhMekh, 11/72, no. 11B336)

Naumova, I. N. Metod kharakteristik dlya ravnovesnykh techeniy nesovershennogo gaza (Method of characteristics for equilibrium imperfect gas flow). AN SSSR, Vychislitel'nyy tsentr, Moskva, 1964, 44p. (RZhMekh, 11/72, no. 11B341 K)

Neuvazhayev, V. Ye., V. D. Frolov, and N. N. Yanenko. Equations of motion of a heat-conducting gas in combined Euler-Lagrange coordinates. IN: Sbornik. Chislennyye metody mehaniki sploshnoy sredy, Novosibirsk, v. 3, no. 1, 1971 (1972), 90-96. (RZhMekh, 11/72, no. 11B681)

Pomerantsev, A. A. Shock wave generation in rarefied gases flowing around heated barriers at supersonic speeds. IN: Sbornik. Teplo-i massoperenos, Minsk, v. 1, 1972, 175-181. (RZhMekh, 11/72, no. 11B302)

iii. Soil Mechanics

Berishvili, G. Vzryv i yego ispol'zovaniye v narodnom khozyaystve (Applications of explosion technology in the economy). Tbilisi, Izd-vo Metsniyereba, 1972, 215p. (KL, 35/72, no. 29549)

Borisovets, V. A., A. M. Kozel, and Ye. B. Revzyuk. Results of an investigation of the stress-strain state of mountain rock masses in the vicinity of underground mines excavated by drilling and blasting. Gornyy zhurnal, no. 7, 1972, 70-73.

Drukovanyy, M. F., L. F. Petryashin, V. A. Belokon', and G. V. Kuznetsov. Metody i sredstva registratsii deystviya vzryva v gornykh porodakh (Methods and equipment for recording the effects of rock blasting). Kiyev, Izd-vo Naukova dumka, 1971, 164p. (FGiV, 3/72, 455)

Drukovanyy, M. F., V. G. Kozlov, and I. A. Semenyuk. Experimental investigation of fracturing in stressed media. IN: Sbornik. Termomechanicheskiye metody razrusheniya gornykh porod, Kiyev, Izd-vo Naukova dumka, part 6, 1972, 11-14. (RZhMekh, 11/72, no. 11V607)

Fadeyev, A. B. Drobyashcheye i seysmicheskoye deystviye vzryva na kirk'erakh (Crushing and seismic effects of blasting in open pits). Moskva, Izd-vo Nedra, 1972, 135p. (FGiV, 3/72, 455)

Kandyba, M. I., O. B. Bakhtin, and E. V. Chudutov. Effect of total explosion delay gap on reduction in seismic oscillation velocity, IN: Sbornik. Akustika v stroitel'stve, Kiyev, Izd-vo Budivel'nik, 1972, 63-67. (RZhMekh, 11/72, no. 11V719)

Kandyba, M. I., and A. S. Zhmudenko. Effect of the number of short-delay explosion stages on seismic wave generation. IN: Sbornik. Akustika v stroitel'stve, Kiyev, Izd-vo Budivel'nik, 1972, 57-62. (RZhMekh, 11/72, no. 11V791)

Komir, V. M., L. M. Geyman, V. S. Kravtsov, and N. I. Myachina. Modelirovaniye razrushayushchego deystviya vzryva v gornykh porodakh (Modelling of destruction in rocks from blasting). Moskva, Izd-vo Nauka, 1972, 216p. (RZhMekh, 11/72, no. 11V803 K)

Korsakov, P. F. Effect of rock anisotropy on delay gap during short-delay explosive blasting. Fiziko-tehnicheskiye problemy razrabotki poleznykh iskopayemykh, no. 2, 1972, 49-56. (RZhMekh, 11/72, no. 11V784)

Kutuzov, B. N., V. K. Rubtsov, and V. N. Marshakov. Fizika vzryvnogo razrusheniya gornykh porod (Physics of rock destruction from blasts). Moskva, 1972, 250p. (KL Dop vyp, 10/72, no. 22246)

Lebedev, T. S., D. V. Korniyets, V. I. Shapoval, and V. A. Korchin. Uprugkiye svoystva gornykh porod pri vysokikh davleniyakh (High pressure elastic properties of rocks). Kiyev, Izd-vo Naukova dumka, 1972, 184p. (RZhMekh, 11/72, no. 11V802 K)

Onishchenko, Yu. A. Tensor properties of rock mass parameters. IN: Sbornik. Problemy voprosov mehaniki gornykh porod, Alma-Ata, Izd-vo Nauka, 1972, 256-263. (RZhMekh, 11/72, no. 11V743)

Savruk, M. P., and A. P. Datsyshin. Limiting-equilibrium state of a body weakened by a system of arbitrarily oriented cracks. IN: Sbornik. Termomekhanicheskiye metody razrusheniya gornykh porod, Kiyev, Izd-vo Naukova dumka, part 2, 1972, 97-102. (RZhMekh, 11/72, no. 11V600)

Timoshin, Yu. V., F. L. Brandt, N. M. Gel'man, A. A. Reznik, and V. D. Shklyarevskiy. Device for converting seismic recordings. Otkr izobr, no. 32, 1972, no. 356608.

Zhubayev, N., and K. Zhunusov. Study of the effectiveness of an air-cushion charge, IN: Sbornik. Problemy voprosov mekhaniki gornykh porod, Alma-Ata, Izd-vo Nauka, 1972, 166-182. (RZhMekh, 11/72, no. 11B265)

iv. Exploding Wire

Rakhuba, V. K., and N. N. Stolovich. Effect of geometric dimensions of an exploding conductor and discharge circuit parameters on energy conversion efficiency. IAN B, Seriya fiziko-energeticheskikh nauk, no. 4, 1972, 119-123.

v. Equations of State

Fortov, V. Ye. Calorimetric equation of state of silicon oxide and liquid silicone, FGIV, no. 3, 1972, 428-433.

Geller, V. Z., A. Ya. Kreyzerova, I. A. Paramonov, and Ye. G. Porichanskiy. Equation of state and thermodynamic properties of liquid F-113, IAN B, Seriya fiziko-energeticheskikh nauk, no. 4, 1972, 65-68.

Mukniddinov, Dzh. Calculating heat capacities of monatomic gases.
IN: Uchenyye zapiski Tashkentskogo gosudarstvennogo
pedagogicheskogo instituta, v. 90, 1971, 71-78. (RZhKh, 22/72,
no. 22B571)

Selevanyuk, V. I., and A. L. Tsykalo. Calculating virial coefficients
of a gas equation of state at low temperatures. Kholodil'naya
tekhnika i tekhnologiya, no. 11, 1971, 94-96. (LZhS, 47/72,
no. 156850)

Toth, J. Equations of state of interphase layers. I. Equations of
state of interphase layers on a solid-gas boundary for an energetically
homogeneous surface. Magyar kemiai folyoirat, v. 76, no. 12, 1970,
643-648. (RZhKh, 22/72, no. 22B1170)

Toth, J. Equations of state of interphase layers. II. Equations of
state of interphase layers on a solid-gas boundary for an energetically-
inhomogeneous surface. Magyar kemiai folyoirat, v. 76, no. 12,
1970, 648-655. (RZhKh, 22/72, no. 22B1171)

vi. Atmospheric Physics

Afonin, V. V., M. I. Verigin, G. L. Gdalevich, B. N. Gorozhankin,
K. I. Gringauz, Yu. I. Logachev, A. P. Remizov, V. G. Stolpovskiy,
M. Z. Khokhlov, and S. M. Sheronova. Effect of scattered electron
and proton flux on the characteristics of the high-latitude ionosphere,
based on observations from the Cosmos-378 satellite. IN: Sbornik.
X Vsesoyuznaya konferentsiya po rasprostraneniyu radiovoln,
Section 1, Moskva, Izd-vo Nauka, 1972, 436-438. (RZhIssledovaniye
kosmicheskogo prostranstva, 11/72, no. 11.62.175)

Biryukov, A. V., I. A. Knorin, Yu. V. Musatov, V. A. Rudakov, and L. A. Shnyreva. Rocket radio-sounding of the high electron density distribution in the ionosphere in 1970-71. IN: ibid., 65-66. (RZhIssledovaniye kosmicheskogo prostranstva, 11/72, no. 11.62.167)

Feoyashev, A. B., and G. A. Tuchkov. Rocket measurements of electrons in the ionospheric D-layer. IN: ibid., 77-80. (RZhIssledovaniye kosmicheskogo prostranstva, 11/72, no. 11.62.170)

Fizika verkhney atmosfery (Physics of the upper atmosphere. Collection of articles). IN: Trudy Instituta eksperimental'noy meteorologii, Moskva, Gidrometeoizdat, no. 1(34), 1972, 176p. (KL, 48/72, no. 38655)

Fizika oblakov i aktivnykh vozdeystviy (Physics of clouds and cloud modification). IN: Trudy Tsentral'noy aerologicheskoy observatorii, Moskva, Gidrometeoizdat, no. 101, 1972, 96p.

Fleyer, A. G. Relationship between variations in the lower ionosphere and earth motion parameters. IN: Sbornik. X Vsesoyuznaya konferentsiya po rasprostraneniyu radiovoln, Section 1, Moskva, Izd-vo Nauka, 1972, 240-244. (RZhIssledovaniye kosmicheskogo prostranstva, 11/72, no. 11.62.174)

Golubitskiy, B. M., T. M. Zhad'ko, and M. V. Tantashov. Effect of optical radar geometric parameters on the applicability of the single-scattering approximation. FAiO, no. 11, 1972, 1226-1229.

Gringauz, K. I. Results of ionospheric probes from the Intercosmos-2 satellite. IN: Sbornik. X Vsesoyuznaya konferentsiya po rasprostraneniyu radiovoln, Section 1, Moskva, Izd-vo Nauka, 1972, 62-64. (RZhIssledovaniye kosmicheskogo prostranstva, 11/72, no. 11.62.166)

Gringauz, K. I., N. M. Shyutte, V. A. Rudakov, and I. A. Knorin. Results of complex rocket probing of upper atmosphere parameters. IN: ibid., 67-68. (RZhIssledovaniye kosmicheskogo prostranstva, 11/72, no. 11.62.168)

Gutshabash, S. D. Diffusion of nonstationary radiation in a semifinite isotropically scattering medium. FAiO, no. 11, 1972, 1154-1165.

Komarnitskaya, N. I. Capture of terrestrial dust particles moving in a near-ecliptic plane. Astronomicheskiy vestnik, no. 1, 1972, 35-43.

Korchak, A. A., L. A. Lobachevskiy, V. V. Migulin, E. Ts. Rapoport, and I. P. Stakhanov. Radiophysics methods of studying the ionosphere and near-Earth space. IN: Sbornik. X Vsesoyuznaya konferentsiya po rasprostraneniyu radiovoln, Section 1, Moskva, Izd-vo Nauka, 1972, 531-535. (RZhIssledovaniye kosmicheskogo prostranstva, 11/72, no. 11.62.176)

Mikhter, Ya. I. Characteristics of VLF electromagnetic wave propagation in the upper ionosphere, based on Intercosmos-3 and Intercosmos-5 satellite observations. IN: ibid., 137-139. (RZhIssledovaniye kosmicheskogo prostranstva, 11/72, no. 11.62.173)

Misyura, V. A., Yu. G. Yerokhin, M. G. Trukhan, V. L. Bludov, V. N. Kudrev, V. I. Ivanov, N. M. Borodin, and N. L. Nisnevich. Vertical gradients and nonstationary electron density, electron composition and ionospheric particle temperatures obtained by an incoherent scattering method during strong solar activity. IN: ibid., Section 3, 89-93. (RZhIssledovaniye kosmicheskogo prostranstva, 11/72, no. 11.62.171)

Misyura, V. A., V. A. Podnos, I. I. Kapanin, A. M. Tsymbal, Yu. G. Yerokhin, and M. G. Trukhan. Effects of wave propagation in the ionosphere based on artificial earth satellite observations and incoherent scattering data. IN: ibid., 99-103. (RZhIssledovaniye kosmicheskogo prostranstva, 11/72, no. 11.62.172)

Mitnik, L. M. Measuring moisture content over ocean waters using SHF radiometers on the Cosmos-243 satellite. IN: Trudy Tsentral'noy aerologicheskoy observatorii, no. 103, 1972, 64-72. (RZhIssledovaniye kosmicheskogo prostranstva, 11/72, no. 11.62.163)

Styro, B. I., and N. K. Shpirkauskayte. Probable correlation between meteorological processes and fallout concentration with density of long-life alpha-radioactive materials. Meteorologiya i gidrologiya, no. 11, 1972, 94-98.

Vasil'yev, G. V., A. I. Galkin, V. Ye. Zasenko, A. S. Kasimanov, Yu. V. Kushnerevskiy, N. S. Mozerov, N. M. Polekh, Yu. A. Sidorov, D. K. Tishchenko, M. D. Fligel', S. V. Fomenkov, and Yu. N. Shaulin. Experiment in pulsed sounding of the ionosphere above the primary maximum of ionization. IN: Sbornik. X Vsesoyuznaya konferentsiya po rasprostraneniyu radiovoln, Section 1, Moskva, Izd-vo Nauka, 1972, 55-58. (RZhIssledovaniye kosmicheskogo prostranstva, 11/72, no. 11.62.165)

X Vsesoyuznaya konferentsiya po rasprostraneniyu radiovoln.
Tezisy dokladov. Sektsiya 1. Ionosfernoye rasprostraneniye
radiovoln (Tenth All-Union Conference on wave propagation,
Section 1. Ionospheric wave propagation). Moskva, Izd-vo
Nauka, 1972, 560p. (RZhF, 10/72, no. 10Zh150 K)

Ibid. Sektsiya 2. Rasprostraneniye UKV v troposfere (Section 2.
Propagation of ultrashort waves in the troposphere). Moskva,
Izd-vo Nauka, 1972, 128p. (RZhF, 10/72, no. 10Zh151 K)

Ibid. Sektsiya 4. Rasprostraneniye elektromagnitnykh voln
millimetrovogo, submillimetrovogo i opticheskogo diapazonov
(Section 4. Propagation of millimeter, submillimeter and optical
waves). Moskva, Izd-vo Nauka, 1972, 388p. (RZhF, 10/72,
no. 10Zh152 K)

Ibid. Sektsiya 5. Rasseyaniye radiovoln zemnoy poverkhnost'yu i
razlichnymi telami. (Section 5. Wave scattering from a terrestrial
surface and various bodies). Moskva, Izd-vo Nauka, 1972, 208p.
(RZhF, 10/72, no. 10Zh153 K)

Ibid. Sektsiya 8. Matematicheskoye modelirovaniye ionosfery
(Section 8. Mathematical modelling of the ionosphere). Moskva,
Izd-vo Nauka, 1972, 166p. (RZhF, 10/72, no. 10Zh155 K)

vii. Miscellaneous Effects of Explosions

Amosov, A. P., S. A. Bostandzhyan, and V. S. Kozlov. Ignition
of solid explosives by heat of dry friction. FGIV, no. 3, 1972,
362-368.

Andriankin, E. I., V. K. Bobolev, and A. V. Dubovik. Shock heating of a liquid explosive layer. FGIV, no. 3, 1972, 408-416.

Baranov, Ye. G. Korotkozamedlennoye vzryvaniye (Short-delay blasting). Frunze, Izd-vo Nilm, 1971, 113p. (FGIV, 3/72, 455)

Deribas, A. A. Fizika uprochneniya i svarki vzryvom (Physics of explosive hardening and explosive welding). Novosibirsk, Izd-vo Nauka, 188p. (RBL, 7/72, no. 604; FGIV, 3/72, 455)

Frolov, Yu. V., V. F. Dubovitskiy, A. I. Korotkov, and v. G. Korostelev. Convective combustion of porous explosives. FGIV, no. 3, 1972, 368-378.

Gol'din, V. Ya., N. N. Kalitkin, Yu. L. Levitan, and B. L. Rozhdestvenskiy. Calculating two-dimensional flow from detonations. ZhVMMF, no. 6, 1972, 1606-1611.

Gorbatskiy, V. G. Kosmicheskiy vzryvy (Explosions in space). Moskva, Izd-vo Nauka, 1972, 208p. (FGIV, 3/72, 455)

Goroyan, T. A., and E. Ye. Khachiyan. Seismic resistance of multi-story frame buildings with reduced rigidity at higher floors. IAN Arm SSR, Seriya tekhnicheskikh nauk, no. 3, 1972, 35-43.

Grayevskiy, M. M., and V. V. Tomasov. Massovoye elektrovzryvan peremennym tokom s pomoshchyu poluprovodnikovykh priborov (Massive a-c electrical explosions using semiconductor devices). Moskva, Izd-vo Vysshaya shkola, 1972, 106p. (KL, 48/72, no. 38752)

Ivanov, G. V., A. M. Viktorenko, and A. G. Tereshchenko.
Physical and chemical properties of methylamine perchlorate.
IVUZ Khim, no. 11, 1972, 1628-1630.

Korovchenko, G. M. Master-vzryvnik (Explosion operations foreman, Training handbook). Moskva, Izd-vo Nedra, 1972, 191p.
(KL, 49/72, no. 39425)

Koshelev, E. A., and Ye. N. Sher. Bubble formation from surface explosions in water. FGIV, no. 3, 1972, 441-443.

Kozachenko, L. S., and B. D. Khristoforov. Surface phenomena from underwater explosions. FGIV, no. 3, 1972, 433-439.

Medvedev, Yu. A., B. S. Punkevich, and B. M. Stepanov. Results of a study of space-time conductivity distribution in a blast zone. FGIV, no. 3, 1972, 417-422.

Shamko, V. V. TNT equivalence of a high power underwater spark discharge. EOM, no. 5, 1972, 16-19.

Sobin, O. A. Experimental study of the destruction zone during cutting of survey pits by cratering explosions. IVUZ Geologiya i razvedka, no. 11, 1972, 120-122.

Walczak, W., and H. Czajkowski. Svarka metallov vzryvom (Explosive welding of metals). Warszawa, Wydawnictwo naukowo-technika, 1970, 91p. (FGIV, 3/72, 458)

Zakharenko, I. D. Critical regimes during explosive welding. FGIV, no. 3, 1972, 422-427.

3. Geosciences

A. Abstracts

Bulin, N. K. Crustal thickness in Pamir. IN: Akademiya nauk. Doklady, v. 204, no. 1, 1972, 167-170.

The results of crustal studies performed in Pamir and southern Tien-Shan in 1963-65, using converted PS-waves from distant earthquakes are described. The observations were made at 110 mobile seismographic stations set up along traverses having a total length exceeding 1500 km (see Fig. 1). Additional data from 35 regional seismological observatories, as well as earlier data obtained by the author, were

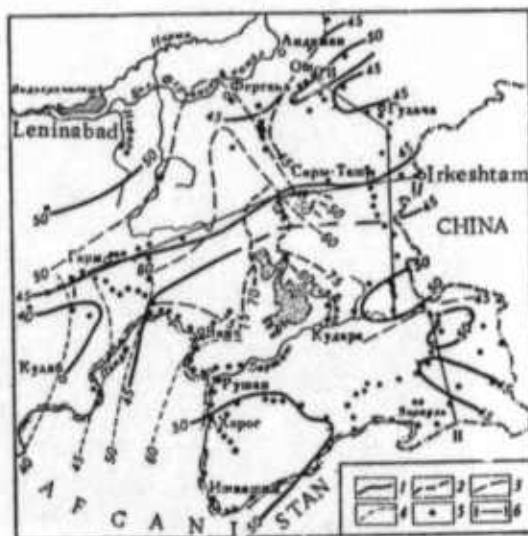


Fig. 1. Surface Relief Map of the Mohorovicic Discontinuity in Pamir and the Eastern Part of Southern Tien-Shan.

- 1 - depth contours from the data on PS-waves from earthquakes obtained in 1961-66;
- 2 - from DSS data (Kosminskaya, 1958)
- 3 - from refracted waves from near earthquakes (Ulomov, 1966)
- 4 - from data on near earthquakes (Kukhtikova, 1967)
- 5 - points of depth determination from PS-wave
- 6 - profile lines of deep seismic sections shown in Fig. 2.

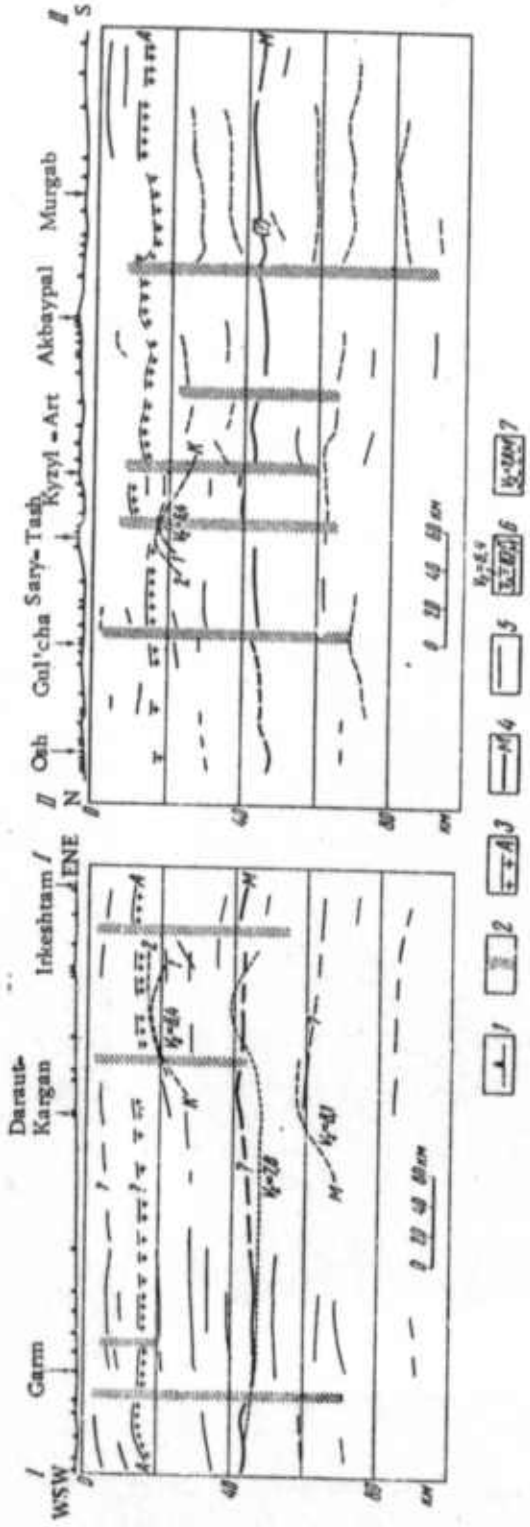


Fig. 2. Deep Seismic Section through Pamir and Southern Tien-Shan along Profiles 1 - 1 and 11 - 11 (Plotted from data on PS-waves from earthquakes in 1961-66).

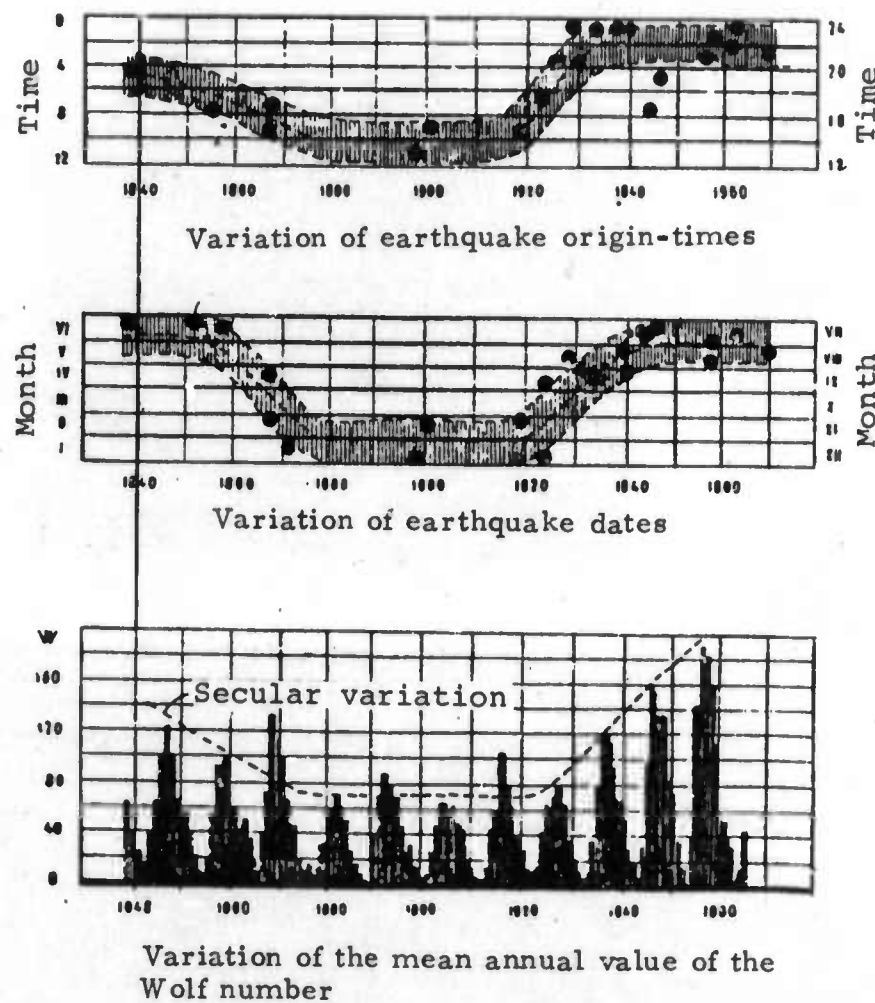
1- Observation points projected onto the profile line; 2- assumed deep-seated faults (clearly revealed parts are shown); 3 - 5- average position of seismic horizons (conversion interfaces): 3 - horizon A within the granitic layer; 4- Moho discontinuity; 5- other crustal and upper mantle horizons; 6- refraction interfaces from DSS data (K- Conrad discontinuity, M- Moho discontinuity, V_r refractor velocity in km/sec); 7- Moho discontinuity from seismological data obtained along profile Hissar valley- Alay valley (Bune, 1960).

used in the interpretation. The results are summarized in two figures: Fig. 1 shows a surface relief map of the Moho discontinuity, and Fig. 2 shows deep seismic sections along profiles I - I and II - II (also indicated in Figure 1). Up to a depth of about 100 km, the crust and upper mantle are characterized by block structure (Fig. 2). Nearly vertical deep zones between large blocks are outlined tentatively. The most distinct conversion interfaces are horizon A within the granitic layer and the Mohorovicic discontinuity.

Depths to the Mohorovicic discontinuity range from 38-52 km with the most frequent value between 46 and 48 km. Thus, the crustal thickness in Pamir (including the Pamir-Alay zone and the northern part of the Tadzhik depression) and the southern Tien-Shan is in accordance with the mean value for all of Central Asia (50 ± 10 from DSS data and 45 ± 5 from near earthquakes). Maximum depths of 50-52 km are found in southwestern Pamir and in some local areas in eastern Pamir and southern Tien-Shan. Thus, great depths are found in Tien-Shan and not exclusively in Pamir. Minimum depths to the Mohorovicic discontinuity (40-45 km) are found in the Tadzhik depression, Alay valley, and Gul'cha basin, but only at one locality in Pamir. The relief of Mohorovicic discontinuity is fairly smooth, with step-wise changes in depth of 3-5 km confined mostly to the junctions of orogenic provinces. The trend of the depth contours of the Mohorovicic discontinuity coincides with the trend of surface Paleozoic and more ancient folded structures. While estimates of the crustal thickness in Pamir compare favorably with a number of seismological data (Treskov, 1957; Lukk and others, 1965; Bune and others, 1960; Kukhtikova and others, 1967), they are in conflict with other seismological (Ulomov, 1966; Nersesov, 1962; Choudkhuri, 1959) and DSS (Kosminskaya, 1958) data. The present results of the most detailed up-to-date seismological studies do not give any evidence of an anomalous (70-75 km) crustal thickness in Pamir, widely accepted on the basis of seimological, DSS, and gravity data.

Lursmanashvili, O. V. Uniform variation
in the date and origin times of strong
earthquakes in Transcaucasia. IN: Akademiya
nauk Gruz SSR. Soobshcheniya, v. 66, no. 3,
1972, 581-583.

The results of the analysis of the variation of the date (month and day) and origin time of earthquakes with $M \geq 5.75$ in Transcaucasia during 1840-1970 are described. It is shown that the variation of the date and origin time for that period were regular and similar, and coincided with the secular variation of solar activity (see Figure 1). A simple empiric expression is derived for the earthquake date/time relation. An attempt is made to predict the date and time of future strong earthquakes over the next decade.



Dubrovskiy, V. A., and V. L. Pan'kov.

Amplitude ratio of PcP and P waves.

IN: Akademiya nauk SSSR. Izvestiya.

Fizika Zemli, no. 6, 1972, 81-84.

An attempt is made to explain anomalously high experimental values of the reflection coefficient of PcP waves. A solution is suggested in which the small changes of the velocity of seismic waves, assumed within a thin layer above and below the solid-fluid boundary, yield an increase of the reflection coefficient sufficient to fit experimental data.

The calculations are made using the expression for the reflection coefficient derived for the case of a P-wave incident through a solid against a plane solid-fluid boundary in terms of $\eta = K/K'$, $p = V_p/V_s$, and $x = \rho'/\rho$. The results are shown in the form of a) $R = f(i_c)$ curves calculated for fixed values of $p = 1.9-1.7$, $\eta = 0.6-0.8$ and $x = 1.7$; and b) $R/R_o = f(i_c)$ curves when R_o is the standard value calculated for $p = 1.9$, $\eta = 1.0$ and $x = 1.7$. It is shown that with a small increase in the shear wave velocity ($\Delta V_s \sim 0.3-0.5$ km/sec) and decrease in the compressional velocity ($\Delta V_p \sim 0.25 - 0.35$ km/sec), R can increase by a factor of 1.5 at intermediate angles of incidence ($30^\circ < i_c < 70^\circ$), and much more at small and large ($30^\circ > i_c > 70^\circ$) angles of incidence.

A physical interpretation is suggested of the assumed increase of shear wave velocity (or shear modulus) and decrease of compressional wave velocity (or incompressibility) on the basis of the hypothesized mechanism of density differentiation in the mantle and expansion of the core.

Kogan, S. D. Study of the dynamics of a compressional wave reflected at the Earth's core. IN: Akademiya nauk SSSR. Izvestiya. Fizika Zemli, no. 6, 1972, 3-20.

The results of a study of the dynamic characteristics of PcP waves are described. The records of P and PcP waves are described. The records of P and PcP waves from nuclear devices exploded at Amchitka Island, in Asia, and in the Arctic Ocean regions obtained for the epicentral distance range at $\Delta = 13-70^\circ$ are analyzed. The following characteristics are considered:

Recording distance range.

PcP waves are observed at all distances in the range $\Delta = 13-70^\circ$. The average observation frequency near 30° is no smaller than at other distances within the $\Delta = 20-60^\circ$ range.

Phase of PcP waves.

Phase correlation of PcP waves generated by the same explosion and reliably recorded by the SVKM and SVK seismograph systems at different epicentral distances revealed no phase reversal relative to P waves at distances $\Delta > 16^\circ$.

Ratio of amplitudes of PcP and P waves.

Dispersion of the A_{PcP}/A_P data points due to different instrument constants are found to be insignificant for the absolute band width $0.7 V_{max} > 0.5$ sec and $T_{max} < 1.0$ sec. A_{PcP}/A_P determined for the waves

generated by different explosions and recorded at the same stations are found to differ greatly, in some cases by a factor of 2. The accuracy of an individual determination of amplitude ratio under optimum conditions is $\pm 0.1 - 0.2$.

Amplitude spectra of P and PcP waves.

Spectral analysis was accomplished using mainly records of the Longshot explosion, recorded by the SVKM seismograph system. The amplitude spectra in the frequency range 0.6 - 1.5 Hz (which corresponds to the absolute bandwidth of the system) corrected for the frequency response of the system were considered. The amplitude spectra of P waves are characterized by pronounced maxima shifting from 0.6 to 0.4 Hz (as epicentral distances increase from 16.5 to 65.6°) and rapid diminution of spectral components towards both the higher and lower frequencies. The comparison to the above, the amplitude spectra of PcP waves have maxima at higher frequencies and a slower diminution of their components, particularly for small epicentral distances. The amplitude spectra $S(f)$ obtained for different epicentral distances are compared using criteria:
a) γ - exponent in the expression $\frac{S(fm)}{S(fi)} = \left(\frac{f_i}{fm}\right)^\gamma$ (in this case $fm = 0.6 \pm 0.1$ Hz,

$f_i = 1.4 \pm 0.1$ Hz) and b) $\operatorname{tg}\alpha$ - slope of cumulative curves $\sum_i S(f_i)$. It was found that γ_P diminishes with epicentral distance. Dispersion of γ_{PcP} is higher than that of γ_P . The average value of γ_{PcP} over the entire distance range ($\bar{\gamma}_{PcP} = 1.73 \pm 0.16$) differs little from the average value of γ_P for distances exceeding 50° ($\bar{\gamma}_P = 1.78 \pm 0.16$), $\operatorname{tg}\alpha_{PcP}$ increases more rapidly than $\operatorname{tg}\alpha_P$ up to $\Delta = 40$ °, while at greater distances, the differences between them either become small or vanish. It is concluded that at $\Delta < 50$ ° absorption of P waves is higher relative to PcP, while at $\Delta > 50$ °, it decreases

relative to the P_cP waves. This conclusion is confirmed by data on the period ratio T_{PcP}/T_P , which is found to be as follows:

$\Delta \leq 50^\circ$		$\Delta > 50^\circ$	
T_{PcP}/T_P	No. of observations	T_{PcP}/T_P	No. of observations
0.86 ± 0.7	17	0.97 ± 0.03	20
0.79 ± 0.03	64	0.96 ± 0.03	30

The ratio of the spectral component of P and P_cP waves $|S_{PcP}(f)/S_P(f)|$ is found to depend on frequency up to $\Delta \sim 40^\circ$. The ratio increases with frequency, reaching a maximum at 1.3 - 1.4 Hz. In the $\Delta = 40-60^\circ$ distance range, the dependence is not very clear; at $\Delta > 60^\circ$ it does not exist.

Differences between experimental and theoretical data
on the ratio A_{PcP}/A_P at $\Delta > 50^\circ$.

The experimental values of A_{PcP}/A_P at $\Delta = 53-68^\circ$ is found to be 0.45 ± 0.4 (averaged from 20 observations, $\sigma = 0.17$). The average values for the ratio of spectral components for P and P_cP waves based on five amplitude spectra at $\Delta = 53.8 - 65.6^\circ$ are greater than 0.2 at all frequencies. Thus, experimental values of A_{PcP}/A_P at $\Delta > 50^\circ$ are:
a) larger by a factor of 2 than the theoretical values calculated for the standard model of the mantle-core boundary with $V_p/V_s = 1.89$, $\rho'/\rho = 1.7$, $K/K' = 1$ (Dana, 1945); b) in agreement with theoretical values calculated for $V_p/V_s = 1.7$, $\rho'/\rho = 1.7$, $K/K' = 0.6 - 0.8$ (Dubrovskiy and others, 1972); c) in agreement with theoretical values obtained for the thin-layered model of the mantle-core transition. Thus, although the nature of the boundary between the mantle and core cannot be determined on the basis of this data, it can be concluded that the elastic parameters of the medium in the mantle-core transition differ from those assumed in Bullen's model A.

Ry kunov, L. N., and Fam Va i Tkhukh.
Study of the effect of local discontinuities
on Rayleigh wave field. IN: Akademiya
nauk SSSR. Izvestiya. Fizika Zemli,
no. 5, 1972, 65-71.

Model studies of the effect of discontinuities on Rayleigh waves were conducted for the following cases: a) abruptly terminated or varying layer thickness in a half-space; b) a vertical slit in a half-space and c) an inclined wall in a full space.

In the first case a two-dimensional model simulated a sedimentary layer over crystalline rock. A noticeable characteristic of the Rayleigh waves is an increase of the amplitude of transmitted waves ($K_t > 1$) at the edge of the layer, regardless of the velocity and density ratios. An explanation for this effect was found through analyzing the distribution of energy and displacement in Rayleigh waves with respect to depth. It was found that as Rayleigh waves propagate from the layer to the halfspace, a redistribution of energy and an increase of the vertical component of the displacement occur.

In the second case, a two-dimensional model simulated a fault with a width of $0.04\lambda_R$ and depth $H = 0 - \lambda_R$. It was found that the amplitude, amplitude spectrum, and trajectory of the particle motion change as the Rayleigh waves propagate across the slit. Immediately after the slit, the amplitude of the vertical component rapidly diminishes forming a "shadow zone". The deeper the slit, the farther from the slit are the amplitude minima in the shadow zone and maxima. The changes of amplitude are accompanied with changes of the trajectory of the particle motion.

Nearly elliptic trajectories correspond to the minimum amplitudes, while very complex ones are attributed to the initial part of the "shadow zone" and

the amplitude maxima. As the distance from the slit increases the trajectories resume their elliptic shape. The amplitude spectra are characterized by a simple shape corresponding to minimum amplitudes and a complex shape corresponding to maximum amplitudes.

In the last case, a change of the relief at a free surface was simulated. It was found that the amplitudes of vertical components of Rayleigh waves decrease abruptly ($K_t = 0.28$, $K_r = 0$), their phase being reverse, as they pass through the lower point of the incline with $\alpha = \pi/2$ (vertical boundary). For $\alpha = 0 - \pi/2$, the relation $K_t = -0.46\alpha + 1$ obtains. An analysis of the radiation pattern of S and P waves generated by Rayleigh waves incident against the corner of the incline with $\alpha = \pi/2$, showed that the predominant motion occurs along its vertical surface.

Yakovleva, I. B. Time-distance curves for western Uzbekistan. IN: Akademiya nauk UzSSR. Institut seismologii. Seismologiya i seismogeologiya Uzbekistana (Seismology and seismogeology of Uzbekistan). Tashkent, Izd-vo Fan, 1971, 52-60.

Theoretical time-distance curves of P and S waves for near earthquakes in western Uzbekistan are constructed. The crustal velocity model, inferred from experimental data assuming a homogeneous multilayered model with horizontal interfaces consists of: 1) the sedimentary layer with $V_{po} = 4.5$ km/sec and $H = 3$ km; 2) the granitic layer with $V_p = 5.8$ km/sec and $H = 10$ km; 3) the basaltic layer with $V_s = 6.5$ km/sec and $H = 18$ km; and

4) the upper mantle with $V_p = 8.1$ km/sec. S-wave velocities are determined from $K = V_p/V_S$ which yields 1.91, 1.74, 1.71 and 1.70 for the four components of the model, respectively. Theoretical time-distance curves are calculated for focal depths of 5-35 km (at 5 km intervals) and epicentral distances 0-800 km (in the 0-300 km range, at 5 km intervals and in 300-800 km range, at 10 km intervals). The curves were found to be valid for the determination of the epicentral coordinates of western Uzbekistan earthquakes. The observed dispersion of experimental data points around the theoretical time-distance curves is explained as being likely due to anomalous travel times in some parts of the region.

Matasova, L. M., and G. V. Gavrilova.

Seismicity of the Chadak reservoir area.

IN: Akademiya nauk Uz SSR. Institut
seismologii. Seismologiya i seismogeologiya
Uzbekistana (Seismology and seismogeology
of Uzbekistan). Tashkent, Izd-vo Fan, 1971,
19-24.

The results of a study of the seismicity of the Chadak reservoir area in eastern Uzbekistan are described. Data on earthquakes with $K = 9-15$ and focal depths of 45-50 km, which occurred in the period 1868-1968, are used for the construction of an epicenter map and a contour map of A_{10} . Observational data on earthquakes with $K \geq 9$ which occurred in 1951-68, represented by their energy class, are used for plotting a recurrence graph. This recurrence graph is characterized by a slope of $\gamma = 0.44 \pm 0.12$ (similar to the values found for other seismic regions in Uzbekistan) and $A_{10} = 0.095$.

Ulomov, V. I., and N. V. Shcheglov.

Study of the dynamic characteristics of seismic waves, using photoelastic models.

IN: Akademiya nauk Uz SSR. Institut seismologii. Seismologiya i seismogeologiya Uzbekistana (Seismology and seismogeology of Uzbekistan). Tashkent, Izd-vo Fan, 1971, 73-77.

A review is given of the basic principles and capabilities of photoelastic methods in seismic model studies.

The photoelastic method provides visualization of stress distribution within models, using polarized lights. The photoelastic stroboscopic model study provides quantitative analysis of the dynamic characteristics of the wave field directly within a model. When combined with oscilloscope records of oscillations on the free surface of the model, it provides unambiguous interpretation of oscilloscopic data.

The method is primarily used in the study of kinematic and dynamic characteristics of seismic waves propagating through a continuously deformed medium, for the purpose of identifying indicators of fracture in an elastic medium.

Tarkov, A. P. Mineralogical-petrological model of the crystalline crust and upper mantle of the Voronezh massif, based on deep seismic sounding. IN: Akademiya nauk SSSR. Izvestiya. Seriya geologicheskaya, no. 4, 1971, 17-28.

Data on seismic velocity obtained through deep seismic sounding (DSS) in the Voronezh crystalline massif is analyzed and a minera-

logical-petrological model of the crystalline crust and upper mantle is inferred. The crustal and upper mantle velocity characteristics were determined from near-vertical incidence reflections and head waves. The average velocity in the crystalline crust varies from 6.2 to 6.6-6.7 km/sec from the southwest to the northeast and of the DSS profile (see Fig. 1). In the upper mantle (at a depth of 75-80 km), the average velocity $V = 7.0$ km/sec. In the crystalline crust, the layer velocities

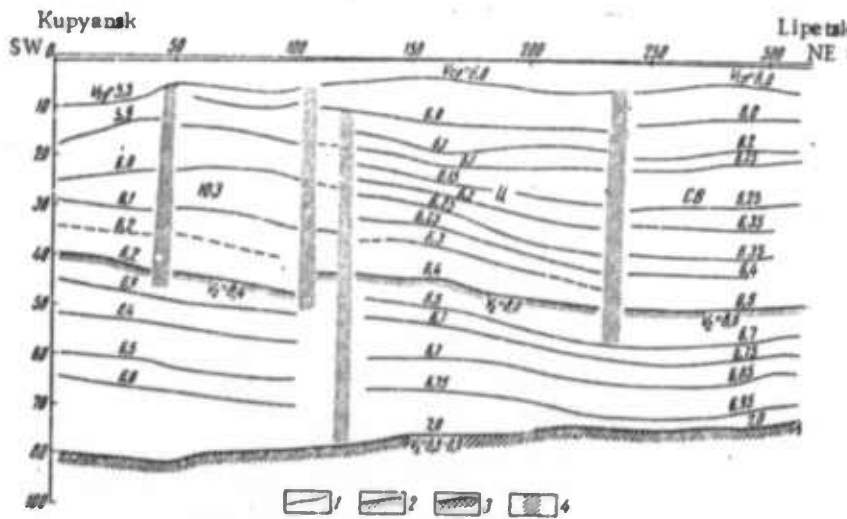


Fig. 1. Velocity Section along the Kupyansk-Lipetsk Profile (after Chamo, S. S., and others, 1968).

1 - Seismic interfaces; 2 - Mohorovicic discontinuity (M_1); 3 - upper mantle interface (M_2); 4 - fault zones.

increase gradually with depth from 6.0-6.2 to 7.3-7.5 km/sec. They continue to increase in the upper mantle reaching 7.5-8.0 km/sec at a depth of 7.5-8.0 km in the southwestern and northeastern part of the profile, respectively. The Mohorovicic discontinuity velocity varies from $V_r = 8.0$ km/sec in the central part of the profile, to 8.6 km/sec in the northeastern

part. The refractor velocity along the deepest upper mantle interface is $V_r = 8.8$ km/sec. Three structural blocks (southwestern, central and northeastern), are characterized by different velocity distributions. Assuming a continuous velocity-depth relation, diagrams of velocity and density distribution $V(Z)$ and $\delta(Z)$ are constructed for each block (see Fig. 2) and a four-layer velocity model is derived. A mineral paragenesis with specific composition corresponds to each layer. In each layer, the

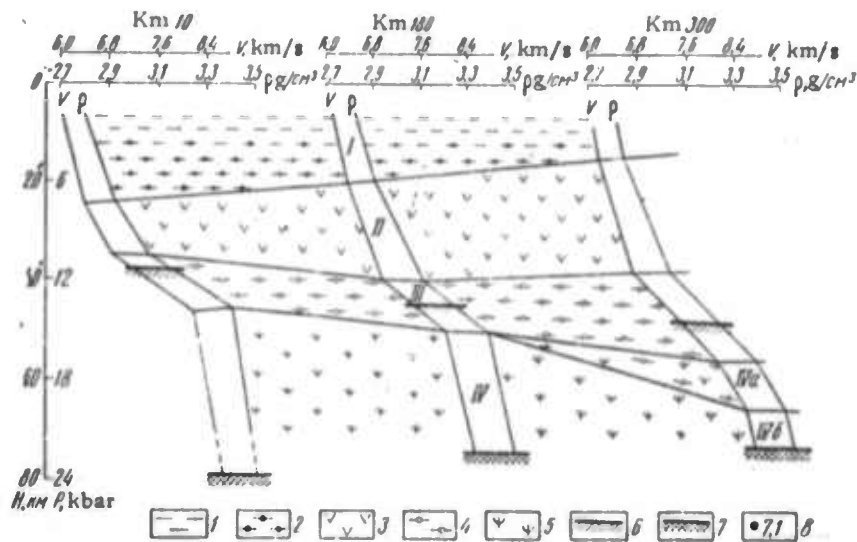


Fig. 2. Crustal and Upper Mantle Velocity and Mineralogical-Petrological Models of the Voronezh Crystalline Massif.

- 1- Facies of green shale; 2- facies of amphibolite;
- 3- facies of basic granulite; 4- facies of charnockite;
- 5- facies of eclogite; 6- Mohorovicic discontinuity (M_1); 7- upper mantle interface M_2); 8- layer velocities.

velocity increase is characterized by a constant vertical gradient dV/dZ which reaches a maximum in the crust-mantle transition layer (layer III). The values determined for dV/dZ exceed laboratory data by increments of

1 and $1.5-1.7 \text{ sec}^{-1}$ for the crust and upper mantle, respectively. dV/dZ increases from the northeast to the southwest in the crust and crust-mantle transitions, while in the upper mantle it increases in the opposite direction. This indicates the existence of different courses in the development of the tectonosphere, related to phases of eclogitization and granitization.

Krylov, S. V., et al. Deep seismic studies in the Transbaykal region. Geologiya i geofizika, no. 12, 1971, 108-112.

The results of deep seismic sounding in the region south of Lake Baykal, which are a continuation of studies begun in the Baykal rift zone in 1968 (Krylov, S. V., et al: Crustal structure along the DSS profile extending across the Baykal rift zone, 1970) are described. The investigations were continued by point seismic sounding along a traverse intersecting the southern margin of the Siberian platform, the Baykal depression and the Baykal mountains characterized by Hercynian, Caledonian and Baikalian folds. (see Fig. 1).

The results of all DSS studies are summarized in the form of a scheme of the Mohorovicic discontinuity structure (Fig. 1) and a seismic (velocity) section along the 700-km-long AG profile (see Fig. 2).

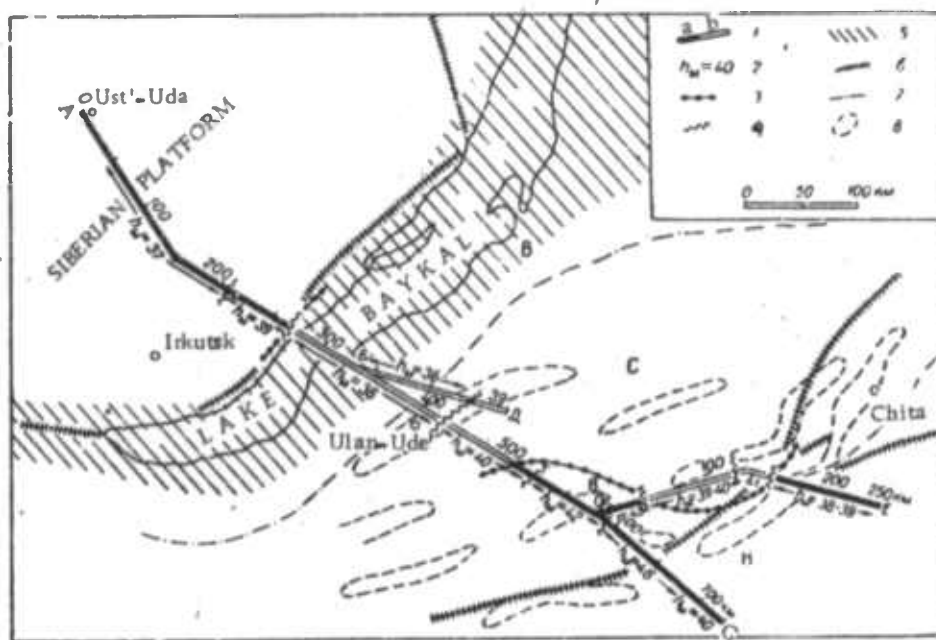


Fig. 1. Outline of the Mohorovicic Discontinuity Structure in the Baykal Rift Zone and Adjoining Regions from DSS Data.

DSS profiles; a- segments with normal Moho discontinuity velocity ($V_r = 8.1$ km/sec), b- segments with low velocity ($V_r = 7.8$ km/sec); 2- averaged depths to the Moho discontinuity (in km); 3- boundary of the low-velocity zone in the Moho discontinuity; 4- segments with sharp escarpments at the Moho discontinuity; 5- the Baykal rift zone (after Solonenko, 1968); 6- major deep-seated faults from geological data; 7- boundaries of folds of different geological age: (B- Baikalian, C- Caledonian, H- Hercyan); 8- boundaries of Mesozoic-Cenozoic basins.

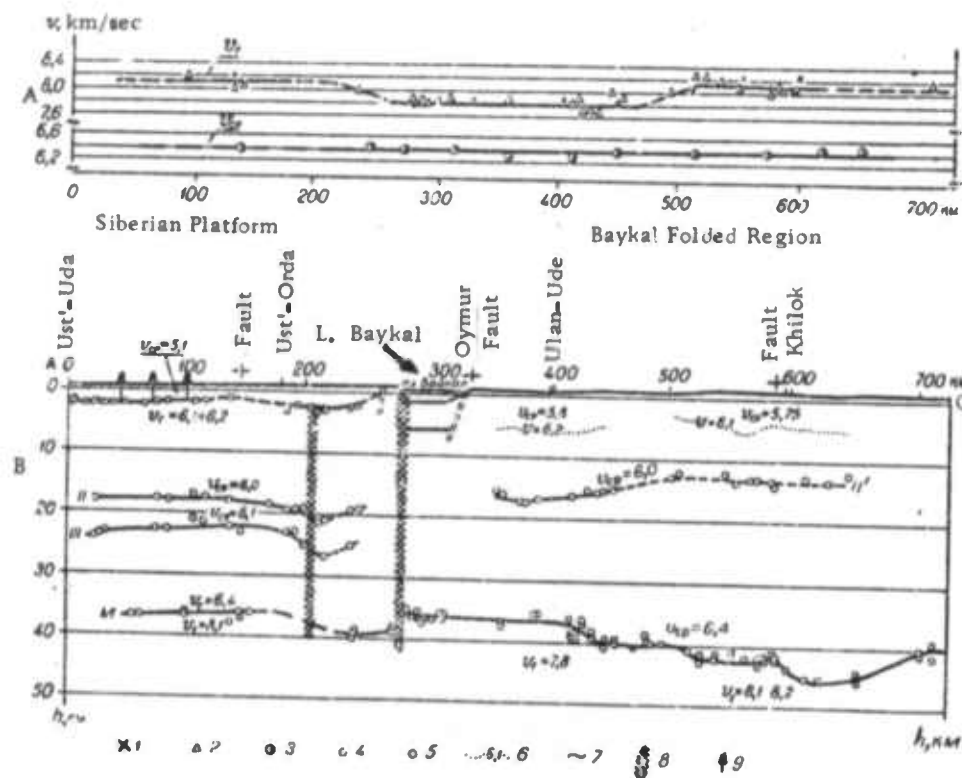


Fig. 2. Mohorovicic Discontinuity Velocity and Average Crustal Velocity (A) and the Seismic (velocity) Section (B) along the AG Profile.

- 1- Moho discontinuity velocity from refraction data;
- 2- the same as 1, determined from refraction and reflection data;
- 3- average crustal velocity from reflection data;
- 4- depths, from refraction data;
- 5- depths, from reflection data;
- 6- lines of equal layer velocities, from refraction data;
- 7- seismic interfaces;
- Φ surface of the basement of the Siberian platform;
- II, III - crustal interfaces, M- Moho discontinuity;
- 8- assumed zones of deep-seated faults;
- 9- bore holes which reach the basement.

The study of a zone of anomalously low upper mantle velocities, revealed by previous DSS work, was continued. This zone extends beyond the Baykal rift zone and over a vast territory. Its northwestern boundaries coincide with the northwestern boundaries of the rift zone, and are located near the northern shore of Lake Baykal. Southeast of Lake Baykal, the zone extends 200-400 km farther and is much wider than the rift zone. Its southeastern boundary is transverse to a large geological paleostructure. In the eastern segment of the BE profile (see Fig. 1), the boundary of the zone coincides with the boundary between the Hercyan and Caledonian folds. Farther to the west (AG profile), the boundary of the zone lies within the Caledonian folds. This nonconformity gives evidence that the zone of low upper mantle velocities was superimposed over older geologic structure.

The crustal structure of the Baykal mountainous region is characterized by the following features: Along the 150-km-long segment of the profile between Lake Baykal and Ulan-Ude (see Fig. 2), the Moho discontinuity occurs at a depth of 36 km, while crustal interface II' lies nearly horizontal at a depth of 16-17 km. Farther to the southeast, the crustal thickness increases stepwise up to 46 km, while interface II' rises to 13 km; thus an inverse relationship of structures occurs at different levels. On the southeasternmost segment of the profile, the crustal thickness sharply decreases to 40 km. The Moho discontinuity relief consists of nearly horizontal segments (100 km and longer) separated by sharp escarpments with heights of 3-4 km. The escarpments of the Moho discontinuity are correlated with Mesozoic and Cenozoic basins. Some basins are located above the segments characterized by abrupt changes in the Moho discontinuity relief. This fact may indicate the existence of deep-seated faults extending to the upper mantle and creating the observed surface structure.

Anomalously low upper mantle velocities as well as high heat flow and anomalously low electric resistivity of rocks, observed in the Baykal rift zone, are suggested to be a consequence of warming up of interior matter due to recent tectonic processes. Gravity anomalies have a complex relationship with the deep structure determined from DSS data, being sometimes uncorrelated or poorly correlated.

Kazinskiy, V. A. Gravity effect of tectonic processes observed in the vicinity of the Kadzharan focal zone. IN: Akademiya nauk SSSR. Doklady, v. 203, no. 3, 1972, 574-577.

Observational data on gravity effects are presented, as obtained in the vicinity of the Kadzharan focal zone (Armenia) by two S-20 gravity variometers during August-October 1970. Simultaneous 8-hour observation periods of air temperature and pressure were also conducted. The temperature and pressure variations do not correlate with the observed gravity variations. Six to eight days prior to the earthquake of 16 October 1970, originating 3-4 km from the observation unit, $W_{\Delta}(t)$ curves obtained by both gravimeters (located 1 meter apart) show an upward trend, while $2W_{xy}(t)$ curves show a downward trend (Fig. 1 a, b). In Fig. 1, the measurements are given separately for each variometer (a and b) and for each recording system (I and II). It is concluded that the observed variations of W_{Δ} and $2W_{xy}$ are induced by tectonic processes preceding an earthquake.

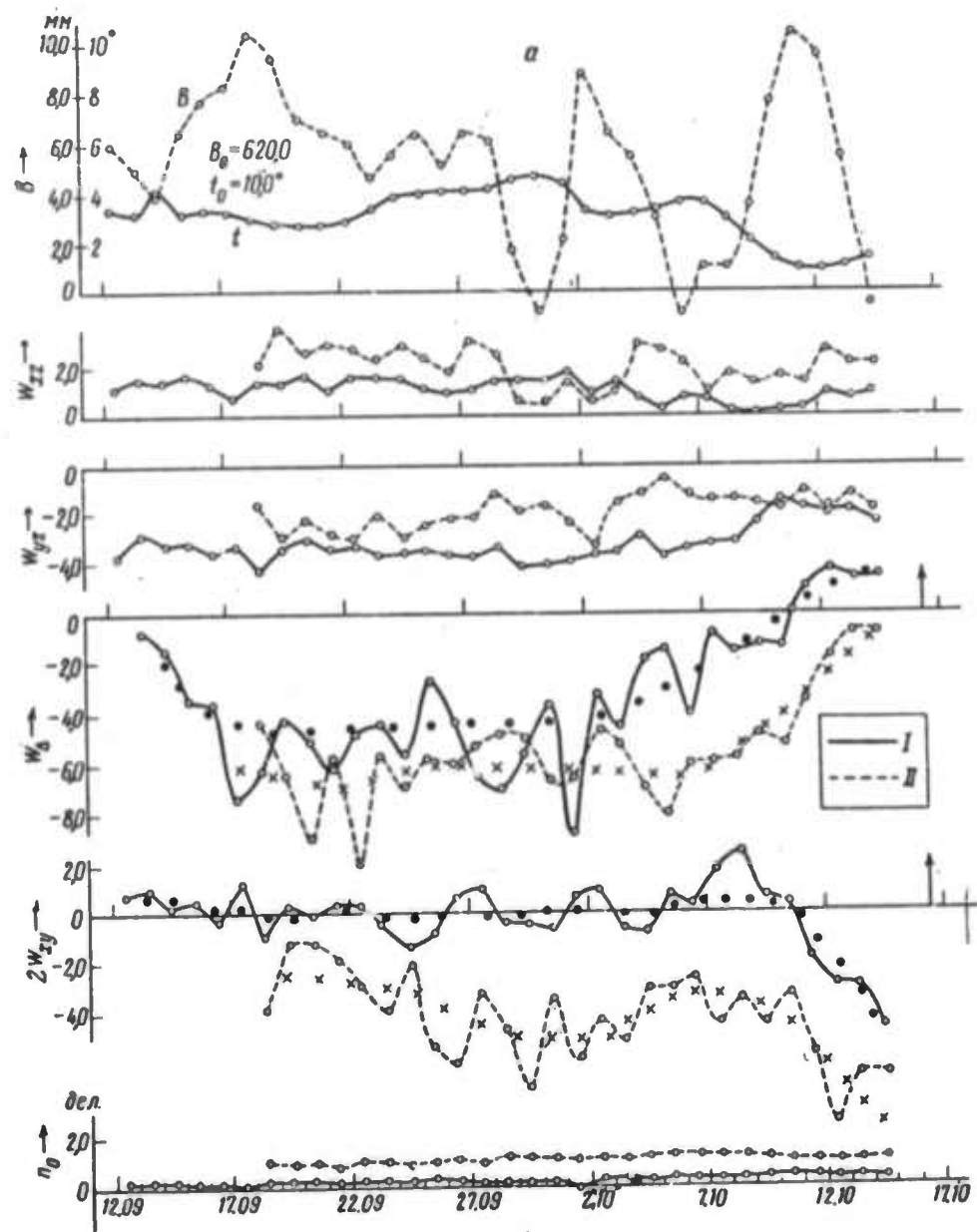


Fig. 1. Variation of Temperature t , Pressure B , and Mean Diurnal Values of Derivatives W_{xz} , W_{yz} , W_Δ and $2W_{xy}$ (vertical arrow indicates time of earthquake occurrence).

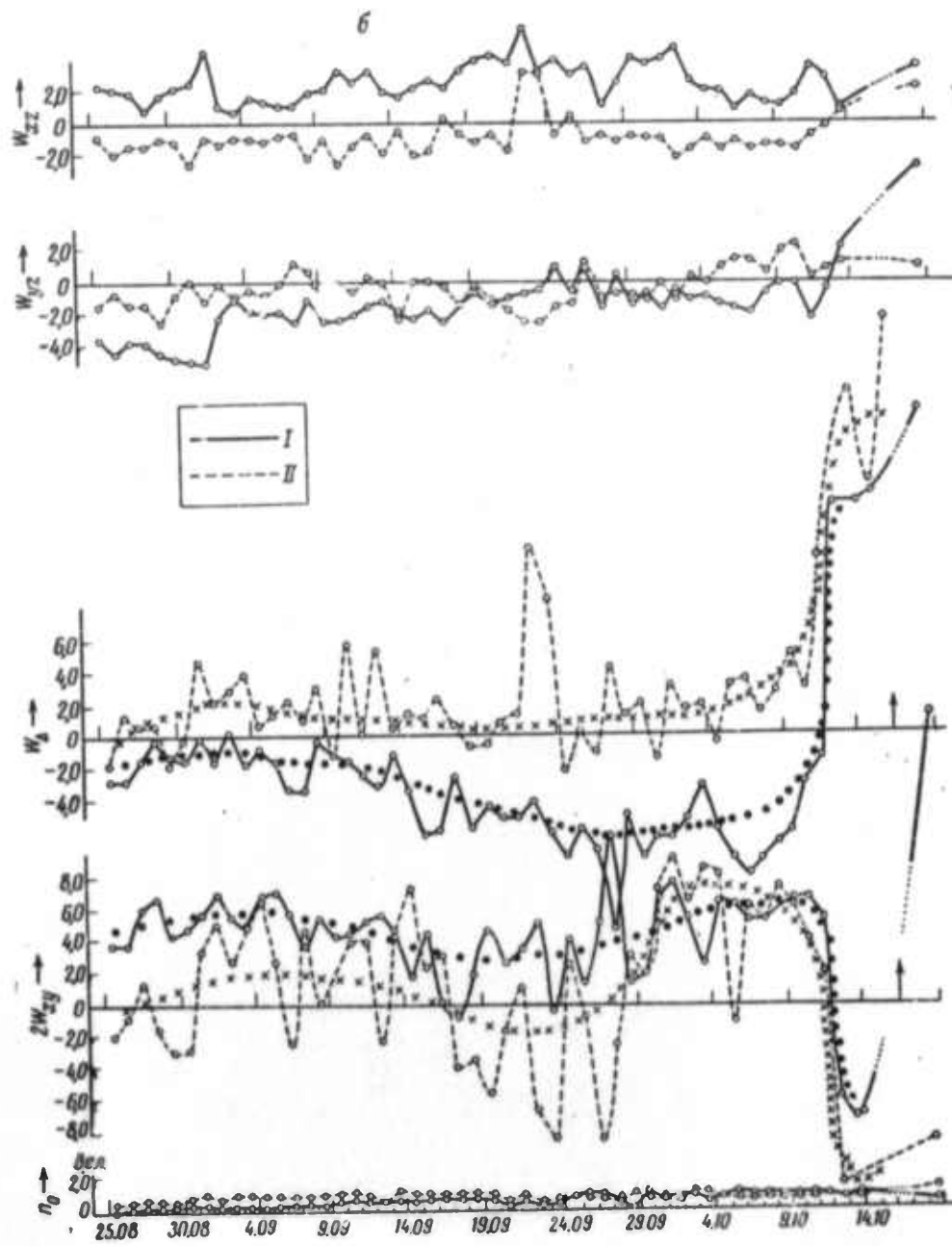


Fig. 1. (continued)

Puzyrev, N. N. General problems of the correlation of seismic waves. IN:
Akademiya nauk SSSR. Sibirskoye otdeleniye.
Institut geologii i geofiziki. Diskretnaya korrelyatsiya seysmicheskikh voln (Discrete correlation of seismic waves). Novosibirsk, Izd-vo Nauka, 1971, 3-15.

A classification of the methods of correlation of seismic waves is proposed, based on the use of a priori information on the wave field, elastic parameter distribution, and geology of the region under study. The methods of correlation of seismic waves are classified as:

1) Positional correlation - defined as tracing of waves by successively comparing their waveform and amplitude in the x, t plane, without using a priori information.

2) Discrete correlation - defined as the tracing waves requiring a priori information.

In contrast to wave correlation, as defined by Gamburtsev (1946), the generalized positional correlation does not require small distances between receivers, established source positions, and exclusively tracing waves (or their phases). In contrast to the previous case, the cophasal axis criterion is not considered necessary. Transpositional correlation, as defined by Gamburtsev (1946), is considered as a particular case of a generalized positional correlation or discrete correlation. The reciprocity condition is not considered necessary in this case. Thus, transpositional correlation is considered to be applicable to asymmetric waves with the introduction of some information on symmetric waves with similar ray geometry. The condition for transpositional correlation of the PPS wave, with information on the PPP wave, is written in the form $T_{12} + t_{01}^{PSS} - t_{01}^{PPP} = T_{21} + t_{02}^{PPS} - t_{02}^{PPP}$.

Two major types of discrete correlation are: 1) discrete wave correlation which uses mainly wave characteristics as criteria, while parametric and geologic characteristics are used only qualitatively and to a lesser extent; and 2) general discrete correlation which to the same degree uses parametric and geological characteristic of the region as criteria as well. It is noted that under actual conditions, the correlation of seismic waves represents a combination of positional and discrete methods.

TRANSLATION

Aksenovich, G. I., R. M. Gal'perina,
Ye. I. Gal'perin, and I. L. Nersesov.
Experience and results of stationary
seismological observations performed in
a deep borehole. Akademiya nauk SSSR.
Doklady, v. 198, no. 4; 1971, 813-815.

Pronounced improvements in sensor sensitivity are required for the study of seismic conditions in large industrial cities in seismically active zones. One method of heightening the sensitivity is to place the seismograph in a deep borehole away from the day surface ^{1, 2}.

Valuable experience applicable to the study of wave fields in internal media points (boreholes) was gained in the seismic prospecting frequency range while developing a method of vertical seismic profiling ³. The method allows a shift to much lower frequencies for stationary seismic observations in deep boreholes.

Preliminary results are presented in this report of test surveying in a deep borehole in Alma-Ata. The currently observed lull in seismic activity drastically hampers seismic studies in this area and emphasize the need for performing such studies. An abandoned borehole (number 10G) in the northeastern outskirts of Alma-Ata was used. This 3200-meter deep borehole is now accessible only down to 2000 meters. The observation conditions in the borehole were below expectations owing to technical problems. Observations were made for about one year between 1968 and 1969. Of the more than 1000 earthquakes detected, about 100 were weak and local ($\Delta t_{S-P} < 13$ sec, including about 15 with a $\Delta t_{S-P} \leq 3$ sec).

A displacement seismograph was used with a flat frequency response between 1.5 and 8-10 Hz. Octave resonance filter recordings were also made on various frequencies. Peak frequencies were 1.5, 3.0, 6.0 and 12 Hz. The signal was transmitted to the day surface by a four-conductor armored logging cable shielded by teflon. Results show that:

1) Underground background seismic noise attenuated more rapidly than the useful signal. Despite the unfavorable survey conditions, seismograph sensitivity at borehole depths was usually restricted by electric rather than seismic noise. Highly variable with time, the electric noise was normally confined to the interval between 2100 and 0200 hours. The optimum recording time was at night when the noise level decreased (Fig. 1). At night the seismograph could be amplified to 2×10^5 .

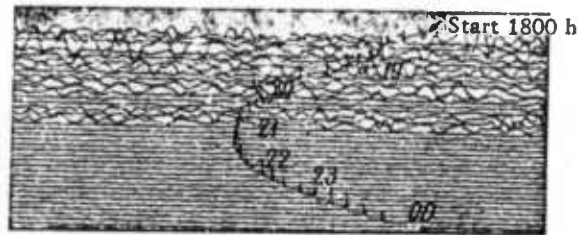


Fig. 1. Electric noise background.

2) The most intense seismic background noise levels on the borehole seismograms usually appeared during severe storms at Issyk-Kul. The noise level was however much lower than that at the day surface (Fig. 2).

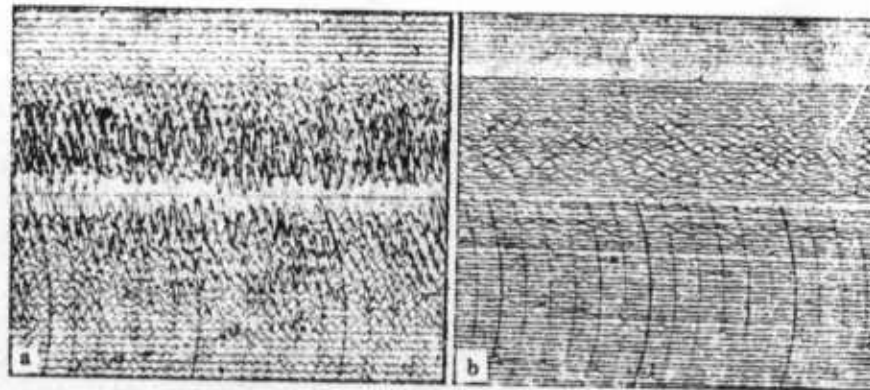


Fig. 2. Microseismic noise from a storm at Issyk-Kul, a - ground level, b - borehole seismogram.

3) Simultaneous recordings from the borehole site and the Alma-Ata Seismographic Station were difficult to compare. Most of the quakes detected by the borehole site were not recorded at Alma-Ata (Fig. 3). Borehole seismograms were indistinct for certain earthquakes that were readable on the Alma-Ata Station seismograms.

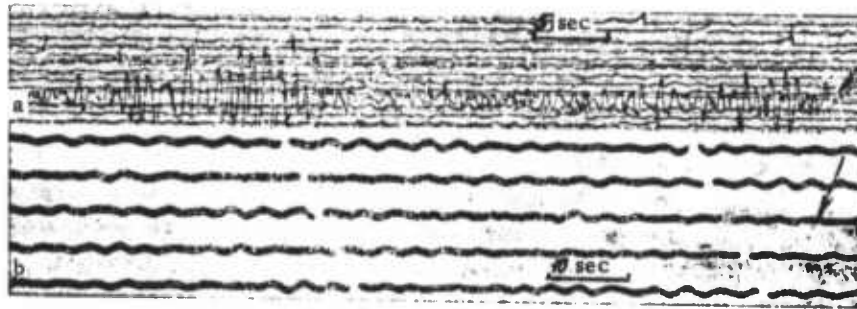


Fig. 3. Earthquake detected at 1357 hours, 15 February 1969; a - borehole, b - Alma-Ata Station seismogram. The arrows denote P-wave arrival.

4) A comparison of borehole recordings with those of the Talgar Seismographic Station, located 25 km from Alma-Ata in a favorable seismic zone, reveals that one-fourth of the borehole recorded earthquakes were detected in the final six weeks of monitoring when the seismograph instruments were more sensitive due to significant reductions in electric noise. (The Talgar seismometers are installed in a 100-meter adit in crystalline rock). Most of the local earthquake recordings in the borehole were of equal or higher intensity than those made at the Talgar Station (Fig. 4). Several earthquakes were detected exclusively by the borehole equipment.

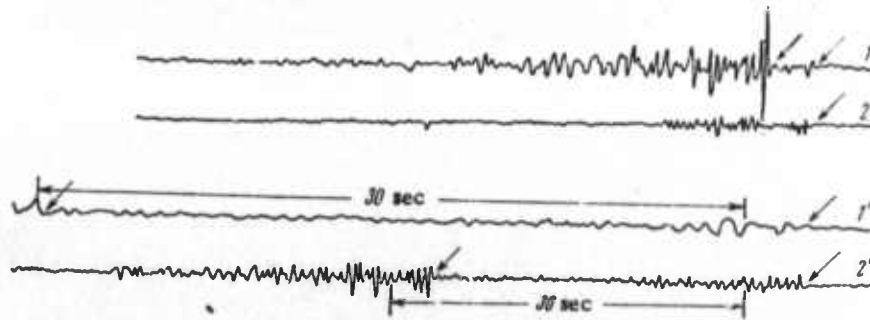


Fig. 4. Recordings of weak local (1, 2) and near (1', 2') earthquakes at 0506 hours (1, 2) and 0358 hours (1', 2') on 11 March 1969 by a borehole site (1, 1') and a ground station (2, 2'). Arrows show the arrival of P and shear waves.

5). Comparison of local earthquake recordings from the borehole site with those of ground stations (located outside the city limits in a favorable seismic zone but on sedimentary rock 2 to 3 km thick) shows that the borehole site detected 30% more earthquakes during the final weeks of observations.

Results verify the feasibility of setting up highly sensitive seismometer sites in deep boreholes on the outskirts of a city for the seismic monitoring of large cities in seismically-active zones.

BIBLIOGRAPHY

1. Tatel, N. E., and M. A. Tuve. In honor of Bena Gutenberg, London, 1958, 152.
2. Takano, K., and T. Haciwaka. Bulletin of the Earth Research Institute, v. 44, 1966, 1135.
3. Gal'perin, Ye. I. VAN SSSR, no. 1, 1966.

B. Recent Selections

Belyayevskiy, N. A. Results of crustal studies by explosion seismology methods (conference). Sovetskaya geologiya, no. 11, 1972, 137-142.

Beranek, B., et al. Chapter II; Deep seismic sounding results by country: Czechoslovakian Socialist Republic. IN: Komissiya mnogostoronnego sotrudничества Akademiy nauk sotsialisticheskikh stran..., et al. Stroyeniye zemnoy kory tsentral'noy i yugo-vostochnoy Evropy; po dannym vzryvnay seysmologii (Crustal structure of central and southeastern Europe; based on explosion seismology data). Kiyev, Izd-vo Naukova dumka, 1971, 182-204.

Borisov, A. A., and G. A. Shenkareva. Seismological and geophysical characteristics of the Caucasus and western Central Asia. Moskovskoye obshchestvo ispytateley prirody. Byulleten'. Otdel geologii, v. 47, no. 6, 1972, 5-16.

Chamo, S. S., et al. Stratification of the crystalline basement of the Russian platform, based on seismic data. IN: Moskovskoye obshchestvo ispytateley prirody. Otdel geologii, v. 47, no. 5, 1972, 72-77.

Dachev, Khr., et al. Chapter II; Deep seismic sounding results by country: People's Republic of Bulgaria. IN: Komissiya mnogostoronnego sotrudничества Akademiy nauk sotsialisticheskikh stran..., et al. Stroyeniye zemnoy kory tsentral'noy i yugo-vostochnoy Evropy; po dannym vzryvnay seysmologii (Crustal structure of central and southeastern Europe; based on explosion seismology data). Kiyev, Izd-vo Naukova dumka, 1971, 47-61.

Fomenko, K. Ye. Deep structure of the Cis-Caspian depression, based on geological and geophysical data. IN: Moskovskoye obshchestvo ispytateley prirody. Byulleten'. Otdel geologii, v. 47, no. 5, 1972, 103-111.

Garkalenko, I. A. Chapter II; Deep seismic sounding results by country: Deep seismic results for the Black Sea. IN: Komissiya mnogostoronnego sotrudничества Akademiy nauk sotsialisticheskikh stran..., et al. Stroyeniye zemnoy kory tsentral'noy i yugo-vostochnoy Evropy; po dannym vzryvnoy seysmologii (Crustal structure of central and southeastern Europe; based on explosion seismology data). Kiyev, Izd-vo Naukova dumka, 1971, 219-231.

Khain, V. Ye., and V. I. Slavin. Chapter I; Concise characteristics of the geological structure of central and southeastern Europe. IN: Komissiya mnogostoronnego sotrudничества Akademiy nauk sotsialisticheskikh stran..., et al. Stroyeniye zemnoy kory tsentral'noy i yugo-vostochnoy Evropy; po dannym vzryvnoy seysmologii (Crustal structure of central and southeastern Europe; based on explosion seismology data). Kiyev, Izd-vo Naukova dumka, 1971, 12-46.

Knote, Kh. Chapter II; Deep seismic sounding results by country: German Democratic Republic. IN: Komissiya mnogostoronnego sotrudничества Akademiy nauk sotsialisticheskikh stran..., et al. Stroyeniye zemnoy kory tsentral'noy i yugo-vostochnoy Evropy; po dannym vzryvnoy seysmologii (Crustal structure of central and southeastern Europe; based on explosion seismology data). Kiyev, Izd-vo Naukova dumka, 1971, 84-99.

Konstantinesku (Constantinescu), P., and I. Kornya. Chapter II; Deep seismic sounding results by country: Socialist Republic of Rumania. IN: Komissiya mnogostoronnego sotrudничества Akademiy nauk sotsialisticheskikh stran..., et al. Stroyeniye zemnoy kory tsentral'noy i yugo-vostochnoy Evropy; po dannym vzryvnoy seysmologii (Crustal structure of central and southeastern Europe; based on explosion seismology data). Kiyev, Izd-vo Naukova dumka, 1971, 108-115.

Lin'kov, Ye. M., et al. Results of a study on seismometer zero-point drift. IN: Leningradskiy universitet. Uchenyye zapiski, no. 366, 1972, 201-223.

Lopatina, N. P., and V. Z. Ryaboy. Velocity and density discontinuities in the upper mantle of the USSR. IN: Akademiya nauk SSSR. Doklady, v. 207, no. 2, 1972, 337-340.

Mitukh, E., and K. Pozhgay. Chapter II; Deep seismic sounding results by country: Hungarian People's Republic. IN: Komissiya mnogostoronnego sotrudничества Akademiy nauk sotsialisticheskikh stran..., et al. Stroyeniye zemnoy kory tsentral'noy i yugo-vostochnoy Evropy; po dannym vzryvnoy seysmologii (Crustal structure of central and southeastern Europe; based on explosion seismology data). Kiyev, Izd-vo Naukova dumka, 1971, 61-84.

Mitukh, E., et al. Chapter III; Deep seismic sounding results for international profiles. IN: Komissiya mnogostoronnego sotrudничества Akademiy nauk sotsialisticheskikh stran..., et al. Stroyeniye zemnoy kory tsentral'noy i yugo-vostochnoy Evropy; po dannym vzryvnoy seysmologii (Crustal structure of central and southeastern Europe; based on explosion seismology data). Kiyev, Izd-vo Naukova dumka, 1971, 232-244.

Prosen, D., et al. Chapter II; Deep seismic sounding results by country: Socialist Federative Republic of Yugoslavia. IN: Komissiya mnogostoronnego sotrudничества Akademiy nauk sotsialisticheskikh stran..., et al. Stroyeniye zemnoy kory tsentral'noy i yugo-vostochnoy Evropy; po dannym vzryvnay seysmologii (Crustal structure of central and southeastern Europe; based on explosion seismology data). Kiyev, Izd-vo Naukova dumka, 1971, 204-219.

Prozorov, A. G., and Ye. Ya. Rantsman. Earthquake statistics and the morphostructure of eastern Central Asia. IN: Akademiya nauk SSSR. Doklady, v. 207, no. 2, 1972, 341-344.

Sobin, O. A. Experimental studies of the destruction zone in excavating prospecting trenches by cratering explosions. IN: IVUZ. Geologiya i razvedka, no. 11, 1972, 120-122.

Sollogub, V. B., and A. V. Chekunov. Chapter II; Deep seismic sounding results by country: Ukrainian Soviet Socialist Republic. IN: Komissiya mnogostoronnego sotrudничества Akademiy nauk sotsialisticheskikh stran..., et al. Stroyeniye zemnoy kory tsentral'noy i yugo-vostochnoy Evropy; po dannym vzryvnay seysmologii (Crustal structure of central and southeastern Europe; based on explosion seismology data). Kiyev, Izd-vo Naukova dumka, 1971, 116-182.

Sollogub, V. B., and A. V. Chekunov. Chapter IV; General conclusions on methodology. IN: Komissiya mnogostoronnego sotrudничества Akademiy nauk sotsialisticheskikh stran..., et al. Stroyeniye zemnoy kory tsentral'noy i yugo-vostochnoy Evropy; po dannym vzryvnay seysmologii (Crustal structure of central and southeastern Europe; based on explosion seismology data). Kiyev, Izd-vo Naukova dumka, 1971, 245-256.

Subbotin, S. I., et al. Chapter V; Certain problems of the structure and evolution of the crust. IN: Komissiya mnogostoronnego sotrudничества Akademiy nauk sotsialisticheskikh stran..., et al. Stroyeniye zemnoy kory tsentral'noy i yugo-vostochnoy Evropy; po dannym vzryvnay seysmologii (Crustal structure of central and southeastern Europe; based on explosion seismology data). Kiyev, Izd-vo Naukova dumka, 1971, 257-281.

Teisseyre, R. Micromorphic mechanics of processes in an earthquake source zone. IN: Academie polonaise des sciences. Bulletin. Serie des sciences de la terre, v. 20, no. 3, 1972, 227-232. (In English)

Troyan, V. N. Resolution in optimum reception of seismic waves with curvilinear cophasal axes. IN: Leningradskiy universitet. Uchenyye zapiski, no. 366, 1972, 194-201.

Troyan, V. N. Statistical methods of separating seismic waves with parabolic cophasal axes. IN: Leningradskiy universitet. Uchenyye zapiski, no. 366, 1972, 244-248.

Ukhman, Ya. Chapter II; Deep seismic sounding results by country: Polish People's Republic. IN: Komissiya mnogostoronnego sotrudничества Akademiy nauk sotsialisticheskikh stran..., et al. Stroyeniye zemnoy kory tsentral'noy i yugo-vostochnoy Evropy; po dannym vzryvnay seysmologii (Crustal structure of central and southeastern Europe; based on explosion seismology data). Kiyev, Izd-vo Naukova dumka, 1971, 99-108.

Volarovich, M. P., et al. Tectonic conditions for the serpentinization of ultrabasites of the Voronezh crystalline massif, based on studies of elastic wave velocities in rock samples under pressures to 25 kbar.
Akademiya nauk SSSR. Izvestiya. Seriya geologicheskaya, no. 12, 1972, 77-86.

Volkov, I. Ye., and T. B. Yanovskaya. Distribution characteristics of P wave amplitudes. IN: Leningradskiy universitet. Uchenyye zapiski, no. 366, 1972, 137-147

4. Particle Beams

A. Abstracts

Mkheidze, G. P., and M. D. Rayzer.

Pulse generator of powerful electron beams. KSpF, no. 4, 1972, 41-45.

A description and test results are given for an electron beam generator with a pulsed current of 20 ka and 20 nsec duration, and an electron energy of 600 kev (Fig. 1). The test pulsed voltage generator

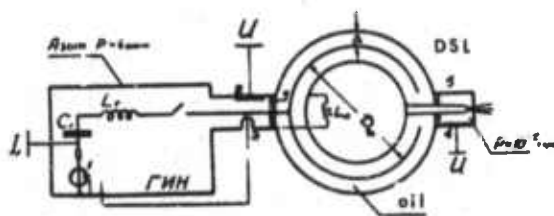


Fig. 1. Experimental sketch

- 1 - ferromagnetic core transformer;
- 2, 4 - capacitive detectors;
- 3 - commutating discharger;
- 5 - bushings.

was a Marx-type condenser impact circuit situated in a 90 cm diameter and 240 cm long tank, filled with nitrogen at 4 atm. The generator consisted of 22 condensers, connected in two sections, with two series-connected condensers in each section. Parameters were: pulse capacitance ≈ 5000 pf, inductance $\approx 2.8\mu\text{h}$, wave resistance ≈ 24 ohms. At an 800 kv pulsed voltage, the system energy capacity was ~ 1.5 joules/dm³. Energy stored in the condenser circuit was used for charging the double shaping line (DSL), made-up of two parallel-connected double-strip lines immersed in castor oil ($\epsilon = 4$). The strip lines were semi-circular, and the whole configuration had a barrel-like shape with a 115 cm diameter and 60 cm height. DSL parameters were: bandwidth-25cm, thickness - 4 cm, gap - 4 cm, line length $l = \pi D/2 \approx 150$ cm, ($\tau = 20$ nsec), capacitance ≈ 2000 pf, and wave resistance ≈ 21 ohms. The commutating discharger operated at the moment

when the voltage U_{DSL} reached a maximum in two regimes: self-breakdown and trigatron ignition. The field emission cathode was stainless steel, 30 mm in diameter and 3 mm thick with 10 2-mm diameter through holes. The cathode chamber pressure was $\sim 10^{-5}$ torr. The anode comprised a titanium foil or stainless steel screen of 10×10 mm² dimension. The gap between anode and cathode was 10 mm. Electron beam current was measured directly in the anode by a shunt resistance in coaxial operation (time constant ≤ 4 nsec). The electron energy flow was measured by a calorimeter, and the electron energy by a magnetic analyser. Fig. 2

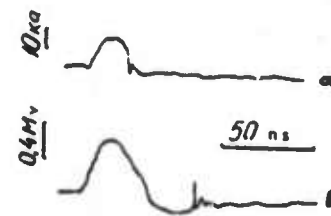


Fig. 2. Typical oscilloscopes
of beam current (a) cathode and
voltage, (b)

shows typical oscilloscopes of cathode voltage and beam current at $U_g = 600$ kv, using a screen anode. The maximum current attained 17 ka, the pulsed current width at mid-height was 20 nsec, and electron energy was 200 joules. Magnetic analyser measurements show the presence of two accelerated particle groups: one with an energy $\epsilon_1 \approx 600$ kev (spectrum width ± 60 kev) and the other with $\epsilon_2 \approx 80$ kev (spectrum width ± 20 kev). Beam current measured in the 50μ thick titanium foil anode showed that the electron current $\epsilon_2 \approx 80$ kev was approximately 12% of total electron current. At $U_g = 600$ kv the shaping line was charged to $U_{DSL} \approx 750$ kev, and the electron energy was $\epsilon_1 \approx 600$ kev. This discrepancy in experimental results, according to the authors, is due to the high resistance of the commutating discharger (discharge channel resistance at a 3.5 cm gap length ≈ 10 ohms, and voltage drop of $U \approx 150-200$ kv). The reason for the appearance of the second group of accelerated electrons ($\epsilon_2 \approx 80$ kev) was not evident from the experimental data.

Tkach, Yu. V., Ya. B. Faynberg, I. I.
Magda, V. D. Shapiro, V. I. Shevchenko,
A. I. Zykov, Ye. A. Lemberg, I. N. Mondrus,
and N. P. Gadetskiy. Collective processes
during high-current relativistic beam transmission
through gas and plasma. ZhETF P, v. 16, no. 7,
1972, 368-371.

Relativistic beam transmission through a 3-meter chamber filled with nitrogen was studied at a pressure of 10^{-2} to 20 torr. A plasma with a density of 10^{12} to $5 \times 10^{13} \text{ cm}^{-3}$ was generated from the collective effects of field ionizations excited by an oscillation beam. The electron beam was compensated by both the charge and the current. Plasma reverse current was 70 to 80 percent of the beam current. Electron beam parameters were: current to 60 ka; electron energy to 1 Mev; energy spread ~ 20 percent; and pulse duration 3×10^{-8} sec. Beam transmission is illustrated in Fig. 1 under the conditions: a) beam current - 30 ka, pressure - 2×10^{-1} torr; a typical periodical structure with constrictions 3 mm in radius along the beam length was observed with a beam relaxation period of the order of 40 to 50 cm; b) beam current - 50 ka, pressure - 4×10^{-1} torr. Beam macroscopic instability develops; this "hose-type" instability led to lateral beam shifts and the formation of "flat kite" type disturbances; c) beam current - 55 ka, pressure - 1 torr.

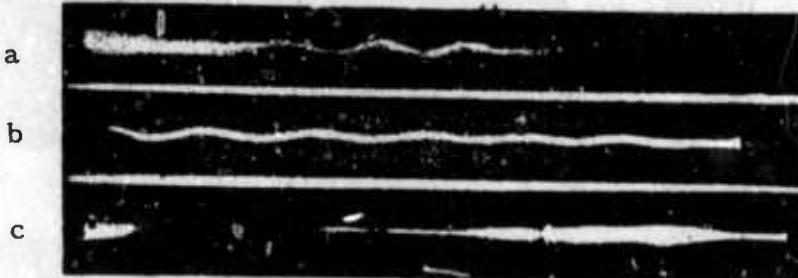


Fig. 1. Electron relativistic beam transmission through gas under varying conditions.

Experiments were made with oscillations induced by hydrodynamic instability during plasma interaction with the modulated relativistic beam. Self-modulations generated during beam interaction with the periodic structure of an iris waveguide sector one meter in length were used for the modulation of high-current beams; the structure was designed for frequencies of 2500 to 2800 MHz and an attenuation of ≈ 0.7 . The length of the waveguide sector in which increased oscillations occurred was $\approx 20-30$ cm, considerably shorter than the length of the sector itself. High-intensity uhf oscillations were generated with a resonance frequency level to 10^7 and a duration of 2×10^{-8} sec. Diagrams of the discharge and modulation apparatus are included.

Kramskoy, G. D., V. I. Kurliko, and
V. A. Shendrik. Theory of lateral beam
instability in an isolated section of a linear
electron accelerator. UFZh, v. 17, no. 10,
1972, 1608-1616.

Lateral beam instability is analyzed in accelerators with long accelerating structures for the conditions $T_p \ll T_f$, where T_p is the particle transit time through the structure ($T_p = L/V_0$; L - system length, V_0 - particle velocity), and T_f is the instability build-up time, equal to the current pulse duration τ_i . A theory is developed for the beam instability in an isolated section owing to the Cerenkov radiation of defocusing axially-asymmetrical waves by beam bunches. Analytical expressions are derived for relationships of bunch lateral displacement to bunch number and the isolated section parameters. Conditions are specified for lateral instability development, and threshold currents are determined. It was noted that in the absence of an accelerating field, the threshold current

was 50 ma, which was approximately 1.3 times less than an experimental critical current value of 67 ma. The threshold and critical currents increased upon application of an accelerating field. The authors point out that for comparison with an experiment in which only critical, and not threshold, current is measured, it is necessary to know the relationship of lateral deviation to the bunch number.

Bol'shakov, V. N. Discharge of an inductive energy storage for obtaining a fast-rise pulse. Elektrichestvo, no. 1, 1972, 56-60.

The author notes that in high current dischargers, capacitive storage is generally preferred over inductive owing to the coupling problems encountered in typical inductive storage. He suggests ways in which the latter difficulties might theoretically be minimized, so as to make inductive storage more attractive in view of its lower cost and size for a given energy capacity. The problem is analyzed for both direct- and transformer-coupled loads, in terms of the two main criteria of delivered power-to-source power ratio and circuit efficiency. Examples are given using simplified equivalent L-R circuits with load circuit interruption.

Katsaurov, L. N. Possibility of using fog particles as a target or acceleration medium.
KSpF, no. 10, 1971, 56-63.

The feasibility is investigated of using fog-particle jets as fine structure targets for contemporary high-current accelerators. The accelerated beam bombards a target particle, heats it and produces additional evaporation of fog droplets in vacuum. To prevent target particle evaporation before passing through the full width of the bombarding beam, the condition $v > I$ must be fulfilled, where v is the particle velocity accelerated by the difference in potential; this velocity is limited by the maximum possible potential of particle charging and I is the current density of the accelerated beam. At a given target thickness the current density is limited by the required maximal capacity of the pump used for maintaining the vacuum. Both linear and cyclic methods of fog particle acceleration are described. The energy of the atomic nucleus is a function of the particle radius r , and is much smaller than the numerical value of the accelerating potential. Each accelerated particle is equivalent to the impulse current I . For ice particles with $r = 10^{-5}$ cm and an accelerating potential of $v = 10^3$ kv, the current is $I = 20$ a. The current pulse duration for these particles equals $\tau_u \cong 10^{-12}$ sec and the current density $I_1 \cong 10^{11}$ a/cm².

When two accelerated fog particles collide and come to rest, a bunch may be generated with a temperature corresponding to the collision energy; and at a velocity expansion rate (disintegration) of $\sim 10^8$ cm/sec a considerable number of nuclear reactions may occur during this process. The author predicts that a neutron yield of 10^{13} neutrons/sec using per 1 kw of beam power could be obtained at $r = 10^{-2}$ cm.

Vavilov, S. P. Determining the plasma expansion rate in a cathode flare during pulsed electric breakdown of millimeter vacuum gaps. IVUZ Fiz, no. 9, 1972, 139-140.

An explosive emission experiment is described in which plasma jet velocity was measured at high voltage and discharge current values. The wire needle cathodes used were 1 mm in diameter; Fig. 1 is a schematic of the circuit. The negative pulsed voltage applied to a

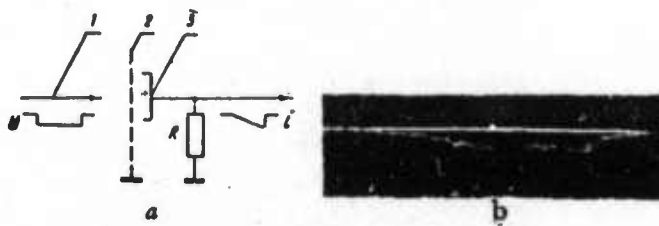


Fig. 1 a) Experimental setup. 1- cathode needle; 2- metal grid; 3 - collector; u, i- collector voltage and electron current.

Fig. 1 b) Typical current oscillogram.

cathode point reached 200 kv, and discharge currents attained 3 ka. Plasma velocity was determined by measuring the current pulse duration T_i in the collector ($v = d/T_i$, where d is the distance between the cathode and the grid). Experiments were conducted at cathode-grid gaps of 1 to 7 mm. Experimental results a molybdenum-cathode are given in Fig. 2. It was seen that the voltage

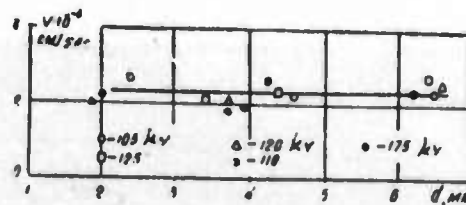


Fig. 2. Relationship between plasma velocity and cathode-grid gap.

had a negligible effect on plasma velocity. Plasma velocities for Al, Mo and Cu cathodes were 2.4×10^6 , 2.2×10^6 and 2.4×10^6 cm/sec, respectively, indicating that the cathode materials also only slightly affected the plasma motion. The author concludes that plasma motion in a cathode flare during a vacuum discharge has a specific velocity independent of the voltage and field intensity; in this case the gradient exceeded 10^8 volt/cm at cathode tip radii of 5-10 μ .

B. Recent Selections

Abramyan, Ye. A., S. B. Vasserman, V. M. Dolgushin, O. P. Pecherskiy, and V. A. Tsukerman. Pulsed accelerator of charged particles. Author's certificate, USSR no. 304895, published March 15, 1972. (RZh Elektr, 12/72, no. 12A391 P)

Akhiyezer, I. A., and V. T. Lazurik-El'tsufin. Dynamic effect from passage of charged particle beams in solids. ZhETF, v. 63, no. 5, 1972, 1776-1779.

Aleynikov, M. S., R. P. Ivanchenkov, V. A. Kochegurov, A. A. Novikov, and V. V. Tsygankov. Problems of automatic optimization in charged particle accelerators. Review. IN: Tr. IV Vses. soveshch. po avtomat. upr. (tekhn. kibernet), 1968. Upr. proiz-vom. Moskva, nauka, 1972, 232-233. (RZh Elektr, 12/72, no. 12A379)

Anishchenko, N. G., N. I. Balalykin, V. A. Vasil'yev, Yu. S. De'endyayev, A. G. Zel'dovich, N. K. Zel'dovich, Yu. V. Muratov, N. B. Rubin, A. A. Sabayev, V. P. Sarantsev, Yu. I. Smirnov, V. G. Shabratov, and Yu. A. Shishov. Progress in developing the accelerator section of a koltsetron. IN: Tr. 2-go Vses. soveshch. po uskoritelyam zaryazhen.chastits, 1970. T. 1, Moskva, nauka, 1972, 221-224. (RZh Elektr, 12/72, no. 12A356)

Bondarenko, B. V., V. I. Makukha, and A. S. Gaydarov. Investigating knife-edge field emitters of disc-like form. RiE, no. 12, 1972, 2634-2637.

Brodskaya, B., G. Trapido, and M. Gubergrits. Light flash intensity and electrical characteristics of high current pulse discharges in electrolytes of different chemical composition.

IAN Est. Khimiya, geologiya, v. 21, no. 4, 1972, 375-378.

Davydov, B. B. Study of the cathode region of a pulsed discharge.
IAN Az. Ser. fiz-tekh. i mat. nauk, no. 2, 1972, 136-140.

Demirkhanov, R. A.; A. K. Gevorkov, A. F. Popov, and O. A. Kolmakov. Investigating the heating mechanism of the electron component of a plasma at unstable beam conditions in a mirror trap.
ZhETF, v. 63, no. 5, 1972, 1653-1663.

Dustman, G., V. Khaynts, G. Germann, P. Kappe, G. Kraut, L. Shteynbok, and L. Tsernial'. Status of the ring electron accelerator project in Karlsruhe. IN: Tr. 2-go Vses. soveshch. po uskoritelyam zaryazhen. chastits, 1970. v. 1, Moskva, nauka, 1972, 214-213.
(RZh Elektr, 12/72, no. 12A357).

Grishayev, I. A., A. N. Dovbnya, and V. V. Petrenko. Method of obtaining charged particle bunches in linear accelerators. Author's certificate, USSR no. 322138, published March 27, 1972. (RZh Elektr, 12/72, no. 12A397 P)

Grishayev, I. A., V. D. Krasnikov, and T. F. Nikitina. Method of phasing the accelerating sections of a linear accelerator. Author's certificate, USSR no. 328531, published April 3, 1972. (RZh Elektr, 12/72, no. 12A395 P)

Ivanov, A. A., V. V. Parail, and T. K. Soboleva. Nonlinear interaction theory of a monoenergetic beam with a dense plasma. ZhETF, v. 63, no. 5, 1972, 1678-1685.

Ivanov, V. G., and T. P. Smirnova. Breakdown phenomenon in p-Ge field emitters. FTT, no. 10, 1972, 3068-3070.

Kazanskiy, L. N. A. A. Kolomenskiy, G. O. Meskhi, and B. N. Yablokov. A heavy-current direct-action electron pulse accelerator. IN: Tr. 2-go Vses. soveshch. po uskoritelyam zaryazhen. chastits, 1970. T. 1. Moskva, nauka, 1972, 95-97. (RZh Elektr, 12/72, no. 12A384)

Kolesnikov, L. M. Elektrodinamicheskoye uskorenienye plazmy. (Electrodynamic acceleration of plasma). Atomizdat, 1971, 390 p. (JPRS USSR Sci abstr, no. 228)

Kolomenskiy, A. A., and I. I. Logachev. Problems on the theory of ion acceleration by electron beam scanning. IN: Tr. 2-go Vses. soveshch. po uskoritelyam zaryazhen. chastits, 1970. T. 1. Moskva, nauka, 1972, 204-206. (RZh Elektr, 12/72, no. 12A383)

Komar, Ye. G., and O. A. Gusev. Charged particle accelerator. Author's certificate, USSR no. 307743, published April 7, 1972. (RZh Elektr, 12/72, no. 12A392 P)

Lavrov'skiy, V. A., I. F. Kharchenko, and Ye. G. Shustin. Single-mode interaction of a plasma-beam discharge in a turbulent regime. ZhETF P, v. 16, no. 11, 1972, 602-606.

Lazarenko, B. R., and N. I. Lazarenko. Plasmoids - a powerful technological factor. EOM, no. 5, 1972, 3-8.

Levin, V. M., V. V. Rumyantsev, K. P. Rybas, and B. N. Telepayev. Electron gun for obtaining intense electron beams. IN: Tr. 2-go Vses. soveshch. po uskoritelyam zaryazhen. chastits, 1970. T. 1. Moskva, nauka, 1972, 92-94. (RZhElektr, 12/72, no. 12A385)

Makarov, G. I., and I. B. Maftul. On the problem of Landau damping in a plasma excited by a monochromatic electron beam. IN: Sbornik. Proble. difraktsii i rasprostr. voln. Leningrad, Leningradskiy universitet, no. 11, 1972, 159-171. (RZhElektr, 10/72, no. 10G234)

Meskhi, G. O., and B. N. Yablokov. Electron gun with a cold-emission cathode. IN: Tr. 2-go vses. soveshch. po uskoritelyam zaryazhen. chastits, 1970 . T. 1. Moskva, nauka, 1972, 90-92. (RZhElektr, 12/72, no. 12A364)

Mesyats, G. A., B. M. Koval'chuk, and Yu. F. Potalitsyn. A method for obtaining an electric discharge in gas. Author's certificate, USSR no. 356824, published February 20, 1970. (Otkr izobr, 32/72, p. 171)

Panasyuk, V. S., A. A. Sokolov, and B. M. Stepanov. Design principles and possible application of accelerators with a superstrong magnetic field, generated by an explosion. Atomnaya energiya, v. 33, no. 5, 1972, 907-912.

Perel'shtejn, E. A., M. S. Perskiy, and V. F. Shevtsov. C rezonanse Q_{ch}^{-1} v kollektivnykh uskoritelyakh. (Q_{ch}^{-1} resonance in collective accelerators). Dubna, 1972, 9 p. (KL, 49/72, no. 39319)

Rabinovich, M. I., and S. M. Faynshteyn. High-frequency instability of electromagnetic waves in a non-equilibrium magnetized plasma. ZhETF, v. 63, no. 5, 1972, 1672-1677.

Rogashkova, A. I., I. F. Kharchenko, M. B. Tseytlin, et al. Razvitiye nelineynykh kolebaniy pri vzaimodeystvii modulirovannogo elektronnogo puchka s plazmoy. (Development of nonlinear oscillations from interaction of a modulated electron beam with plasma). Moskva, 1972, 24 p. (KL Dop vyp, 10/72, no. 21720)

Sarantsev, V. P. The collective ion accelerator - a new instrument in elementary particle physics. IN: Tr. 2-go vses. soveshch. po uskoritelyam zaryazhen.chastits, 1970. T. 1. Moskva, nauka, 1972, 201-204. (RZhElektr, 12/72, no. 12A360).

Savchenko, O. Ya. Powerful ion beam formation by grid electrodes. IN: Tr. 2-go vses. soveshch. po uskoritelyam zaryazhen.chastits, 1970. T. 1. Moskva, nauka, 1972, 128-129. (RZhElektr, 12/72, no. 12A354)

Tsytovich, V. N., and A. S. Chikhachev. On the structure of the exponential spectra of relativistic electrons in a turbulent plasma. Moskva, Fizika plazmy, no. 3, 1971, 97-103. (JPRS USSR Sci abstr no. 228)

Uskoreniye zaryazhennykh chastits. Eksperimenty na uskoritelyakh. (Charged particle acceleration. Experiments with accelerators). AN SSSR. Trudy Radiotekhn. in-ta, no. 9, Moskva, 1972, 221 p. (KL, 48/72, no. 38625)

Vishnyakov, V. A., I. A. Grishchayev, Yu. I. Dobrolyubov, V. M. Kobezskiy, V. V. Kondratenko, and V. I. Makota. The 2 Gev linear electron accelerator at FTI, AN UkrSSR. IN: Tr. 2-go vses. soveshch. po uskoritelyam zaryazhen. chastits, 1970. T. 1. Moskva, nauka, 1972, 66-70. (RZhElektr, 12/72, no. 12A362)

Voronkov, R. M., V. A. Danilichev, B. Yu. Bogdanchich, and V. F. Gass. Experimental study of field-emission gun parameters. IN: Tr. 2-go vses. soveshch. po uskoritelyam zaryazhen. chastits, 1970, T. 1. Moskva, 1972, 126-127. (RZhElektr, 12/72, no. 12A355)

Yakushev, V. P., and A. N. Serbinov. Stable operating conditions for high-voltage accelerator tubes. IN: Tr. 2-go vses. soveshch. po uskoritelyam zaryazhen. chastits, 1970. T. 1. Moskva, nauka, 1972, 86-88. (RZhElektr, 12/72, no. 12A380).

5. Material Science

A. Abstracts

Verzhinskaya, A. B., Yu. D. Il'yukhin,
and V. B. Nesterenko. Experimental stand
for investigating isobaric heat capacity of
dissociative nitrogen tetroxide at 140-550° C
and 25-350 kg/cm². VAN BSSR, Ser. fiziko-
energet. nauk, no. 3, 1972, 84-88.

An experimental stand has been developed at the Institute of Atomic Energy, Academy of Sciences, BSSR for investigating the specific heat of the dissociating gas system $N_2O_1 \rightleftharpoons 2N_2O_2 \rightleftharpoons 2NO + O_2$ at 140-550° C and 25-350 kg/cm². The isobaric specific heat of nitrogen tetroxide is measured by the method of a flow-through adiabatic calorimeter and a closed circulation system, with calorimetric measurement of the flow rate, developed by the All-Union Institute of Heat Engineering imeni Dzerzhinskii. A diagram of the stand is presented in Fig. 1.

In order to test the operation of the stand, control experiments were conducted to determine the specific heat of water at isobars of 151 and 201 kg/cm² in the temperature range of 200-300° C. The experiments were conducted on the basis of isotherms. Analysis of the experimental error showed that the limit error in determining the specific heat c_p of water amounts to 0.7%. A preliminary analysis of possible errors permits the limit error of measurement of the specific heat of dissociation-promoting nitrogen tetroxide to be estimated at 0.9-1% (disregarding errors of attribution).

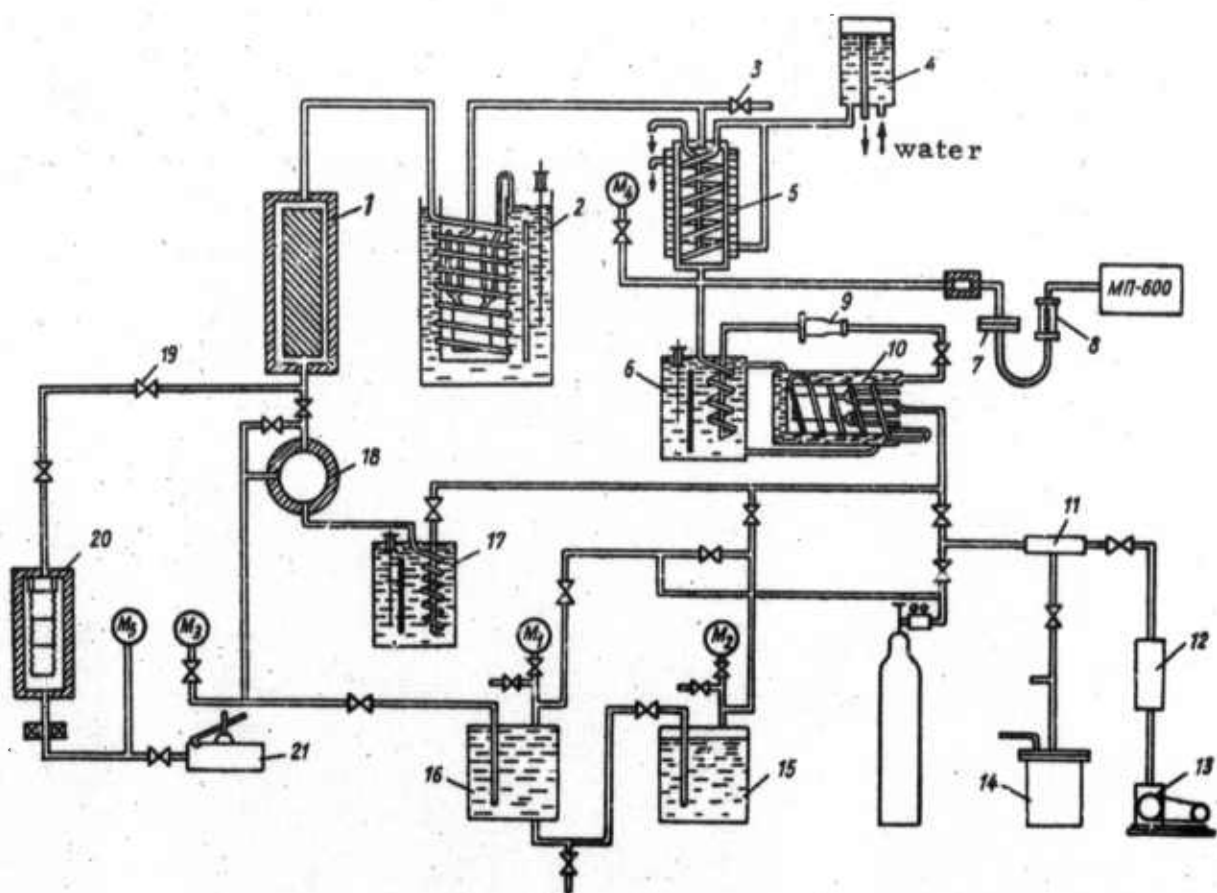


Fig. 1. Experimental stand for investigating the isobaric specific heat c_p of nitrogen tetroxide.

Vertogradskiy, V. A., and V. Ya.
Chekhovskoy. Electrical resistivity
of tungsten-rhenium cermet alloys.
Poroshkovaya metallurgiya, no. 10,
1972, 68-70.

Electrical resistivity ρ data are presented for W-Re alloys over a wide range of solid solution compositions (5-27 wt % Re) at 1,200-3,000° K. Resistivity was measured in wire specimens, annealed at 2,500° K by the potentiometric technique described earlier by the authors (TVT, v. 9, no. 2, 1971, 438). The experimental error was < 1% and the additional error due to uncertainties in composition was 0.5-1.1% at 1200° K and 0.3-0.6% at 3,000° K. The experimental ρ plots (Fig. 1) show a linear relationship between ρ and $C(100-C)$ at %, in which the alloys generally satisfy the Nordheim rule. The 20% and 21% Re alloys of run no. 1 were the only exceptions to the rule at temperatures above 1,700° K. In agreement with the literature, this deviation is explained by the presence of intermediate phases. A relative decrease of ~5% was found in ρ of the 20% Re alloy (run no. 1) at 2,800° K.

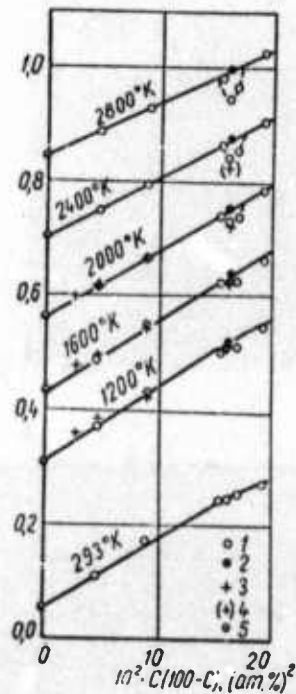


Fig. 1. Electrical resistivity ρ of W-Re alloys versus the product of atomic concentrations of the components: 1- authors' data, 2- same for alloys with 20% Re (runs no. 2 and 3), 3- literature data for the 20% Re alloy, 4- same data extrapolated to 2,400°K, 5- literature data for pure W.

Stulov, V. P. Gas flow on a surface vaporizing from radiant heating. IN:
Sbornik. Teplo-i massoperenos,
Minsk, v. 1, 1972, 423-432. (RZhMekh
9/72, no. 9B469)(Translation).

A numerical solution is given to equations of supersonic flow around a sphere with extraneous gas subsonic injection through the front surface according to a given law. The solution is obtained by iteration with alternating application of the Telenin method to the flow between the shock wave and the vapor layer and the flow in the vapor layer. The profile of the discontinuity contact surface is determined. The calculated numerical data are compared to known analytical solutions. One of these solutions was obtained on assumption of constant but different gas densities in the shock layer and the vapor layer (Hill spherical vortex). Another solution was obtained by a boundary layer approximation of perfect compressible gas equations. The cited solutions disagree quantitatively with numerical solutions for an arbitrary injection law. An approximate flow analysis was performed for the radiation absorbing but nonemitting vapor layer near the axis. The temperature and thickness of the vapor layer are determined.

Shapiro, Ye. G. Static high temperature supersonic air flow around a sphere. IN:
Sbornik. Nauchnaya konferentsiya. Institut mekhaniki Moskovskogo universiteta, 22-24 May 1972, Moskva, 1972, 34. (RZhMekh, 9/72, no. 9B470)(Translation)

A numerical investigation is presented of equilibrium air flow around a sphere at oncoming flow Mach numbers in the 1.5-6 range, temperatures of $2,000\text{-}6,000^{\circ}\text{K}$, and pressures of 10^{-4} to 10 atm.

Sultanov, M. A. Effect of degree of oriented stretching on destruction mechanism in polymer films under supersonic plasma flow. Vysokomolekulyarnyye soyedineniya, v. 14, no. 2, 1972, 94-96.

The destruction pattern of the surface and interior of a teflon film under supersonic plasma flow, depending upon the degree of its stretching, is reported. Photographs of surface and interior destruction at 100, 250, and 410% orientational stretching, are given. The pattern of surface destruction changes as the degree of orientation increases: the number of fibers decreases, and the distances between them increase. In all cases of change of the degree of stretching, the volume of the material undergoes intensive destruction. As the degree of orientation increases, the effect of destruction in the volume increases. The destruction pattern of the surface and interior of the material, shown by photographs, indicates that as the degree of stretching increases, a teflon film is subjected to more intensive destruction. The same is also true for other polymer films. The destruction of the material is caused basically by a combination of shock wave action and internal effect of plasma flux.

Lebedev, D. P., and V. V. Samsonov.
Characteristics of external heat and mass transfer in a vacuum during sublimation.
I-FZh, v. 23, no. 3, 1972, 424-429.

Vacuum sublimation ($1-5 \times 10^{-3}$ torr) of ice from a permeable cermet plate, a free ice surface, and quartz sand was studied experimentally at thermal loads from 10^3 to 2×10^4 w/m². Vapor velocity and temperature

profiles over the sublimation flare were determined at different vapor flow rates and vacuum depths. The existence of three regions in the vapor flare was established. Molar heat and mass transfer occurs in the diffusion wall layer with a turbulent structure and constant temperature. The core of the sublimation flare is distinguished by a constant temperature gradient. In all experiments, the process of vapor flow from the sublimation surface into the vacuum was identical, and similar to the submerged jet outflow. The height and dimensions of the vapor flare depend on the heat load and degree of vacuum. The effect of additional vibration on the sublimation rate in vacuum is also considered.

B. Recent Selections

i. Crack Propagation

Fremel', T. V., R. V. Torner, L. M. Luk'yanova, and L. A. Flekser. High pressure failure of polyethylene in an [insulator] element. MP, no. 5, 1972, 935-936.

Krasovskiy, A. Ya., Ye. E. Zasimchuk, and I. A. Makovetskaya. Local plastic deformation in a microcrack terminus from cleavage fracture of polycrystalline iron. Problemy prochnosti, no. 11, 1972, 44-46.

Peter, V. E. Calculation of crack resistance of prestressed concrete structural elements from torsional buckling. IN: Nauchnyye trudy Omskogo instituta inzhenerov zhelezno-dorozhnogo transporta, v. 120, no. 1, 1971, 53-56. (LZhS, 46/72, no. 153846)

Peter, V. E. Calculation of crack resistance and deformation capacity of a prestressed concrete support from torsional buckling. IN: Nauchnyye trudy Omskogo instituta inzhenerov zhelezno-dorozhnogo transporta, v. 120, no. 1, 1971, 57-62. (LZhS, 46/72 no. 153845)

Tomashevskaya, I. S., and Ya. N. Khamidullin. Feasibility of predicting time of breakdown of rock samples based on crack growth fluctuations. DAN SSSR, v. 207, no. 3, 1972, 580-582.

ii. High Pressure Research

Mukhamedzyanov, I. Kh., G. Kh. Mukhamedzyanov, and A. G. Usmanov. Thermal conductivity of liquid-saturated hydrocarbons at pressures to 2250 bar. IN: Trudy Kazanskogo khimiko-tehnologichesk instituta, no. 47, 1971, 22-28. (LZhS, 47/72, no. 156822)

Mukhamedzyanov, I. Kh., G. Kh. Mukhamedzyanov, and A. G. Usmanov. Generalization of test data on thermal conductivity of liquids at high pressures. IN: Trudy Kazanskogo khimiko-tehnologicheskogo instituta, no. 47, 1971, 29-34. (LZhS, 47/72, no. 156821)

Nesterenko, V. B., Yu. D. Il'yukhin, A. B. Verzhinskaya, G. P. Povedaylo, and A. N. Dashuk. Experimental investigation of isobaric heat capacity of dissociable nitrogen tetroxide at subcritical pressures. IAN B, Seriya fiziko-energeticheskikh nauk, no. 4, 1972, 54-58.

Shmin, Yu. I. Application of the capacitance barometric dependence of a flat quartz condenser to measurements of high hydrostatic pressure. Metrologiya, no. 11, 1972, 25-28.

Tarzimanov, A. A., and V. A. Arslanov. Experimental device for measuring thermal conductivity of gases at temperatures to 500 C and pressures to 2000 bar. IN: Trudy Kazanskogo khimiko-tehnologicheskogo instituta, no. 47, 1971, 150-156. (LZhS, 47/72, no. 156858)

Tarzimanov, A. A., and V. A. Arslanov. Thermal conductivity of argon at high pressures. IN: Trudy Kazanskogo khimiko-tehnologicheskogo instituta, no. 47, 1971, 157-160. (LZhS, 47/72, no. 156857)

Volarovich, M. P., A. I. Levykin, and V. D. Parfenov. Plastic deformation and longitudinal wave velocity in barite at high pressure. DAN SSSR, v. 207, no. 1, 1972, 79-80.

iii. High Temperature Research

Cukic, R. Coupled and uncoupled theory and the problem of thermal shock on shells of revolution surfaces. Bulletin de l'Academie Polonaise des Sciences, Serie des sciences techniques, v. 20, no. 10, 1972, 393(763)-400(770).

Dzhafarov, E. O., O. A. Golikova, and L. S. Stil'bans. High temperature thermal conductivity of group IV transition metal carbides. IAN Az, no. 2, 1972, 123-126.

Jarzebski, Z. M. Electrical properties of NiO at high temperatures. APP, v. A42, no. 4, 1972, 371-381.

Jarzebski, Z. M., B. Muszynska, and J. Oblakowski. Electrical properties of CdO at high temperatures. APP, v. A42, no. 4, 1972, 383-391.

Kalashnikov, V. I. Device for measuring electrical resistance of metals at high temperatures in a vacuum. IN: Sbornik nauchnykh trudov. Kiyevskiy institut inzhenerov grazhdanskoy aviatsii, no. 2, 1971, 96-99. (RZhMetrolog, 10/72, no. 10.32.1123)

Kashcheyev, V. N. Ferromagnetism pri vysokikh temperaturakh (Ferromagnetism at high temperatures). Riga, Izd-vo Zinatne, 1972, 162p. (KL, 49/72, no. 39313)

Konkin, A. A., and N. F. Konnova. Carbon fibers. Zhurnal Vsesoyuznogo khimicheskogo obshchestva, no. 6, 1972, 632-639.

Korolev, V. P., M. V. Nikulin, V. N. Uvarov, and G. Ye. Chernenko. Measuring thermal insulation materials ablation using loaded shell strain data. MP, no. 5, 1972, 824-828.

Kutateladze, S. S., and A. I. Leont'yev. Teplomassoobmen i treniye v turbulentnom pogranichnom sloye (Heat and mass transfer and friction in a turbulent boundary layer), Moskva, Izd-vo Energiya, 1972, 342p. (KL, 48/72, no. 38615)

Lidorenko, N. S., S. P. Chizhik, Ya. T. Shermazanyan, V. V. Shakhparonyan, T. V. Yefimovskaya, A. A. Lanin, L. A. Lyutsareva, and S. P. Shumanova. Preparing transparent zirconium dioxide in a high temperature solar device. IAN Arm, Seriya tekhnicheskikh nauk, v. 25, no. 4, 1972, 10-13.

Murav'yev, A. I., I. V. Chernyshevich, and S. L. Fofanov. Method for solving Stefan problems. IAN B, Seriya fiziko-energeticheskikh nauk, no. 4, 1972, 108-112.

Shestaka, I. S. Coefficient of meteor ablation and maximum brilliance. Astronomicheskiy vestnik, v. 6, no. 3, 1972, 186-194.

Stovbun, V. P., T. I. Kedrova, and V. V. Barzykin. Ignition system with refractory reaction products. FGIV, no. 3, 1972, 349-354.

Teoriya i metody rascheta luchistogo teploobmena v teplovых ustroystvakh. Fiziko-tehnicheskaya sektsiya (Theory and methods for calculating radiative heat transfer in thermal devices). Trudy Krasnodarskogo politekhnicheskogo instituta, Krasnodar, no. 39, 1971, 150p. (KL, 48/72, no. 38744)

Udovskiy, A. L., Ye. S. Shmakova, and Yu. I. Mikhin. Physical source of temperature variations in modulus of elasticity of carbon materials, Khimiya tverdogo topliva, no. 6, 1972, 88-94.

Yermolenko, I. N., A. M. Safonova, and Zh. V. Malashevich.

Structure of metal-carbon fibers made from oxycellulose salts.

IAN B, Seriya khimicheskikh nauk, no. 6, 1972, 60-66.

Zashchitnyye vysokotemperaturnyye pokrytiya. Trudy 5-go
Vsesoyuznogo soveshchaniya po zharostoykim pokrytiyam. Khar'kov,
12-16 Maya 1970 g. (High temperature protective coatings. Transactions
of Fifth All-Union conference on heat resistant coatings, Khar'kov,
12-16 May 1970). Leningrad, Izd-vo Nauka, 1972, 368p. (KL, 46/72,
no. 37458)

iv. Miscellaneous Material Properties

Aref'yev, I. M., V. N. Biryukov, V. A. Gladkiy, S. V. Krivokhizha,
I. L. Fabelinskiy, and I. G. Chistyakov. Hypersonic and ultrasonic
propagation in a nematic liquid crystal isotropic phase in a region of
phase transition. ZhETF, v. 63, no. 5, 1972, 1729-1734.

Chaykovskiy, V. M., and I. G. Chistyakov. Feasibility of an
approximation analysis of the average angle of inclination of molecules
and the degree of orientation in a liquid crystal specimen. IN:
Uchenyye zapiski Ivanovskogo gosudarstvennogo pedagogicheskogo
instituta, v. 99, 1972, 298-300. (RZhKh, 22/72, no. 22B603)

Chaykovskiy, V. M., and I. G. Chistyakov. Structural change of
smectic and nematic liquid crystals in a magnetic field with a temperature
rise. IN: Uchenyye zapiski Ivanovskogo gosudarstvennogo pedagogiches-
kogo instituta, v. 99, 1972, 301-320. (RZhKh, 22/72, no. 22B608)

Chistyakov, I. G., and L. S. Shabyshev. Liquid crystal structure of p-anisoamino cinnamic acid ethyl ether. IN: Uchenyye zapiski Ivanovskogo gosudarstvennogo pedagogicheskogo instituta, v. 99, 1972, 43-49. (RZhKh, 22/72, no. 22B602)

Chistyakov, I. G., and L. S. Shabyshev. Structure of p-nonyloxybenzoic acid in a stationary electric field. IN: Uchenyye zapiski Ivanovskogo gosudarstvennogo pedagogicheskogo instituta, v. 99, 1972, 50-55. (RZhKh, 22/72, no. 22B612)

Chistyakov, I. G. Temperature dependence of the degree of orientation of nematic p-azoxyanisole. IN: Uchenyye zapiski Ivanovskogo gosudarstvennogo pedagogicheskogo instituta, v. 99, 1972, 19-25. (RZhKh, 22/72, no. 22B609)

Chistyakov, I. G., and S. K. Sukharev. Effect of flow on nematic p-azoxyanisole orientation. IN: Uchenyye zapiski Ivanovskogo gosudarstvennogo pedagogicheskogo instituta, v. 99, 1972, 108-111. (RZhKh, 22/72, no. 22B613)

Chuvyrov, A. N., and A. N. Trofimov. Orientation oscillations of liquid crystal domain structures. Mechanism of hexagonal domain structure formation in stationary electric fields. Kristall, v. 17, no. 6, 1972, 1205-1209.

Dashevskiy, Ye. M. Method of discrete elements numerical solution to a two-dimensional problem in linear destruction mechanics. IN: Trudy Tsentral'nogo nauchno-issledovatel'skogo instituta stroitel'nykh konstruktsiy, no. 20, 1971, 77-86. (LZhS, 46/72, no. 153834)

Demenkov, A. P., V. A. Likhachev, and N. S. Frantsuzov.
Priroda sverkhplastichnosti (Nature of superplasticity). AN SSSR.
Fiz.-tekhn. inst. imeni A. F. Ioffe. Leningrad, 1972, 56p. (KL,
Dop vyp, 10/72, no. 21622)

Gusakova, L. A., and I. G. Chistyakov. Structure of nematic
mixtures of binary liquid crystal systems. IN: Uchenyye zapiski
Ivanovskogo gosudarstvennogo pedagogicheskogo instituta, v. 99,
1972, 26-32. (RZhKh, 22/72, no. 22B600)

Vysokoskorostnaya deformatsiya. Voprosy povedeniya metallicheskikh
materialov pri impul'snom nagruzhenii (High speed deformation.
Behavior of metal materials under impulse loads), Moskva,
Izd-vo Nauka, 1971, 128p. (FGiV, 3/72, 455, no. 4)

Inozemtseva, A. D. Application of optical modelling to studies of
liquid crystal materials structure. IN: Uchenyye zapiski Ivanovskogo
gosudarstvennogo pedagogicheskogo instituta, v. 99, 1972, 33-42.
(RZhKh, 22/72, no. 22B604)

Kapustin, A. P., and L. I. Mart'yanova. Ultrasonic spectroscopy
of liquid crystals. IN: Uchenyye zapiski Ivanovskogo gosudarstvennogo
pedagogicheskogo instituta, v. 99, 1972, 71-76. (RZhKh, 22/72, no.
22B618)

Korovskiy, Sh. Ya. Fracture structure characteristics in surface-
active media. DAN SSSR, v. 207, no. 3, 1972, 576-579.

Kudryavtsev, G. I. Method for preparing heat resistant fibers.
Zhurnal Vsesoyuznogo khimicheskogo obshchestva, no. 6, 1972,
625-631.

Lependin, L. F., A. P. Kapustin, and V. A. Poyarkova. Methods of ultrasonic measurement of liquid crystal rheological properties. IN: Uchenyye zapiski Ivanovskogo gosudarstvennogo pedagogicheskogo instituta, v. 99, 1972, 77-82. (RZhKh, 22/72, no. 22B617)

Lozovik, G. Ya., and I. Ya. Klinov. Protective properties of chlorosulfonated polyethylene coatings on steel. IN: Trudy Moskovskogo instituta khimicheskogo mashinostroyeniya, no. 37, 1971, 135-143. (LZhS, 46/72, no. 154312)

Maydachenko, G. G., and B. N. Makarov. Methods for preparing n-(p-alkyloxybenzylidene)-p'-azyloxyaniline series of liquid crystal materials. IN: Uchenyye zapiski Ivanovskogo gosudarstvennogo pedagogicheskogo instituta, v. 99, 1972, 250-253. (RZhKh, 22/72, no. 22B597)

Mikhaylov, V. M. Small-angle x-ray analysis of p-anisoamino cinnamic acid ethyl ether in a stationary electric field. IN: Uchenyye zapiski Ivanovskogo gosudarstvennogo pedagogicheskogo instituta, v. 99, 1972, 105-107. (RZhKh, 22/72, no. 22B607)

Mochalin, S. N., and P. P. Pugachevich. Temperature dependence of cholesteric mesophase density, IN: Uchenyye zapiski Ivanovskogo gosudarstvennogo pedagogicheskogo instituta, v. 99, 1972, 200-207. (RZhKh, 22/72, no. 22B614)

Nazin, V. P. Optical analysis of a Rivanol (2-etoxy-6, 9-diaminoacridine lactate) liquid crystal layer under effects of various chemical substances. IN: Uchenyye zapiski Ivanovskogo gosudarstvennogo pedagogicheskogo instituta, v. 99, 1972, 189-199. (RZhKh, 22/72, no. 22B598)

Sakevich, N. M. Formation kinetics of liquid crystal nuclei and centers. IN: Uchenyye zapiski Ivanovskogo gosudarstvennogo pedagogicheskogo instituta, v. 99, 1972, 83-88. (RZhKh, 22/72, no. 22B755)

Samodurova, I. D., and A. S. Sonin. Investigation of p-azoxyanizole domain structure. IN: Uchenyye zapiski Ivanovskogo gosudarstvennogo pedagogicheskogo instituta, v. 99, 1972, 89-94. (RZhKh, 22/72, no. 22B611)

Shaltyko, L. G., A. A. Shepelevskiy, and S. Ya. Frenkel'. Small-angle light scattering in liquid crystals. IN: Uchenyye zapiski Ivanovskogo gosudarstvennogo pedagogicheskogo instituta, v. 99, 1972, 124-146. (RZhKh, 22/72, no. 22B601)

Shepurev, E. I. Polymeric fiber optics (review). OMP, no. 11, 1972, 56-59.

Shuvalov, I. V. Temperature dependence of electrical conductivity of cholesteric liquid crystal substances. IN: Uchenyye zapiski Ivanovskogo gosudarstvennogo pedagogicheskogo instituta, v. 99, 1972, 95-100. (RZhKh, 22/72, no. 22B616)

Sukhoverkhov, V. F., and V. S. Barkman. Liquid-solid phase equilibrium in a ClF₅-ClF₃ system. DAN SSSR, v. 207, no. 1, 1972, 117-120.

Tolstykh, S. A., and V. M. Vyglovskiy. Investigation of silicon nitride properties. IN: Sb. Fizika poluprovodnikov i mikroelectron, Voronezh, 1972, 42-45. (RZhKh, 22/72, no. 22L76)

Vaynshteyn, B. K., Ye. A. Kosterin, and I. G. Chistyakov. Structural analysis of liquid crystals using two-dimensional functions of interatomic distances. IN: Uchenyye zapiski Ivanovskogo gosudarstvennogo pedagogicheskogo instituta, v. 99, 1972, 5-18. (RZhKh, 22/72, no. 22B605)

Vorob'yev, A. A., G. A. Vorob'yev, et al. Impul'snyy proboy i razrusheniye dielektrikov i gornykh porod (Pulsed breakdown and destruction of dielectrics and rocks). Tomsk, Izd-vo Tomskogo universiteta, 1971, 70p. (FGiV, 3/72, 455).

Zharenov, R. I., and I. G. Chistyakov. Structure of p-azoxybenzoles in a stationary electric field. IN: Uchenyye zapiski Ivanovskogo gosudarstvennogo pedagogicheskogo instituta, v. 99, 1972, 216-226. (RZhKh, 22/7~, no. 22B606)

v. Superconductivity

Alfeyev, V. N., B. N. Formozov, and V. P. Yarotskiy. Combined superconducting film memory cell. Otkr izobr, no. 32, 1972, no. 356693.

Aronov, A. G., and V. L. Gurevich. Tunneling excitation from a superconductor and increased T_c . ZhETF, v. 63, no. 5, 1972, 1809-1821.

Batakov, Yu. P., N. I. Doynikov, A. G. Zhikhareva, N. A. Monoszon, G. V. Trokhachev, and G. F. Churakov. Superconducting magnets with iron shields. IN: Trudy 2-go Vsesoyuznogo soveshchaniya po uskoritelyam zapryazhennykh chastits, 1970. Moskva, Izd-vo Nauka, v. 1, 1972, 241-243. (RZhElektr, 12/72, no. 12A376)

Bohdziewicz, A., J. Szymaszek, and B. Makiej. Critical magnetic field of superconducting cylindrical layers of indium. APP, v. A42, no. 4, 1972, 419-422.

Borodovskiy, V. S., and D. Ya. Gal'perovich. Nanosecond pulse transmission through a superconducting coaxial cable. Radiotekh, no. 11, 1972, 51-55.

Golovanov, L. B. Fourth International Conference on cryogenics (May, 1972, Eindhoven, the Netherlands). Atomniya energiya, v. 33, no. 5, 1972, 943-944.

Grigor'yev, Yu. M., V. F. Degtyareva, A. G. Merzhanov, and A. G. Rabin'kin. Superconductivity of metal and alloy nitride films prepared by an electrothermal method. FTT, no. 10, 1972, 3071-3072.

Ivlev, B. I. Characteristics of superconducting films in a variable frequency field close to threshold. ZhETF P, v. 16, no. 10, 1972, 567-570.

Kiselev, Yu. F. Stabilizator toka sverkhprovodyashchego solenoida (Superconducting solenoid current stabilizer). Dubna, 1972, 19p. (KL Dop vyp, 10/72, no. 22118)

Mints, A. L., A. A. Vasil'yev, E. L. Burshteyn, and Ye. S. Mironov. Application of high GeV superconducting cybernetic proton synchrotrons as low repetition frequency accelerator injectors. IN: Trudy 2-go Vsesoyuznogo soveshchaniya po uskoritelyam zapryazhennykh chastits, 1970. Moskva, Izd-vo Nauka, v. 1, 1972, 13-15. (RZhElektr, 12/72, no. 12A347)

Popova, S. V., L. N. Fomicheva, and L. G. Khvostantsev.
Synthesis and superconducting properties of cubic rhenium monocarbide.
ZhETF P, v. 16, no. 11, 1972, 609-610.

Zarubina, O. A. Superconductivity of lanthanum at pressures to 250 kbar. FTT, no. 10, 1972, 2890-2893.

Zenkevich, V. B., et al. Magnitnyye sistemy na sverkhprovodnikakh (Superconductor magnetic systems). Moskva, Izd-vo Nauka, 1972, 260p. (RBL, 7/72, no. 474)

vi. Epitaxial Films

Alferov, Zh. I., V. M. Andreyev, D. Z. Garbuzov, A. N. Yermakova, Ye. P. Morozov, and M. K. Trukan. Electroluminescent properties of epitaxial GaAs p-n junctions with precompensated p- and n-regions. FTP, no. 10, 1972, 2027-2033.

Alferov, Zh. I., V. M. Andreyev, D. Z. Garbuzov, and M. K. Trukan. Radiative recombination in epitaxially compensated gallium arsenide. FTP, no. 10, 1972, 2015-2026.

Alferov, Zh. I., V. I. Amosov, D. Z. Garbuzov, Yu. V. Zhilyayev, S. G. Konnikov, P. S. Kop'yev, and V. G. Trofim. Composition dependence of luminescence properties of n- and p- $\text{GaP}_{x}\text{As}_{1-x}$ and $\text{Al}_x\text{Ga}_{1-x}$ solid solutions. FTP, no. 10, 1972, 1879-1887.

Chistyakov, Yu. D. Role of phase equilibria in processes of orientation growth (epitaxy). IN: Sbornik. Splavy tsvetnoy metallurgii, Moskva, Izd-vo Nauka, 1972, 82-92. (RZhKh, 22/72, no. 22B766)

Dorfman, V. F., B. N. Pypkin, and A. L. Ocheretyanskiy. Effect of growth rate and crystallization conditions on defect formation in GaAs and GaP epitaxial layers. Kristall, v. 17, no. 6, 1972, 1225-1231.

Dueweritz, L. Probability of twin development in semiconductor thin layers with a diamond and sphalerite structure. Krist. und Techn., v. 7, no. 1-3, 1972, 167-177. (RZhKh, 23/72, no. 23B603)

Lozovskiy, V. N., and V. P. Popov. Stability of a zone melting process with a temperature gradient. Kristall, v. 17, no. 6, 1972, 1232-1237.

Mietz, I., and H. Sprenger. High vacuum condensation preparation of antimonide thin oriented films from single crystal substrates. Krist. und Techn., v. 7, no. 1-3, 1972, 123-131. (RZhKh, 23/72, no. 23B691)

Pedos, S. I., A. V. Vanyukov, Ye. D. Yukhtanov, N. P. Artamonov, and G. V. Indenbaum. Dissolving and crystallization processes in a $Hg-Cd_xHg_{1-x}Te$ system. IN: Sbornik. Problemy fizicheskikh sovremenennykh A^{II}B^{VI}, Vil'nyus, v. 1, 1972, 160-164. (RZhKh, 23/72, no. 23B836)

Stepanova, A. N., and N. N. Sheftal. Effect of $AsCl_3$ impurity on growth mechanism and structural improvement of germanium autoepitaxial films. Krist. und Techn., v. 7, no. 1-3, 1972, 133-140. (RZhKh, 23/72, no. 23B592)

Zotov, Yu. A., I. F. Chernomordin, V. N. Maslov, L. I. D'yakonov, and L. A. Nisel'son. Method of producing epitaxial films. Otkr izobr, no. 32, 1972, no. 330811.

vii. Magnetic Bubble Materials

Okorokov, A. I., and Ya. A. Kasman. Magnetization of $Y_3Fe_5O_{12}$ close to the Curie point. FTT, no. 10, 1972, 3065-3068.

Zvezdin, A. K., and S. G. Kalenkov. Effect on phase transition of orthoferrite domain structure near the spin reorientation temperature. FTT, no. 10, 1972, 2835-2840.

6. Miscellaneous Interest

A. Abstracts

Narayeva, M. K., I. A. Telegin,
and T. L. Kulakova. Phototelevision
image readout system for Mars-2 and
Mars-3 automatic interplanetary
stations. OMP, no. 7, 1972, 27-29.

The phototelevision units of the "Mars-2" and "Mars-3" space stations employ an optomechanical scanner of the autocollimation type. Line scanning is accomplished by the turning of mirror 8 about its axis of rotation 12 (see Fig. 1), resulting in translational movement of the

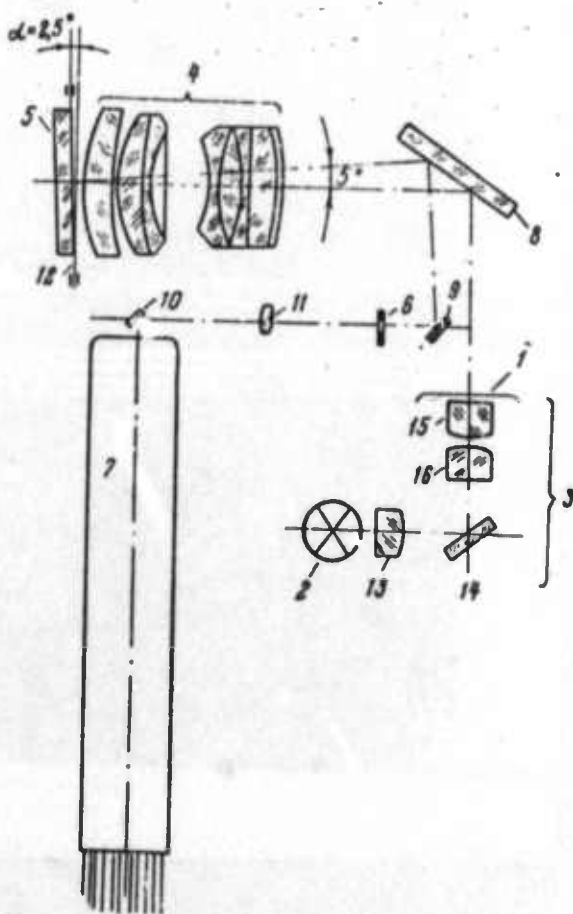


Fig. 1. Optical diagram of an autocollimation-type scanner: 1- photofilm, 2- incandescent lamp, 3- condenser, 4- objective, 5, 8, 9, 10, 14- mirrors, 6- diaphragm, 7- photomultiplier, 11- lens.

photofilm image with respect to a stationary diaphragm. Since the image shift takes place in the focal plane of the objective, defocusing is absent in autocollimation scanners; they are essentially two-dimensional. The objective is of the photographic type.

Due to the inclination of rocking mirror 5 to axis 12 by angle α , scanning in the focal plane is not rectilinear, but takes place along a curve approximating a quadratic parabola. The smaller the focal distance of the objective, the greater is the deviation of the trajectory of motion from rectilinearity with a given line length. As a result, images taken on standard photography ground equipment (drum recording) are characterized by distortions that vary along the line and remain constant with respect to the frame field. In the present device, the value of these distortions is within the permissible range, and comprises 2-3%.

To compensate for the change of line illuminance of the scanner, a condenser has been developed which creates an illuminance with a law inverse to the law of illuminance drop in the scanner. As a result, the change of the composite signal along the line does not exceed the permissible value, equal to 3-4%.

Prokhorov, V. G. Piezoelectric matrices
for registering acoustic images and holograms.
Akusticheskiy zhurnal, no. 3, 1972, 482-484.

The characteristics and test results for three types of piezoelectric matrix composites are described. The first matrix is a large surface area metal plate containing longitudinal-transverse grooves

on one side forming a lattice of metal ridges and a thin uniform base layer. The piezoelements are applied to the reverse side of the uniform layer opposite to the ridges to form a multiple core converter system. The grooves significantly weaken the elastic bond between elements. Each matrix element is a dual-layer core converter with an approximate quarter-wave layer thickness and a plane of zero displacement along the uniform layer. Plate materials are steel, aluminum and brass. The second matrix type is a simple configuration in which the piezoelements are bonded into a uniform system by self-setting plastics to attain satisfactory strength and hermetic sealing. The third matrix was prepared by pouring an organosilicon hermetic seal between the piezoelectric elements. Transient characteristics data for the three matrix types (types 1 and 3 containing 2500, and type 2 5776 piezoelectric elements) reveal good image threshold values from simple test models, and support the application of the matrices as millimeter and microwave ultrasonic image converters.

Mel'nicenko, I. P. Effectiveness of using a boundary layer as a working body. PM, no. 10, 1972, 129-132.

A theoretical evaluation is presented of the external efficiency η of two ramjet engine configurations from the standpoint of using the boundary layer to attain the highest possible body speed in a continuous medium. The boundary layer is defined as the wake formed along a body. A ramjet engine design which uses the boundary layer as a working body for attachment in the leading edge region is compared with a design which achieves the attachment in the trailing edge region. Analysis of the thrust power balance

$$P = P_T + P_L \quad (1),$$

where P_T is the engine thrust power and P_L is the exit loss, yields $\eta = P_T/P$ for both engine designs, as a function of the thrust power fraction k converted into the wake mechanical energy and the blowing rates β_0 in the boundary layer and β in the jet stream. The η formulas for the two designs were

combined into a single design formula

$$\eta = \frac{2v}{v + w} \quad (2)$$

where v and w are the moduli of the body absolute velocity and the relative effective detachment velocity, respectively. Assuming identical structural geometry and equal k , w , and β for both engine designs, the ratio of structural velocities is given as

$$\frac{v_1}{v_2} = \frac{\beta + 2k\beta_{02}}{\beta + 2k(\beta_{01} - \beta)} \quad (3).$$

At the limit of $\beta \rightarrow \beta_{01}$ and high Reynolds numbers, Eq. (3) gives the value $V_1/V_2 \approx 1.42$ for a streamlined axisymmetric body. It is concluded that the design using the boundary layer as a working body is more advantageous for high propulsion velocities.

Grekhev, I. V., M. Ye. Levinshteyr,
T. V. L'vova, A. Ye. Otblesk, and A. I.
Serbin. Silicon injection modulator of
infrared radiation. FTP, no. 7, 1972,
1327-1334.

The performance of silicon injection modulators of infrared radiation was experimentally and theoretically investigated. Tests were made using two specimens of geometrically similar n-type silicon specimens, with a specific resistance of 50 to 70 ohm \times cm ($n_o \approx 10^{14}/\text{cm}^3$). The p-n-transitions were generated by boron diffusion from borosilicate glass, formed on a silicon plate. Boron surface concentration after diffusion was $\sim 10^{19}/\text{cm}^3$. One of the diffused layers was removed after diffusion by polishing and an R^+ contact (a type 1 diode) was made on this surface by the standard chemical techniques of nickel plating and brazing. The type 2 diodes

had n^+ -type contacts which were obtained by diffusing phosphorus from phosphorosilicate glass; phosphorus surface concentration after diffusion was $10^{20}/cm^3$. Polished specimen edges were flat. The n-base thickness of both specimens was $390\ \mu$, and the p-n-junction depth was $50\ \mu$. The n-n-junction depth was $8\ \mu$ in type 2 diodes; diode length was $Z_0 \sim 3.5\text{mm}$. Hole lifetime in the n-base was $25\ \mu\text{sec}$. Experiments were conducted in the device shown in Fig. 1, using a CO_2 laser ($\lambda = 10.6\ \mu\text{m}$), and results

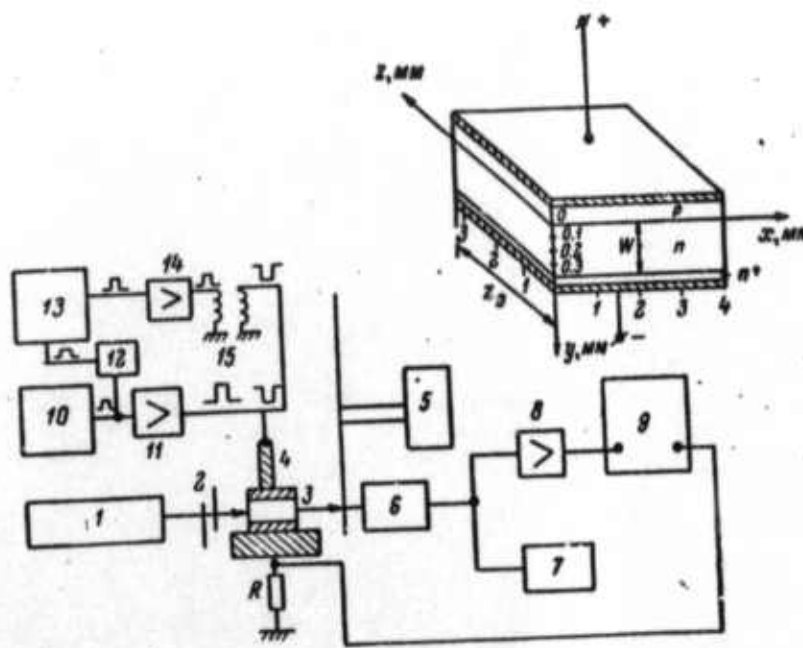


Fig. 1. Experimental device. 1- laser;
2- gap; 3- specimen; 4- metal shield;
5- chopper; 6- photodetector; 7- voltmeter;
8- broadband amplifier; 9- oscilloscope;
10, 13- pulse generators; 11, 14- emitter
followers; 12- delay line; 15- pulse transformer.
In the upper-right hand corner is a typical
specimen configuration.

were plotted. For $k = 80\%$ modulation of a 400μ width light beam, the required current density J_0 was $\sim 10 \text{ a/cm}^2$ in a c-w and $\sim 50 \text{ a/cm}^2$ in a pulsed regime at a pulse duration $\tau = 5 \mu\text{sec}$. At $\tau = 0.2 \mu\text{sec}$ and $J_0 = 10 \text{ a/cm}^2$, the permissible pulse repetition rate was $\sim 2 \times 10^5 \text{ pulse/sec}$ at $k \sim 10\%$. A generalized method is suggested for injection modulator calculations in the continuous as well as pulsed regimes. Calculations and experimental results were in good agreement.

Ivanov, A. P., I. I. Kalinin, A. L.
Skrelin, and I. D. Sherbaf. Spatial-
time structure of light pulses in water.
FAiO, n°. 8, 1972, 884-890.

Shipboard measurements are reported of the effect of sea water optical parameters and experimental configuration geometry on the time structure of reflected laser pulses. The pulse emitter and detector devices were installed on a horizontal crossbeam and could be shifted relative to each other for distances of 1.8 to 3.14 m. The device optical axes were oriented on the target, which was submerged at various depths in relationship to the emitter-detector. The crossbeam was hung on the ship's boom and lowered by a winch to a depth of 5 m. The light source was a Q-switched neodymium laser with frequency doubler. The radiated power at 550 nm wavelength was 100 kw at a 40 nsec pulse duration; beam angle of divergence was $20'$. Using a semitransparent plane-parallel glass plate, the portion of the emission in the water was shunted onto a coaxial photoelectric cell to control the sensor output radiation pulse parameters. The light detector comprised an objective with a 300 mm focusing distance, an aperture ratio of 1:4.5, an interchangeable diaphragm and light filter circuit, a polarization light filter and a photomultiplier. Placing the inter-

changeable diaphragm circuit in the objective focal plane permitted variation of the detector aperture angle from $17'$ to $56''$. The polarization light filter was rotated or held in two mutually-perpendicular positions to investigate the polarization characteristics of emissions from the water. The function $Y(t) = F(t)/W_o$ was analyzed, where $F(t)$ is the light flux diffusion and W_o is the output pulse energy. In clear waters, $Y(t)$ agrees with the transfer function given earlier by the authors (FAiO, 6, 9, 1970), which characterizes the time dependence of the intensive scattering medium of a δ -pulse energy unit. Data reported by Timofeyeva et al (FAiO, 2, 3, 1966) were used for the sea water scattering indicatrix. Figure 1 is a plot (five similar plots are included) of Y/Y_{\max} as a function of depth for a submerged 1 m diameter target with a reflection coefficient of 0.46. The detector aperture angle in the figure is $17'$ and the emitter-detector interval is 3.14 m. The condition is analyzed when the emitter-detector optical axes intersect in the plane of the target. Test data are based on averaging 5 to 10 oscilograms.

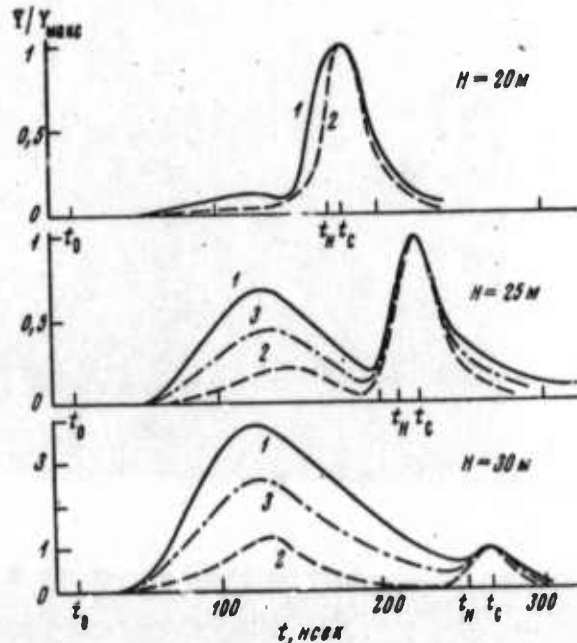


Fig. 1. Dependence of Y/Y_{\max} as a function of various depths (H). The attenuation index = 0.25 m^{-1} and the absorption index is 0.05 m^{-1} : 1 - parallel polaroids, 2 - crossed polaroids, and 3 - without polaroids.

Yeshchenko, S. D., and B. Sh. Lande.
Radar imaging of sea surfaces. RiE,
no. 8, 1972, 1590-1597.

Theoretical and experimental data on microwave radiation reflection from a sea surface are presented. Relationships are derived which show that when the wave parameters of velocity, upper and lower limits of capillary wave spectra, and the spatial q-factor are varied in sea surface zones, the radar images should differ from zone to zone as a function of the mechanism of capillary wave spectra development; in actuality, the capillary waves are normally formed as a result of the simultaneous effects of several mechanisms. Experimental data were recorded to support an investigation of radar signals in steady and transient wind and sea states; specifically in a windless and calm sea state, in a mild wind state of irregular direction, and in a steady wind and two-dimensional wave state at a stage of moderate seas and strong storm swells. Airborne radar measurements were made in the 2 and 3 cm wave range with vertically polarized signals. Multiple passes were flown over the sea surface at varying angles of illumination in relation to the sea wave front, wind direction, and various hydrometeorological conditions. Aerial photographs of the surfaces were also recorded for comparison; flight altitudes were from 500 to 200 m at speeds of 450 to 550 km/hr. The receiver-recorder channel was calibrated before each flight to achieve sequential measurement of signal strength by photometric radar imagery. Wave surface reflected signals were recorded in a side-looking mode using an electronic photorecorder, providing photographic signal storage and simultaneous shaping of large-scale radar images. This procedure allowed the measurement of signal strength as well as an evaluation of the configuration and dimensions of zones with varying intensity. Vertical radar images were formed in range-path coordinates, with an experimental range of 15 km and an image expansion along the flight path of units and tens

of kilometers.

The experimental data show that 2 and 3 cm wavelength sea surface reflected signals are associated with the presence of capillary wave saturated components on wave crests, which are also in the saturated portion of the spectrum. Conclusions are: 1) Sea surface microwave scattering has a selective characteristic mainly due to the wave field saturated components with highest amplitudes. This affects the radar signal strength; 2) The surface zone configurations containing the saturated components, as a function of the capillary wave formation mechanism, are variable but with narrow boundaries. This supports the use of the given formulas and also verifies the finding of Phillips (Dinamika verkhnego sloya okeana, 1969) on the restricted range of upper and lower boundaries of capillary wave saturated components; 3) The saturated spectra components of resonant capillary waves are correlated with the crests of large saturated gravitation waves, which confirms the periodic structure of sea surface radar images.

Chebotayev, V. P. Unconstricted linear direct-current glow discharge at atmospheric pressures. DAN SSSR, v. 206, no. 2, 1972, 334-336.

A steady continuous uniform discharge of direct current was generated in subsonic and supersonic gas flow at pressures between 1 and 2 atm. Tests were conducted in several types of discharge tubes up to 4 cm in diameter and 20 cm in length, in most cases containing helium. The chambers were designed so that air, CO₂ or N₂ could be added. The length of the discharge was dependent on the size of the power supply. At a

gas pressure exceeding 1.5 atm, the discharge in the tube became uniform in cross-section. The discharge glow at high pressures was similar to that generated at low pressures. With increased tube gas velocity the glow intensity decreased and became less uniform due to gas compression and dilution in the flow. A uniform cross-section unconstricted discharge was studied in various types of gas flow using subsonic and supersonic nozzles. It was established that the flow turbulence did not affect the uniformity pattern of the discharge. When the discharge current was increased, it was however necessary to also increase the flow velocity to maintain discharge uniformity. Rapid changes in the gas state affected the thermal processes and deconstriction of the discharges. The cited results are applicable to high-pressure gas lasers, the study of plasma, and to properties of subsonic and supersonic flows.

Batenin, V. M., V. S. Zrodnikov, I. I.
Klimovskiy, and N. I. Tsemko. Mechanism
of propagation from an shf discharge in air.
ZhETF, v. 63, no. 3, 1972, 854-860.

Effects are studied of plasma nonequilibrium in a discharge on the velocity of ionization front movement in strong shf fields in air under atmospheric pressure. An electromagnetic wave occurs in front of the discharge in an area heated by gas thermal conductivity. The electromagnetic wave is composed of the incident wave and the wave reflected from the plasma plug; the reflection coefficient is ~25% according to experimental data. It is assumed that discharge movement is governed by the breakdown of heated gas, and the ionization temperature by the electric field in front of the discharge. Qualitative comparison of experimental and theoretical data confirms the role of the breakdown mechanism in ionization development.

Since it was not possible to obtain accurate data on the reflection phase, the computed values of discharge movement velocities are not uniform. The authors therefore conducted a series of experiments aimed at analyzing the velocities of discharge movement in a region with a uniform magnetic field of three possible orientations: $\vec{H} \perp \vec{E}$, $\vec{H} \parallel \vec{u}$; $\vec{H} \perp \vec{E}$, $\vec{H} \parallel \vec{u}$; and $\vec{H} \perp \vec{u}$, $\vec{H} \parallel \vec{E}$.

The magnetic field of any chosen orientation should not affect the thermal conductivity heating of gas in front of the discharge. However, when the discharge moves due to gas heating in front of the discharge and ends in a breakdown, the magnetic field may affect the discharge movement only under the condition $H \perp E$. The authors conducted additional experiments in a 6.5 cm discharge tube, which was calculated for optimal performance, excluding the impact of the ionization breakdown mechanism.

The experiments with magnetic fields and discharge tubes of diverse diameters corroborated the assumption that the mechanism of shf discharge movement can be of a two-step type and occur in the thermal conductivity heating of gas in front of the discharge with a subsequent breakdown. The process and its nature depend on gas pressure and electric field strength. Even at high gas pressures, the breakdown mechanism may be dominant whenever the incident wave field strength is substantial.

The cited mechanism differs from the model developed by Rayzer (ZhETF, 61, 222, 1971) which is based upon similarity with flame propagation in a combustible mixture, when the temperature of ionization jump under the condition of equilibrium heating is determined by the thermal gas ionization.

Gabovich, M. D., P. D. Starchik, and
V. F. Semenyuk. Transportation of
plasma flux by magnetic fields of up to
100 koe. UFZh, no. 3, 1972, 353-355.

The article presents an experimental study of plasma flux in a relatively strong magnetic field, when both electrons and ions are magnetized under the condition $\rho_e \ll \rho_i \ll R$, where ρ_e is the Larmor radius of electrons, ρ_i is the Larmor radius of ions, and R - the outlet radius. The object is to show that it is feasible to transport plasma by ion-magnetizing magnetic fields.

The plasma flux along a magnetic field to 100 koe intensity flowed from the pulsed discharge gap into a vacuum region. Argon or helium at 10^{-2} torr was used in the discharge chamber. The helium plasma ion component (density = $3 \times 10^{12} \text{ cm}^{-3}$) in a 80 koe magnetic field propagated at a velocity of $v \approx 10^6 \text{ cm/sec}$, and the argon plasma ion component (density - $8 \times 10^{12} \text{ cm}^{-3}$) at a velocity of $\approx 5 \times 10^5 \text{ cm/sec}$. Figure 1 shows a relationship for collector ion current. The results reveal that in the 80 koe field the 1 mm flux plasma propagates more than 100 mm almost without diffusion. The Larmor radius of helium ions (1 ev at $H = 80$ koe) is $\sim 5 \times 10^{-2} \text{ mm}$, considerably smaller than that of the outlet radius. Even at $H = 40$ koe, the flux of emerging ions is concentrated in a cone whose apex angle is $\leq 1^\circ$. The experiments with argon yielded similar results, i.e. the flux similarly propagated without diffusion even at $H = 40$ to 80 koe, and the cone apex angle did not exceed $\sim 1^\circ$.

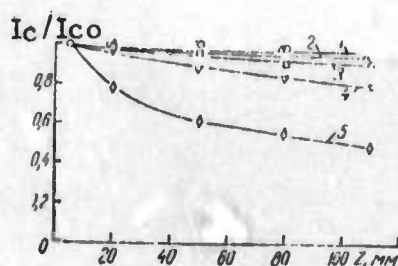


Fig. 1. Relationship of collector ion current at a point z to a corresponding current at $z = 5 \text{ nm}$ away from the magnetic field z - coordinate. Magnetic intensities (H): 1 = 180 koe; 2 = 70 koe; 3 = 60 koe; 4 = 50 koe; 5 = 40 koe.

B. Recent Selections

Aleksandrov, V. V., and O. S. Ryzhov. Nonlinear acoustics of a radiating gas. 1. Combined analysis of equations. ZhVMMF, no. 6, 1972, 1489-1511.

Budushcheye nauki. Mezhdunarodnyy yezhegodnik. Vypusk pyatyy (The future of science. International yearbook. No. 5). Moskva, Izd-vo Znaniye, 1972, 335 p. (RBL, 7/72, no. 368)

Burshteyn, R. Kh., A. G. Pshenichnikov, M. R. Tarasevich, Yu. A. Chizmadzhev, and Yu. G. Chirkov. Moisture exchange in a hydrogen-oxygen fuel cell with a capillary membrane. Elektrokhimiya, no. 11, 1972, 1688-1692.

Fiziki o fizike. Fizika tverdogo tela: novyye idei i metody (Physicists on physics. Solid state physics: new ideas and methods). Moskva, Izd-vo Znaniye, 1972, 64 p. (RBL, 7/72, no. 388)

Garshka, E., V. Kunigelis, B. Ketis, and A. Sereyka. Extrinsic nonlinearity of electroacoustic interactions. IN: Nauchnyye trudy vuzov LitSSR, Ul'trazvukh, v. 3, 1971, 37-41. (LZhS, 46/72, no. 153301)

Kazantsev, A. P. Acceleration of atoms by a resonant field. ZhETF, v. 63, no. 5, 1972, 1628-1634.

Ketis, B., V. Kunigelis, E. Garshka, and V. Ilgunas. Aspects of nonlinear electroacoustic interactions. IN: Nauchnyye trudy vuzov LitSSR, Ul'trazvukh, v. 3, 1971, 43-45. (LZhS, 46/72, no. 153271)

Kunigelis, V., and E. Garshka. Nonlinearity of electroacoustic interactions. IN: Nauchnyye trudy vuzov LitSSR, Ul'trazvukh, v. 3, 1971, 47-50. (LZhS, 46/72, no. 153244)

Molchanov, A. D., and V. P. Kosyk. Optimum parameters of the discharge gap for high voltage spark discharges in a liquid. EOM, no. 5, 1972, 43-48.

Okorokov, V. V., D. L. Tolchenkov, I. S. Khizhnyakov, Yu. N. Cheblukov, Yu. Ya. Lapitskiy, G. A. Iferov, and Yu. I. Zhukova. Coherent excitation of atoms passing through a crystal. ZhETF P, v. 63, no. 11, 1972, 588-592.

Protopopova, L. F., and A. M. Fedorchenco. Rayleigh waves in semiconductors and ionic crystals with cubic symmetry. IN: Nauchnyye trudy vuzov LitSSR, Ul'trazvukh, v. 3, 1971, 61-67. (LZhS, 46/72, no. 153302)

Ratnikov, E. V., and A. D. Khudokormov. Flame conductivity during a corona discharge. IAN B. Seriya fiziko-tehnicheskikh nauk, no. 4, 1972, 117-120.

Vinogradov, A. P., V. I. Nefedov, V. S. Urusov, and N. M. Zhavoronkov. X-ray analysis of metallic iron in lunar regolith. DAN SSSR, v. 207, no. 2, 1972, 433-436.

Volkov, S. V., and V. D. Prisyazhnyy. Kholodnoye gorenije. (Problema toplivnykh elementov)(Cold combustion: problem of fuel cells). Kiyev, Izd-vo Naukova dumka, 1972, 175 p. (KL, 48/72, no. 38722)

Voynich, B. A., G. A. Volkova, M. V. Andreychuk, and V. A. Andrianov. Effect of a priori data on target location on the quality of radar detection. IN: Trudy Moskovskogo aviationsionnogo instituta, no. 207, 1971, 190-197. (LZhS, 47/72, no. 157668)

Yuzonene, L., and A. Ribikauskas. Measuring ultrasonic waves. IN: Nauchnyye trudy vuzov LitSSR, Ul'trazvukh, v. 3, 1971, 127-133. (LZhS, 46/72, no. 153354)

Zhitkovskiy, Yu. Yu. Correlation between reflection and scattering of sound from the ocean bottom. Akusticheskiy zhurnal, no. 4, 1972, 533-536.

7. SOURCE ABBREVIATIONS

AiT	-	Avtomatika i telemekhanika
APP	-	Acta physica polonica
DAN ArmSSR	-	Akademiya nauk Armyanskoy SSR. Doklady
DAN AzSSR	-	Akademiya nauk Azerbaydzhanskoy SSR. Doklady
DAN BSSR	-	Akademiya nauk Belorusskoy SSR. Doklady
DAN SSSR	-	Akademiya nauk SSSR. Doklady
DAN TadSSR	-	Akademiya nauk Tadzhikskoy SSR. Doklady
DAN UkrSSR	-	Akademiya nauk Ukrainskoy SSR. Dopovidi
DAN UzbSSR	-	Akademiya nauk Uzbekskoy SSR. Doklady
DBAN	-	Bulgarska akademiya na naukite. Doklady
EOM	-	Elektronnaya obrabotka materialov
FAiO	-	Akademiya nauk SSSR. Izvestiya. Fizika atmosfery i okeana
FGiV	-	Fizika goreniya i vzryva
FiKhOM	-	Fizika i khimiya obrabotka materialov
F-KhMM	-	Fiziko-khimicheskaya mekhanika materialov
FMiM	-	Fizika metallov i metallovedeniye
FTP	-	Fizika i tekhnika poluprovodnikov
FTT	-	Fizika tverdogo tela
FZh	-	Fiziologicheskiy zhurnal
GiA	-	Geomagnetizm i aeronomiya
GiK	-	Geodeziya i kartografiya
IAN Arm	-	Akademiya nauk Armyanskoy SSR. Izvestiya. Fizika
IAN Az	-	Akademiya nauk Azerbaydzhanskoy SSR. Izvestiya. Seriya fiziko-tehnicheskikh i matematicheskikh nauk

IAN B	-	Akademiya nauk Belorusskoy SSR. Izvestiya. Seriya fiziko-matematicheskikh nauk
IAN Biol	-	Akademiya nauk SSSR. Izvestiya. Seriya biologicheskaya
IAN Energ	-	Akademiya nauk SSSR. Izvestiya. Energetika i transport
IAN Est	-	Akademiya nauk Estonskoy SSR. Izvestiya. Fizika matematika
IAN Fiz	-	Akademiya nauk SSSR. Izvestiya. Seriya fizicheskaya
IAN Fizika zemli	-	Akademiya nauk SSSR. Izvestiya. Fizika zemli
IAN Kh	-	Akademiya nauk SSSR. Izvestiya. Seriya khimicheskaya
IAN Lat	-	Akademika nauk Latviyskoy SSR. Izvestiya
IAN Met	-	Akademika nauk SSSR. Izvestiya. Metally
IAN Mold	-	Akademika nauk Moldavskoy SSR. Izvestiya. Seriya fiziko-tehnicheskikh i matematicheskikh nauk
IAN SO SSSR	-	Akademika nauk SSSR. Sibirskoye otdeleniye. Izvestiya
IAN Tadzh	-	Akademika nauk Tadzhikskoy SSR. Izvestiya. Otdeleniye fiziko-matematicheskikh i geologo-khimicheskikh nauk
IAN TK	-	Akademika nauk SSSR. Izvestiya. Tekhnicheskaya kibernetika
IAN Turk	-	Akademika nauk Turkmenskoy SSR. Izvestiya. Seriya fiziko-tehnicheskikh, khimicheskikh, i geologicheskikh nauk
IAN Uzb	-	Akademika nauk Uzbekskoy SSR. Izvestiya. Seriya fiziko-matematicheskikh nauk
IBAN	-	Bulgarska akademiya na naukite. Fizicheski institut. Izvestiya na fizicheskaya institut s ANEB
I-FZh	-	Inzhenerno-fizicheskiy zhurnal

IiR	-	Izobretatel' i ratsionalizator
ILEI	-	Leningradskiy elektrotekhnicheskiy institut. Izvestiya
IT	-	Izmeritel'naya tekhnika
IVUZ Avia	-	Izvestiya vysshikh uchebnykh zavedeniy. Aviatsionnaya tekhnika
IVUZ Cher	-	Izvestiya vysshikh uchebnykh zavedeniy. Chernaya metallurgiya
IVUZ Energ	-	Izvestiya vysshikh uchebnykh zavedeniy. Energetika
IVUZ Fiz	-	Izvestiya vysshikh uchebnykh zavedeniy. Fizika
IVUZ Geod	-	Izvestiya vysshikh uchebnykh zavedeniy. Geodeziya i aerofotos"yemka
IVUZ Geol	-	Izvestiya vysshikh uchebnykh zavedeniy. Geologiya i razvedka
IVUZ Gorn	-	Izvestiya vysshikh uchebnykh zavedeniy. Gornyy zhurnal
IVUZ Mash	-	Izvestiya vysshikh uchebnykh zavedeniy. Mashinostroeniye
IVUZ Priboro	-	Izvestiya vysshikh uchebnykh zavedeniy. Priborostroyeniye
IVUZ Radioelektr	-	Izvestiya vysshikh uchebnykh zavedeniy. Radioelektronika
IVUZ Radiofiz	-	Izvestiya vysshikh uchebnykh zavedeniy. Radiofizika
IVUZ Stroi	-	Izvestiya vysshikh uchebnykh zavedeniy. Stroitel'stvo i arkhitektura
KhVE	-	Khimiya vysokikh energiy
KiK	-	Kinetika i kataliz
KL	-	Knizhnaya letopis'
Kristall	-	Kristallografiya
KSpF	-	Kratkiye soobshcheniya po fizike

LZhS	-	Letopis' zhurnal'nykh statey
MiTOM	-	Metallovedeniye i termicheskaya obrabotka materialov
MP	-	Mekhanika polimerov
MTT	-	Akademiya nauk SSSR. Izvestiya. Mekhanika tverdogo tela
MZhiG	-	Akademiya nauk SSSR. Izvestiya. Mekhanika zhidkosti i gaza
NK	-	Novyye knigi
NM	-	Akademiya nauk SSSR. Izvestiya. Neorganicheskiye materialy
NTO SSSR	-	Nauchno-tehnicheskiye obshchestva SSSR
OiS	-	Optika i spektroskopiya
OMP	-	Optiko-mekhanicheskaya promyshlennost'
Otkr izobr	-	Otkrytiya, izobreteniya, promyshlennyye obraztsy, tovarnyye znaki
PF	-	Postupy fizyki
Phys abs	-	Physics abstracts
PM	-	Prikladnaya mekanika
PMM	-	Prikladnaya matematika i mekanika
PSS	-	Physica status solidi
PSU	-	Pribory i sistemy upravleniya
PTE	-	Pribory i tekhnika eksperimenta
Radiotekh	-	Radiotekhnika
RiE	-	Radiotekhnika i elektronika
RZhAvtom	-	Referativnyy zhurnal. Avtomatika, telemekhanika i vychislitel'naya tekhnika
RZhElektr	-	Referativnyy zhurnal. Elektronika i yeye primeneniye

RZhF	-	Referativnyy zhurnal. Fizika
RZhFoto	-	Referativnyy zhurnal. Fotokinotekhnika
RZhGeod	-	Referativnyy zhurnal. Geodeziya i aeros"-yemka
RZhGeofiz	-	Referativnyy zhurnal. Geofizika
RZhInf	-	Referativnyy zhurnal. Informatics
RZhKh	-	Referativnyy zhurnal. Khimiya
RZhMekh	-	Referativnyy zhurnal. Mekhanika
RZhMetrolog	-	Referativnyy zhurnal. Metrologiya i izmeritel'naya tekhnika
RZhRadiot	-	Referativnyy zhurnal. Radiotekhnika
SovSciRev	-	Soviet science review
TiEKh	-	Teoreticheskaya i eksperimental'naya khimiya
TKiT	-	Tekhnika kino i televideniya
TMF	-	Teoreticheskaya i matematicheskaya fizika
TVT	-	Teplofizika vysokikh temperatur
UFN	-	Uspekhi fizicheskikh nauk
UFZh	-	Ukrainskiy fizicheskiy zhurnal
UMS	-	Ustalost' metallov i splavov
UNF	-	Uspekhi nauchnoy fotografii
VAN	-	Akademiya nauk SSSR. Vestnik
VAN BSSR	-	Akademiya nauk Belorusskoy SSR. Vestnik
VAN KazSSR	-	Akademiya nauk Kazakhskoy SSR. Vestnik
VBU	-	Belorusskiy universitet. Vestnik
VNDKh SSSR	-	VNDKh SSSR. Informatsionnyy byulleten'
VLU	-	Leningradskiy universitet. Vestnik. Fizika, khimiya
VMU	-	Moskovskiy universitet. Vestnik. Seriya fizika, astronomiya

ZhETF	-	Zhurnal eksperimental'noy i teoreticheskoy fiziki
ZhETF P	-	Pis'ma v Zhurnal eksperimental'noy i teoreticheskoy fiziki
ZhFKh	-	Zhurnal fizicheskoy khimii
ZhNiPFIK	-	Zhurnal nauchnoy i prikladnoy fotografii i kinematografii
ZhNKh	-	Zhurnal neorganicheskoy khimii
ZhPK	-	Zhurnal prikladnoy khimii
ZhPMTF	-	Zhurnal prikladnoy mekhaniki i tekhnicheskoy fiziki
ZhPS	-	Zhurnal prikladnoy spektroskopii
ZhTF	-	Zhurnal tekhnicheskoy fiziki
ZhVMMF	-	Zhurnal vychislitel'noy matematiki i matematicheskoy fiziki
ZL	-	Zavodskaya laboratoriya

8. AUTHOR INDEX

A

Afonina, N. Ye. 23
Aksenovich, G. I. 91
Alimov, V. A. 37
Alkhimov, A. P. 8
Arifov, T. U. 8
Arsen'yan, T. I. 39

B

Batanov, B. A. 6
Batanov, V. A. 4
Batenin, V. M. 144
Berlyand, O. S. 35
Blagosklonov, V. I. 22
Bogolyubskiy, I. L. 24
Bol'shakov, V. N. 105
Boronin, A. P. 47
Bulin, N. V. 68

C

Chastov, A. A. 15
Chebotayev, V. P. 143

D

Danileyko, Yu. K. 1
Dubrovskiy, V. A. 72

G

Gabovich, M. D. 146
Gershbein, E. A. 25
Gilinskiy, S. M. 23
Golovachev, Yu. P. 21
Gorinov, A. S. 25
Grekhov, I. V. 138

I

Ivanov, A. P. 140

K

Kapitanov, V. A. 38
Katsaurov, L. N. 106

Kazinskiy, V. A. 86
Klyatskin, V. I. 33
Knyazev, I. N. 10
Kogan, S. D. 73
Kopytenko, Yu. A. 43
Kramskoy, G. D. 104
Krylov, S. V. 82

L

Lebedev, D. P. 119
Lebedev, S. V. 29
Lokhov, Yu. N. 2
Lomakin, B. N. 31
Lursmanashvili, O. V. 71

M

Magnitskiy, B. V. 41
Markov, A. A. 49
Matasova, L. M. 78
Mel'nichenko, I. P. 137
Mel'nikova, N. S. 50
Mkheidze, G. P. 101
Moshnenko, Yu. I. 27

N

Narayeva, M. K. 135
Nikolayev, F. A. 28

P

Petukhova, T. M. 16
Pilyugin, N. N. 27
Polyakov, Yu. A. 20
Prokhorov, V. G. 136
Puzyrev, N. N. 89

R

Rezvov, A. V. 11
Ry kunov, L. N. 76

S

Savinov, K. G. 26
Shapiro, Ye. G. 118

Shvets, A. I. 22
Stulov, V. P. 118
Sultanov, M. A. 119
Sychev, V. V. 31

T

Tarkov, A. P. 79
Tkach, Yu. V. 103
Tyurin, Ye. L. 12

U

Ulomov, V. I. 79

V

Vavilov, S. P. 107
Vertogradskiy, V. A. 117
Verzhinskaya, A. B. 115
Vinogradov, A. I. 44

Y

Yakovleva, I. B. 77
Yeshchenko, S. D. 142

Z

Zak, L. I. 24
Zayko, Yu. N. 13
Zuyev, V. Ye. 46
Zvolinskiy, N. V. 52

9. CUMULATIVE AUTHOR INDEX:
JANUARY - DECEMBER 1972

A

Abdullabekov, K. N. 9:128, 10:69
Abramova, K. B. 4:24, 2:62
Abramovich, V. U. 5:103
Abramyan, E. A. 6:95
Adadurov, G. A. 2:48, 9:38, 40
Adam, A. 10:4
Adeyshvili, D. I. 9:136
Afanasenkov, A. N. 5:21
Afanas'yev, A. A. 3:5
Afanas'yev, Yu. V. 4:9
Afonina, N. Ye. 12:23
Akhiyezer, A. I. 3:23
Aksenovich, G. I. 12:91
Alekhin, V. P. 7:149
Aleksandrov, A. F. 2:57
Aleksandrov, V. V. 6:19, 10:15
Alekseyev, E. I. 4:7
Alekseyev, Yu. L. 2:53
Alenichev, V. S. 2:60
Aleynikov, A. L. 9:129
Alimov, V. A. 4:36, 5:57, 6:24,
 12:37
Alinovskiy, N. I. 2:19, 9:50
Aliyev, F. 7:104
Alkhimov, A. P. 12:8
Al'tshuler, L. V. 2:54
Anan'in, O. B. 3:6
Anatsky, A. N. 3:79
Andreyev, A. A. 5:86
Andreyev, V. G. 9:159
Andreyev, V. P. 2:36
Andreyev, Yu. P. 9:171
Andriankin, E. I. 9:73
Andrionov, A. M. 2:103
Anik'yev, I. I. 2:62
Anisimov, S. I. 4:12, 11:1
Anoshin, A. N. 11:11
Antipov, Ye. A. 11:112
Antonenko, A. N. 5:89
Antonets, A. V. 5:34, 35
Antonova, A. M. 9:63
Antonova, L. V. 4:57
Apshteyn, E. Z. 5:33
Aptikayev, F. F. 4:63

Arifov, T. U. 12:8
Arifov, U. A. 3:1, 11:7
Aristov, A. V. 9:25
Aristov, V. V. 5:69
Arkhangel'skiy, N. A. 2:59
Arsen'yan, T. I. 12:39
Artem'yev, M. Ye. 4:58
Artyukh, V. G. 5:129
Arutyunyan, G. M. 5:37
Asabayev, Ch. 11:67
Aseyev, G. I. 7:9, 11:9, 10
Ashmarin, I. I. 5:1
Askar'yan, G. A. 4:10, 6:2,
 9:1
Aslanov, S. K. 5:11
Assovskiy, I. G. 2:1
Avdeyenko, N. S. 6:62
Avduyevskiy, V. S. 6:25
Averin, V. G. 10:98
Avotin, S. S. 4:1
Ayvazov, V. Ya. 5:103

B

Babaritskiy, A. I. 2:99
Babenko, K. I. 9:66
Bagdoyev, A. G. 2:56
Bagirov, M. A. 5:115
Bakal, S. Z. 5:109
Bakhshiyyev, N. G. 9:24
Baksht, R. B. 2:111
Baksik, A. 9:20
Balakin, V. B. 5:11, 9:63
Balkarey, Yu. I. 6:69
Balter, M. A. 10:130
Barinov, V. I. 4:79
Barinova, T. Ya. 10:28
Barmin, A. A. 9:9
Baron, V. V. 6:92
Bartashyus, I. Yu. 2:94
Barwicz, W. 3:89, 90
Barzykin, V. V. 9:79, 10:48
Bashkatov, A. V. 7:45
Bashurov, V. 11:34
Basman, A. R. 9:139
Basov, N. G. 2:1, 65, 6:7

Batanov, B. A. 12:6
Batanov, V. A. 7:8, 12:4
Batenin, V. M. 12:144
Batsanov, S. S. 9:77
Bayev, V. K. 9:76
Bayramov, B. Kh. 3:6
Bedilov, M. R. 7:10
Begoulev, P. B. 11:34
Bek-Bulatov, I. Kh. 5:117
Belan, N. V. 3:97, 102, 11:116
Belikov, A. G. 10:94
Belkin, N. V. 2:98
Bel'kov, Ye. P. 2:108, 7:59
Belobrovik, V. I. 11:6
Belozerov, S. A. 4:2, 11:5
Belyayevskiy, N. A. 6:56
Benediktov, Ye. A. 9:88, 90
Berezin, Yu. A. 10:19
Bereznyak, P. A. 3:96
Berlyand, O. S. 12:35
Berzon, I. S. 11:71
Bessarab, Ya. Ya. 5:4
Beylis, I. I. 9:144
Bezdomnyy, N. 5:148
Bezhanov, K. A. 5:30
Bezrodnyy, Ye. M. 5:92, 10:65
Biberman, L. M. 3:24, 9:53
Blagosklonov, V. I. 12:22
Blitshteyn, Yu. M. 10:16
Bobolev, V. K. 9:80
Bogachev, I. N. 6:91, 11:109
Bogashchenko, I. A. 4:21, 5:44
Bogdankevich, L. S. 10:87
Bogolyubskiy, I. L. 12:24
Bogomolova, L. A. 2:51
Bol'shakov, V. N. 12:105
Bonch-Bruyevich, A. M. 10:6
Borisov, A. A. 3:24
Borisov, D. G. 10:97
Borisov, M. B. 3:25
Borisov, V. V. 2:10
Boronin, A. P. 2:50, 12:47
Borovich, B. L. 2:101
Borovoy, V. Ya. 5:30, 7:19
Boyko, M. M. 9:48
Boyko, Yu. I. 2:2, 9:10
Bozhkov, A. I. 6:1
Brazhnev, V. V. 10:113
Brekovskikh, V. P. 3:7
Brodskaya, B. Kh. 6:73
Bronin, S. Ya. 2:28
Brudnyy, V. N. 4:20
Bud'ko, N. I. 2:10

Buechl, K. 7:7
Bugayevskiy, G. N. 3:71
Bukin, G. V. 11:44
Bulakh, B. M. 9:62
Bulin, N. K. 3:66, 5:82, 95, 12:68
Bunin, V. A. 9:207
Burakov, V. S. 6:11, 9:17
Buravova, S. N. 6:15
Burminskiy, E. P. 2:28
Butenin, A. V. 3:1
Buzhinskiy, O. I. 11:21
Bykov, B. P. 5:56
Bystrov, L. N. 7:46

C

Chagelishvili, E. Sh. 9:82
Chamo, S. S. 6:48
Chastov, A. A. 12:15
Chebotayev, V. P. 12:143
Chekalin, E. K. 2:30
Cherkun, Yu. P. 5:2
Chernyshevich, I. V. 7:173
Churayev, V. A. 3:98

D

Danileyko, Yu. K. 12:1
Danilov, V. V. 9:26
Danilovskaya, V. I. 3:100
Danilychev, V. A. 2:106
Davlet-Kil'deyev, R. Z. 9:54
Davydov, B. B. 3:104
Demidov, M. I. 9:133
Denisov, Yu. P. 3:14
Denyak, V. M. 3:89
Deryagin, B. V. 11:52
Derzhavina, A. I. 3:14
Deryabina, V. I. 10:111
Dikhter, I. Ya. 2:63
Dimakov, A. I. 10:68
Dmitriyev, M. T. 2:97
Dmitriyevskiy, V. A. 5:18
Dolmatov, K. I. 7:23
Dombrovskiy, G. A. 11:23
Doroshenko, A. N. 5:108
Dremin, A. N. 2:48, 49, 5:21, 70
Drobyshev, Yu. P. 4:66
Druker, I. G. 10:121
Dubnov, L. V. 6:15
Dubovik, A. V. 9:83
Dubrovin, V. M. 9:45
Dubrovskiy, V. A. 12:72

Dunin, S. Z. 5:140
Duntsova, Zh. S. 2:33
Dyadyusha, G. G. 9:22

E

Epshteyn, E. M. 5:3
Eydmann, V. Ya. 7:54

F

Fadina, M. P. 11:64
Fal'kovskiy, N. I. 2:106
Fanchenko, S. D. 7:2
Fateyeva, N. S. 7:97
Fedotov, B. N. 9:67
Fekeshgazi, I. V. 2:2
Ferdinandov, E. S. 6:23
Fetisova, M. M. 11:110
Filatov, Ye. I. 5:45
Fokin, L. R. 10:32
Fortov, V. Ye. 2:67, 10:18
Fridlender, B. A. 10:117
Frolov, V. V. 5:4
Fursey, G. N. 2:90, 92, 93, 10:89

G

Gabovich, M. D. 12:146
Gadion, V. N. 9:71
Galaktionov, I. I. 2:32
Galeev, A. A. 2:19
Gal'perina, R. M. 4:64
Gaponenko, N. P. 10:123
Gaponov, S. A. 10:23
Gaponov, V. A. 6:75
Garber, R. I. 3:3
Garkalenko, I. A. 6:52
Gashchenko, A. G. 9:160
Gavrilenko, T. B. 5:126
Gavrilenko, V. G. 6:23
Gayskiy, V. N. 3:75
Geguzin, Ya. Ye. 7:5
Gel'fand, I. M. 11:68
Gel'tsel', M. Yu. 2:100
Generalov, N. A. 2:11, 3:15
Geogdzhayev, V. O. 7:111
Georg, E. B. 7:94
Gershbeyn, E. A. 12:25
Gilinskiy, S. M. 12:23
Godunov, S. K. 4:17
Gogosov, V. V. 3:17
Golant, V. Ye. 4:9
Gol'din, S. V. 9:126, 127

Gol'dman, A. Ya. 9:177
Gol'dshteyn, R. V. 10:108
Goloborod'ko, V. T. 7:52
Goloskokov, Ye. G. 10:132
Gelov, A. A. 7:61
Golovachev, Yu. P. 2:29, 12:21
Golovanivskiy, K. S. 5:123
Golovina, Ye. S. 10:118
Golyanov, V. M. 7:112
Goncharov, V. K. 7:1
Gorbenko, V. G. 11:92
Gorelov, V. A. 2:38, 41, 3:17, 6:21
Gorinov, A. S. 12:25
Goriin, G. B. 7:148
Girekhov, I. V. 12:138
Grigor'yev, S. S. 9:123
Grigor'yev, Yu. N. 10:101
Grishin, V. K. 3:104
Groshev, I. N. 7:148
Gryaznovskaya, F. V. 9:121
Gubarev, V. Ya. 3:93
Gulyayeva, A. S. 11:3
Gurevich, A. V. 7:29
Gurevich, V. I. 6:4
Gusev, N. V. 3:3
Gusev, V. K. 9:16
Gutova, L. A. 3:80

I

Inogamov, I. I. 9:86
Iremashvili, D. V. 3:99
Iskakbayev, A. 6:30
Ivanov, A. A. 3:19, 6:21
Ivanov, A. P. 12:140
Ivanov, N. V. 5:122
Ivanov, V. V. 10:119
Ivanov, Yu. S. 4:77
Ilev, B. I. 7:106

J

Jelen, J. 9:136
Juza, J. 11:40

K

Kabanov, A. N. 6:72
Kachanov, M. L. 10:107
Kaliski, S. 7:7, 25
Kalitkin, N. N. 7:101
Kallistratova, M. A. 10:39
Kalyatskiy, I. I. 5:128
Kantorovich, I. I. 9:5

Kapel'yan, S. N. 6:5
 Kapitanov, V. A. 12:38
 Kapustyanskiy, S. M. 10:29
 Karakhanov, S. M. 2:61
 Karasev, A. B. 5:42, 43
 Karashokov, K. Ye. 3:81
 Karchevskiy, A. I. 9:147
 Karnozhitskiy, V. P. 7:109
 Karpinos, D. M. 9:182
 Karпов, V. P. 2:46
 Kasatochkin, V. I. 2:8
 Kashirskiy, A. V. 11:47
 Katasev, L. A. 9:94
 Katsaurov, L. N. 12:106
 Katskova, O. N. 9:61
 Kaytmazov, S. D. 4:7
 Kazakov, A. Ye. 2:12
 Kazansky, L. N. 11:86
 Kazinskiy, V. A. 12:86
 Kestenboym, Kh. S. 3:19, 7:28
 Khalturin, V. I. 3:75
 Khannanov, Sh. Kh. 7:74, 76
 Khazov, L. D. 7:12
 Khirseli, E. M. 11:88
 Khristoforov, B. D. 5:22, 9:56
 Kichayeva, G. S. 7:57
 Kikvidze, R. R. 3:86, 11:85
 Kirichenko, G. S. 10:91
 Kiryushchenko, A. I. 5:141
 Kiseleva, L. G. 11:64
 Kislykh, V. V. 10:114
 Kit, G. S. 7:91
 Klyatskin, V. I. 12:33
 Knyazev, I. N. 12:10
 Kochelap, V. A. 10:8
 Kochmanova, L. V. 2:27
 Kogan, S. D. 12:73
 Kokin, G. A. 5:52
 Kolesnikov, P. M. 4:77, 5:106
 Kolokolov, A. A. 3:7
 Kolomenskiy, A. A. 10:86
 Komel'kov, V. S. 2:107
 Kondorskaya, N. V. 5:98
 Kondrya, A. K. 11:30
 Kon'kov, A. A. 9:172
 Konobeyevskiy, S. T. 5:117
 Kopan', V. S. 7:107
 Kopecky, V. 11:87
 Kopytenko, Yu. A. 12:43
 Korchagina, O. A. 11:66
 Kornev, V. M. 10:128
 Korobeynikov, V. P. 5:64, 10:27
 Korotin, A. V. 6:6
 Korotkov, V. A. 11:36
 Korshunov, G. S. 2:105
 Korsunkaya, I. A. 11:107
 Kosarev, I. B. 11:49
 Kosarev, V. I. 3:21
 Kosorukov, A. L. 9:64
 Kostylev, V. M. 6:10
 Kotenko, V. G. 4:75
 Kovadlo, M. 5:148
 Kovalchuk, V. M. 11:88
 Kovalev, A. A. 9:33
 Kovalev, V. P. 5:105
 Kovalevskiy, G. L. 6:65, 10:64
 Kozachenko, L. S. 5:14
 Kozlov, V. I. 4:29
 Kozyrev, B. P. 10:45
 Kraft, V. V. 6:78
 Kramskoy, G. D. 12:104
 Krasovitskiy, V. B. 6:84, 7:62
 Krasovskiy, A. Ya. 2:52
 Krasyuk, I. K. 6:9
 Krestin, G. S. 7:77
 Krishtal, M. A. 9:149
 Krivitskiy, Ye. V. 5:131, 10:157
 Krivoshchekov, G. V. 2:101
 Krupina, A. Ye. 9:89
 Krupnikov, K. K. 5:66
 Krylov, S. V. 3:64, 9:112, 12:82
 Kryukova, S. G. 9:68
 Kukarkina, M. A. 9:60
 Kukhtevich, V. I. 5:62
 Kulagina, M. V. 6:60
 Kul'man, V. G. 6:76
 Kurbanov, M. 5:93, 99
 Kurtmullayev, R. Kh. 2:44
 Kuz'menko, N. Ye. 7:16
 Kuzmicheva, A. Ye. 9:92
 Kuznetsov, A. Ya. 9:2
 Kuznetsov, A. Ye. 9:7
 Kuznetsov, V. S. 11:87
 Kvartskhava, I. F. 10:95

L

Larin, O. B. 3:21
 Lavrovskiy, V. A. 5:118
 Lazarenko, B. R. 11:89
 Lazarev, B. G. 7:117
 Lazareva, L. D. 9:29
 Lazovskaya, V. R. 3:22
 Lebedev, D. P. 12:119
 Lebedev, D. V. 7:84
 Lebedev, S. V. 2:58, 59, 12:29
 Lerman, M. I. 10:25
 Letokhov, V. S. 11:8

Levin, M. L. 11:95
Libatskiy, L. L. 7:83
Liberman, M. A. 4:6
Lidorenko, M. S. 5:70
Lifshits, Yu. B. 5:45
Limarev, A. Ye. 5:12
Lisin, V. N. 10:99
Lisitsa, M. P. 2:3
Lisovets, Yu. P. 3:2
Lobanov, V. F. 7:18
Lokhov, Yu. N. 11:11, 12:2
Lomakin, B. N. 10:21, 12:31
Lomakin, Ye. V. 10:134
Lominadze, D. G. 11:26
Lopatin, V. V. 5:112
Losev, S. A. 2:21
Lozhkin, V. L. 11:115
Lukk, A. A. 3:74, 4:51
Lunev, V. V. 5:36, 39
Lursmanashvili, O. V. 12:71
Lutkov, A. I. 7:95
Lutts, B. G. 6:58

M

Magnetova, N. N. 3:27
Magnitskiy, B. V. 12:41
Maksimov, A. M. 3:32
Malinochka, Ya. N. 7:93
Malkin, O. A. 4:72
Malyshev, G. M. 11:15
Malyshev, V. V. 2:70, 7:26
Mamadaliyev, N. A. 5:38
Mandzhikov, V. F. 5:139
Mardukhayev, I. R. 2:50
Markov, A. A. 12:49
Martynov, Ye. P. 2:110
Mar'yamov, A. N. 2:50
Matasova, L. M. 12:78
Matora, I. M. 3:86
Mattheck, C. 11:140
Maykapar, G. I. 9:65
Mel'nichenko, I. P. 12:137
Mel'nik, V. I. 9:151
Mel'nikova, N. S. 12:50
Merzhanov, A. G. 5:61
Meshkov, Ye. Ye. 2:23
Mesyats, G. A. 2:95, 96, 97, 10:82, 84,
 11:82, 84
Mevlyudov, S. I. 9:69
Migdal, A. A. 10:33
Mikhaylov, V. N. 6:27
Mikhaylova, R. S. 6:64
Mirkin, L. I. 3:4, 6:4
Mironov, V. L. 9:91
Mitsuk, V. E. 10:5

Mkheidze, G. P. 3:87, 10:84, 12:101
Molchanov, A. Ye. 10:109
Molodtsov, V. K. 9:59
Momaklov, F. N. 4:65
Morozov, A. I. 5:106
Morozova, L. V. 3:35
Moshnenko, Yu. I. 12:27
Motulevich, V. P. 9:167
Mozzhilkin, V. V. 2:46
Muminov, M. M. 3:26
Musin, A. K. 5:121
Myshenkov, V. I. 5:31, 6:16

N

Naboko, I. M. 3:33
Nagaybekov, R. B. 5:114
Namitokov, K. K. 5:116
Narayeva, M. K. 12:135
Naumenko, I. G. 7:114
Naumov, A. P. 10:45
Nazarov, A. G. 9:120
Nematzov, L. 7:23
Nemchinov, I. V. 2:5
Nevskiy, A. P. 2:4
Nevskiy, L. B. 6:20
Neyland, V. Ya. 5:43
Nikiforov, Yu. N. 9:10
Nikitenko, A. F. 6:98
Nikolayev, F. A. 11:37, 12:28
Nikolayevskiy, V. G. 3:90
Nitskevich, V. P. 6:91
Norinskiy, L. V. 4:6
Noskov, D. A. 3:84
Novikov, B. V. 3:94
Novikov, M. I. 10:158
Novikov, N. P. 6:8
Nurgozhin, B. I. 11:42

O

Ocheretin, V. N. 2:60, 5:67
Omel'chenko, A. Ya. 11:16
Onishcherko, I. N. 3:84
Orehov, M. V. 3:8
Orlov, V. S. 10:66
Osadin, B. A. 10:5
Osipov, V. G. 6:94

P

Panasyuk, V. V. 7:88, 9:176
Pataraya, A. D. 2:37
Pavlenkova, N. I. 6:55
Pavlov, A. I. 7:18
Pavlov, B. M. 9:56

Pavlov, V. D. 4:58
Pavlova, I. N. 4:60
Perevodchikov, V. I. 3:82
Perminov, V. D. 9:58
Petrenko, V. I. 9:142
Petukhova, T. M. 12:16
Pevnev, A. K. 3:73
Pidstryhach, Ya. S. 7:79
Pilyugin, N. N. 12:27
Plotnikov, M. A. 2:68
Plyatsko, G. V. 3:9
Podstrigach, T. S. 2:25
Podurets, M. A. 4:19
Pogodayev, V. A. 2:9
Pogorelov, V. I. 5:13
Poltavtsev, Yu. G. 4:130
Poluboyarinov, A. K. 3:31, 5:18
Polyakov, L. M. 4:89
Polyakov, Ye. V. 7:103
Polyakov, Yu. A. 12:20
Polyanskiy, O. Yu. 11:27
Ponomarev, V. S. 4:63
Poplavskiy, A. A. 10:9
Popov, F. D. 9:58
Popov, S. P. 10:3
Popov, V. N. 5:72
Poshekhanov, P. V. 2:113
Postnikov, V. V. 7:116
Pranevichyus, I. I. 7:62
Pridatchenko, Yu. V. 9:97
Prokhorov, V. G. 12:136
Proskurovskiy, D. I. 2:112
Pryadkin, K. K. 7:152
Puchkov, S. V. 5:92
Pustovalov, V. K. 5:20, 6:6
Pustovitenko, B. G. 9:117
Putrenko, O. I. 2:5
Puzyrev, N. N. 12:89

R

Rabinovich, L. B. 9:170
Raicheff, R. G. 7:73
Rakhmatulin, Kh. A. 9:68
Ratner, S. B. 7:80
Rats, B. 9:31
Rautian, T. G. 9:119
Rauzin, Ya. R. 10:124
Rayzer, Yu. P. 2:11
Regel', V. P. 9:179
Reshetnikova, K. A. 11:89
Rezanov, I. A. 6:57, 59

Rezvov, A. V. 12:11
Rodichev, Yu. M. 9:162
Rodionov, K. P. 2:69
Rodionov, V. N. 5:64, 6:30
Rosinskiy, S. Ye. 6:80
Roytburd, A. L. 2:71
Rubinov, A. N. 9:32
Rukhadze, A. A. 6:84
Rulev, B. G. 3:70
Rykunov, L. N. 12:76
Rysakov, V. M. 11:7
Ryutov, D. D. 3:96

S

Sabun, L. B. 11:120
Salamandra, G. D. 5:26
Saltanov, G. A. 7:16
Samarskiy, A. A. 11:97
Savinov, K. G. 12:26
Savityuk, V. I. 7:22
Savruk, M. P. 7:86
Sedova, Ye. N. 4:55
Semenova, V. I. 9:2
Semkin, B. V. 11:82
Serensen, S. V. 11:118
Sergeyev, V. L. 10:115
Shafer, Yu. G. 4:30
Shamina, O. G. 3:71
Shapiro, Ye. G. 5:49, 12:118
Shchepetov, V. N. 6:74
Shcherbakova, B. Ye. 10:70
Shem'i-Zade, A. E. 10:46
Shermergor, T. D. 9:181
Shidlovskiy, V. P. 11:51
Shifrin, E. G. 5:32, 6:18
Shigorin, V. D. 9:21
Shlyapnikov, V. V. 11:40
Shtessel', E. A. 9:73
Shul'gin, B. V. 5:142
Shurshalov, L. V. 4:22
Shvets, A. I. 12:22
Siller, G. 3:4
Sil'vestrov, V. V. 9:54
Simbireva, I. G. 4:67
Simonov, I. V. 5:22
Simonov, V. A. 4:27
Sinkevich, O. A. 2:24, 3:30
Skripov, V. P. 2:57
Skupskaya, E. V. 7:113
Smekhov, G. D. 2:45
Smiryan, O. D. 7:60

Smol'skaya, T. I. 9:27
Sokolov, R. N. 4:128
Solodovnikov, A. P. 3:79
Soshko, A. I. 7:81
Starobinets, I. A. 10:42
Stepanov, G. V. 2:48
Stepanov, Yu. S. 2:55
Stesik, L. N. 6:31
Stulov, V. P. 5:32, 6:28, 9:56,
12:118
Suladze, K. Ye. 3:85
Sultanov, M. A. 2:4, 3:101, 5:6,
10:4, 12:119
Summ, B. D. 7:90
Suntsova, S. P. 9:141
Suslov, A. A. 2:35
Suvorov, V. D. 5:89
Sychev, V. V. 12:31
S"yedin, V. Ya. 10:42
Sysun, V. V. 3:34
Syutkin, N. N. 2:112

T

Tarasov, V. D. 2:111
Tarkov, A. P. 12:79
Temkin, L. A. 5:48
Terent'yev, V. F. 7:108
Ternov, I. M. 5:107
Testov, V. G. 3:36
Tkach, Yu. V. 12:103
Tregub, F. S. 4:61, 6:63
Tret'yachenko, G. N. 9:161
Trubnikov, B. A. 7:150
Trufakin, N. Ye. 9:74
Tsaplin, V. S. 9:93
Tsukerman, V. A. 4:122
Tsvetkov, Ye. P. 3:74
Tsvetkova, M. V. 9:52
Tsytovich, V. N. 9:148
Tugazakov, R. Ya. 3:39
Tumakayev, G. K. 3:38
Tumanov, A. T. 11:113
Turhanov, Ye. N. 9:55
Tyurikova, L. A. 4:120
Tyurin, Ye. L. 12:12

U

Udovskiy, A. L. 9:165
Uglov, A. A. 4:4, 9:13
Ulomov, V. I. 12:79

Ul'yanov, K. N. 7:53
Ur'yash, F. V. 3:89
Urzhumtsev, Yu. S. 10:124

V

Vagin, Yu. P. 6:81
Vagner, S. D. 7:55
Vakatov, V. P. 4:26
Vakhrushin, Yu. P. 3:92
Vashchenko, V. I. 5:60
Vasil'yev, M. M. 9:64
Vasil'yev, Yu. F. 4:53
Vasil'yeva, R. V. 2:40
Vasserman, A. A. 2:72, 10:35
Vatolin, Yu. N. 11:25
Vavilov, S. P. 12:107
Vaynshteyn, B. I. 5:69
Ventova, I. D. 3:91
Verbitskiy, V. A. 9:207
Vereshchagin, L. F. 7:98, 100, 102
Vereshchagin, V. L. 10:92
Vertogradskiy, V. A. 12:117
Verzhinskaya, A. B. 12:115
Veytsman, P. S. 3:72
Vinogradov, A. I. 12:44
Vinokurov, A. Ya. 9:41
Vishnevskiy, A. I. 6:77
Vlasov, V. I. 11:33
Vodovatov, F. F. 3:5
Volson, L. Yu. 3:80
Volosevich, P. P. 9:8
Voloshin, V. A. 6:97
Volosov, V. I. 2:98
Vorob'yev, A. A. 3:93, 5:120
Vorob'yev, V. F. 10:130
Veronin, V. I. 7:96
Voronkin, V. G. 5:36
Voskoboinikov, I. M. 2:67
Vovk, A. A. 9:85
Vozhzhova, N. N. 6:55
Vul'ffson, N. I. 6:24
Vystavkin, A. N. 7:119

W

Wlodarczyk, E. 11:27

Y

Yakovleva, I. B. 12:77
Yakushev, V. V. 2:47

Yakusheva, O. B. 11:28
Yampol'skiy, P. A. 2:49
Yefimov, A. S. 3:37
Yegorkin, A. V. 9:125
Yegorov, N. V. 6:71
Yeliseyev, B. V. 6:82
Yeliseyev, Yu. B. 5:19
Yel'yashevich, M. A. 6:22
Yepifanov, A. A. 5:94
Yepinat'yeva, A. M. 9:124
Yermak, Yu. N. 7:19
Yesmchenko, S. D. 12:142
Yevtushenko, T. P. 4:11
Yurgens, D. I. 11:52

Z

Zagorodnikov, S. P. 2:43, 3:28
Zak, L. I. 12:24
Zak, M. A. 9:48
Zakatov, L. P. 5:110
Zakharchenko, V. F. 5:54
Zakharenko, I. O. 9:82
Zakharkin, R. Ya. 10:90
Zakharov, M. N. 10:30
Zakharov, S. D. 2:13
Zakharov, V. P. 3:9, 6:3
Zakharova, A. I. 9:118, 11:76
Zamyshlyayev, B. V. 2:70
Zapol'skiy, K. K. 4:59
Zaritskiy, A. R. 10:7
Zavadovskaya, Ye. K. 10:126
Zaydel', R. M. 5:27
Zayko, Yu. N. 12:13
Zaytsev, A. V. 4:131
Zaytsev, S. G. 3:29
Zelenskiy, K. F. 4:125
Zhak, V. M. 9:128
Zhdanov, V. A. 9:98
Zhdanov, V. V. 6:57
Zheleznyak, M. B. 2:21
Zhidkova, Z. V. 6:93
Zhigulev, V. N. 11:110
Zhikhareva, T. V. 2:39
Zhmayeva, Ye. A. 10:22
Zhukov, M. F. 7:48
Zolotovskiy, O. A. 3:37
Zolotykh, B. N. 6:85
Zubarev, V. N. 2:54
Zubkov, I. P. 3:106
Zubkov, P. I. 9:75
Zunnunov, F. Kh. 5:94
Zuyev, V. Ye. 10:37, 12:46
Zverev, G. M. 4:2, 10:1
Zvolinskiy, N. V. 12:52